REPUBLIQUE ALGERIENNE DEMOCRATIQUE ET POPULAIRE

Ministère de l'Enseignement Supérieur et de la Recherche Scientifique

ECOLE NATIONALE POLYTECHNIQUE

Mechanical Engineering Department

Algerian Transport Industrial Company

End-of-study project dissertation for obtaining the state engineer diploma in Mechanical Engineering

Analysis of the breakage defect of the mechanical parts of the tramway bridges and proposition of solutions

Presented and defended on 14/07/2022 by :

Ouiam MESSAADI

Abdellah DAHOUMANE

Composition of the jury

President	**M. Brahim GUERGUEB**	**MAA**	**ENP**
Promoter	**M. Djamel SAIDI**	**MCB**	**ENP**
Promoter	**M. Hakim SIGUERDJIDJENE**	**MCA**	**UMBB**
Promoter	**M. Abdelhak ABDI**	**Engineer**	**CITAL**
Examiner	**M. Hamid SEDJAL**	**MAA**	**ENP**
Guest of honor	**M. Mohamed BOUAZIZ**	**Pr**	**ENP**

ENP 2022

REPUBLIQUE ALGERIENNE DEMOCRATIQUE ET POPULAIRE

Ministère de l'Enseignement Supérieur et de la Recherche Scientifique

ECOLE NATIONALE POLYTECHNIQUE

Mechanical Engineering Department

Algerian Transport Industrial Company

End-of-study project dissertation for obtaining the state engineer diploma in Mechanical Engineering

Analysis of the breakage defect of the mechanical parts of the tramway bridges and proposition of solutions

Presented and defended on 14/07/2022 by :

Ouiam MESSAADI

Abdellah DAHOUMANE

Composition of the jury

President	**M. Brahim GUERGUEB**	**MAA**	**ENP**
Promoter	**M. Djamel SAIDI**	**MCB**	**ENP**
Promoter	**M. Hakim SIGUERDJIDJENE**	**MCA**	**UMBB**
Promoter	**M. Abdelhak ABDI**	**Engineer**	**CITAL**
Examiner	**M. Hamid SEDJAL**	**MAA**	**ENP**
Guest of honor	**M. Mohamed BOUAZIZ**	**Pr**	**ENP**

ENP 2022

REPUBLIQUE ALGERIENNE DEMOCRATIQUE ET POPULAIRE

Ministère de l'Enseignement Supérieur et de la Recherche Scientifique

ECOLE NATIONALE POLYTECHNIQUE

Département de génie mécanique

Compagnie industrielle des transports algériens

Mémoire de projet de fin d'études pour l'obtention du diplôme d'ingénieur d'état en Génie Mécanique

Analyse du défaut casse des pièces mécaniques des ponts de tramway et proposition de solutions

Présenté et soutenu le 14/07/2022 par :

Ouiam MESSAADI

Abdellah DAHOUMANE

Composition du jury

Président	**M. Brahim GUERGUEB**	**MAA**	**ENP**
Promoteur	**M. Djamel SAIDI**	**MCB**	**ENP**
Promoteur	**M. Hakim SIGUERDJIDJENE**	**MCA**	**UMBB**
Promoteur	**M. Abdelhak ABDI**	**Ingénieur**	**CITAL**
Examinateur	**M. Hamid SEDJAL**	**MAA**	**ENP**
Invité d'honneur	**M. Mohamed BOUAZIZ**	**Pr**	**ENP**

ENP 2022

ملخص

الغرض من هذا المشروع هو تحليل وتقديم حلول للمشاكل التي تواجهها سيتال أثناء اشتغال مخفض السرعات الخاص بالجسر وخاصة مشكلة انكسار المسننات (عمليا، قص الأسنان من جذورها).
تم تحليل هذه المشكلة من عدة جوانب، بدءًا من تحليل الموثوقية متبوعًا بالتركيب الكيميائي، وانتهاءً بالتحقق من مقاومة المادة باستخدام معياري ضغط السطح والتمزق.

الكلمات المفتاحية: المسننات، الموثوقية، مخفض السرعات، التحليل.

Résumé

Ce projet a pour but d'analyser et d'apporter des solutions aux problèmes rencontrés par l'entreprise CITAL au sujet du fonctionnement du pont, en particulier, l'usure et l'endommagement (pratiquement, cisaillement des dentures à leur racine) du couple pignon fritté-couronne. Le problème a été analysé sous plusieurs aspects : analyse de la fiabilité, composition chimique et vérification des deux critères de résistance du matériau à la pression superficielle et à la rupture.

Mots-clés : Engrenages, Fiabilité, Réducteur, Caractérisation.

Abstract

The purpose of this project is to analyze and provide solutions to the problems encountered by the CITAL company during the operation of the bridge, in particular wear and breakage (practically, shearing of the teeth at their root) of the sintered pinion-crown pair. The problem has been analyzed under several aspects starting with the analysis of the reliability followed by the chemical composition, to finish with the verification of the resistance of the material using the two criteria of the surface pressure and the rupture.

Keywords: Gears, Reliability, Reducer, Characterization.

Dedication

To my parents, my grandparents and all my family.

DAHOUMANE Abdellah

First of all, I want to dedicate this modest work to my dear parents, I thank them for their unconditional moral and financial support. To my dear sister "CHAIMA", and my bothers "SABER","LOUAI","NIDAL" and "IYAD" who have given me this desire to learn and know -how, I wish you all the best in your life, may ALLAH protect you. To my dear professor "Mr. BOUAZIZ" I wish for you all happiness in your life. To all my friends, especially my best friend "AMIRA".

MASSAADI Ouiam

Thanking

First of all, we thank ALLAH the Almighty for giving us the courage and patience to complete this work.

Secondly, we would like to sincerely thank our supervisors in this project Mr. Djamel SAIDI, Mr. Mohamed BOUAZIZ, Mr. Hakim SIGUERDJIDJENE and Mr. Abdelhak ABDI, for their availability and for guiding us throughout this project.

We would also like to thank the members of the jury Mr. Hamid SEDJAL and Mr. Brahim GUERGUEB for the interest they have shown in our work by accepting to examine it.

We also thank the SNVI factory, and especially Mr. Hakim AGGOUNE for welcoming us and letting us use their laboratories.

Finally, we address our most sincere thanks to all our family and friends, who have always supported and encouraged us during the realization of this thesis. Thank's everyone.

Table of contents

Table of figures

List of tables

Nomenclature

Chapter 2:

$\boldsymbol{MTBF}$	Mean Time Between Failure	**Hour**
$\boldsymbol{\lambda}$	Failure rate	**1/Hour**
$\boldsymbol{\eta}$	Scale parameter	
$\boldsymbol{\gamma}$	Position parameter	
$\boldsymbol{\beta}$	Shape parameter	
$\boldsymbol{\sigma}$	Standard deviation	
$\boldsymbol{MTTR}$	Mean Time To Repair	**Hour**
$\boldsymbol{\mu}$	Repair rate	**1/Hour**
$\boldsymbol{A_i}$	Inherent availability	
$\boldsymbol{A_o}$	Operational availability	

Chapter 4:

$\boldsymbol{b}$	Tooth width	$\boldsymbol{mm}$
$\boldsymbol{d_i}$	Pitch diameter	$\boldsymbol{mm}$
$\mathbf{d_{bi}}$	Base diameter	$\boldsymbol{mm}$
$\mathbf{h_{ai}}$	Projection height	$\boldsymbol{mm}$
$\mathbf{h_i}$	Tooth height	$\boldsymbol{mm}$
$\mathbf{d_{ai}}$	Head diameter	$\boldsymbol{mm}$
$\mathbf{d_{fi}}$	Foot diameter	$\boldsymbol{mm}$
$\boldsymbol{\alpha_t}$	Apparent pressure angle	°
$\boldsymbol{m_n}$	Normalized modulus	$\boldsymbol{mm}$
$\boldsymbol{k}$	The minimum width coefficient	$\boldsymbol{mm}$
$\boldsymbol{\alpha}$	Pressure angle	°
$\boldsymbol{\beta}$	Pitch helix angle	°
$\boldsymbol{P}$	Engine power	$\boldsymbol{W}$

σ_H	The maximum contact pressure	**MPa**
K_A	The application factor	
K_V	The dynamic factor	
$K_{H\beta}$	The load's longitudinal distribution factor	
$K_{H\alpha}$	The load's transversal distribution factor	
σ_{HB}	The surface pressure calculated in the contact point	**MPa**
Z_B	The Inclination factor	
Z_β	The high contact factor	
σ_{HO}	The reference (basic) surface pressure	**MPa**
Z_H	The geometric factor	
Z_ε	The conduct factor	
Z_E	The elasticity factor	$\sqrt{\text{MPa}}$
σ_{HP}	The allowable contact (Hertz) pressure	**MPa**
σ_{Hlim}	The nominal reference stress (contact pressure)	**MPa**
S_{Hmin}	The minimum safety coefficient (puncture formation)	
V	Tangential velocity	$^{m}/_{s}$
Z_N	Duration factor	
Z_L	Viscosity factor	
Z_v	Speed factor	
Z_W	Hardness ratio factor	
Z_X	Dimension factor	

List of abbreviations

SEM : Scanning electron microscopy

TEM : Transmission electron microscopy

FIM : Field ion microscopy

SPM : Scanning probe microscopy

AFM : Atomic force microscopy

STM : Scanning tunneling microscopy

XRT : X-ray diffraction topography

DTA : Differential thermal analysis

DEA : Dielectric thermal analysis

TGA : Thermo Gravimetric Analysis

DSC : Differential Scanning Calorimetric

IET : Impulse excitation technique

General introduction

The tramway is a catalyst for the process of modernizing cities, by guaranteeing access to urban centers. Tramways has several features, it is a fundamental element in guaranteeing the sustainable mobility of citizens in increasingly constrained and saturated urban spaces, it also strengthens the interconnection capacity with other means of transport (TGV, TER, city buses, etc.). For all those reasons, the tramway is part of a clearly announced and planned urban regeneration strategy.

Algeria witnesses a remarkable expansion of tramway networks. Since 2011, a total of six completely new built tram systems with modern low-floor vehicles have started regular operations with four other systems currently under construction.

The CITAL company improved from the assembly of tramways to an activity centered on maintenance and mainly the maintenance of bogie bridges. This transformation was not without impact and the company saw the need to integrate a specialized design office to carry out reverse-engineering in order to break away from the TEXILIS supplier and take over the maintenance activity. It's in this context that our work fits, particularly within the framework of the analysis of the breakage defect motor bogie bridges of the CITADIS tramway encounter.

Due to the absence of plans and technical data related to the various tramway components, the analysis of the causes of the defect of the bridge reducer cannot be carried out at present, therefore the question asked is how to help CITAL to analyze the causes of failures at the level of the bridges of bogies? In order to meet the needs of CITAL, we approached this project by determining at first point the technical data that is essential to process the reverse-engineering.

To carry out our work, we have organized our dissertation into four chapters. The first chapter is devoted to the presentation of the CITAL company, a state-of-the-art presentation of tramways equipment and the statement of the problematic. The second chapter presents the analysis of the reliability of the bridge of the tramway. Followed by the third chapter, in which material analysis concerning the defectuous part of the bridge. Concluding with the fourth chapter in which verification calculations about the breakage defect are presented.

Chapter 1

Company presentation, state of the art and problematic

1.1 INTRODUCTION:

In this chapter we will present the CITAL company, as well as all of its activities, its objectives and its vision. Followed by a state-of-the-art presentation regarding the railway industry and especially the tramways, in order to have an overall idea of its industrial environment. To conclude whit the statement of the problematic of this subject, what will enrich our future observations in order to process better the problem analysis part.

1.2 PRESENTATION OF CITAL:

1.2.1 General presentation:

CITAL is a joint stock company which was born in 2011 from the will of Algeria to acquire modern industrial capacities in the assembly and maintenance facilities in the rail sector, it is responsible for meeting the tram needs of current and future projects in Algeria. To the present day, 6 tramways systems are maintained by CITAL: Algiers since December 2010; Oran since April 2013 and Constantine since June 2013, Sidi-Bel-Abbes since July 2017, Ouargla since March 2018 and Setif since May 2018. Soon the maintenance of the Mostaganem trams and that of the CORADIA ALGERIA mainline trains will also be provided by CITAL.

Figure 1-1: The logo of CITAL

CITAL is certified ISO 9001, 2015 version and has in its track record:

• 145 tram ramps produced.

• Development of a railway economic and industrial fabric in Annaba around the factory, and throughout Algeria around CITAL maintenance centers.

• The recruitment of more than 500 local managers and employees, who are trained in Europe and in Algeria, to become highly qualified and master advanced technologies.

• 3 Major Partners EMA, FERROVIAL and ALSTOM.

• Quality at the highest world level attested by ISO 9001 certifications.

• The commitment to the preservation of our environment attested by ISO certifications 14001.[1]

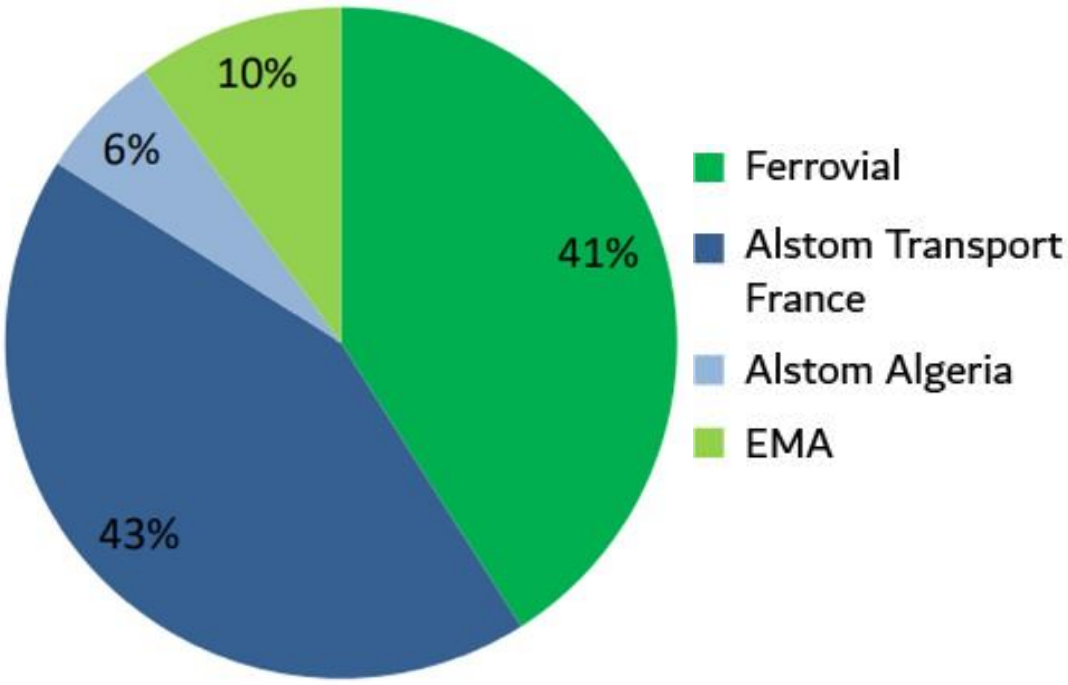

Figure 1-2: CITAL shareholders

1.2.2 History:

It all started on November 14, 2010, with the signing of the Framework Agreement and the Pact of Shareholders. Then on March 15, 2011, followed the creation of CITAL, the unit of assembly and maintenance of Citadis 302 and Citadis 402 type tram sets, in continuation in December 13 2012, the rolling stock supply program contracts (EMA) were signed. In May 12, 2015, the Annaba factory was inaugurated. And on April 10, 2016 the signing of the framework agreement between Alstom, Ferrovial, EMA and SNTF for the extension of CITAL's activities to the family of Coradia hybrid trains was agreed.[1]

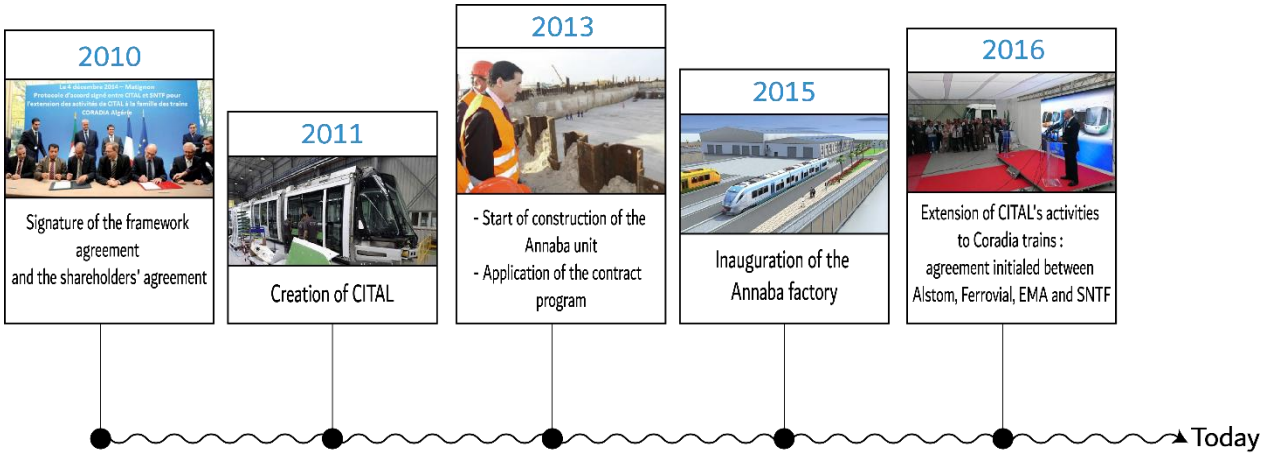

Figure 1-3: Timeline of CITAL's major events

1.2.3 Organization of CITAL:

CITAL includes 6 maintenance sites in service and the Annaba factory where we have done our internship:

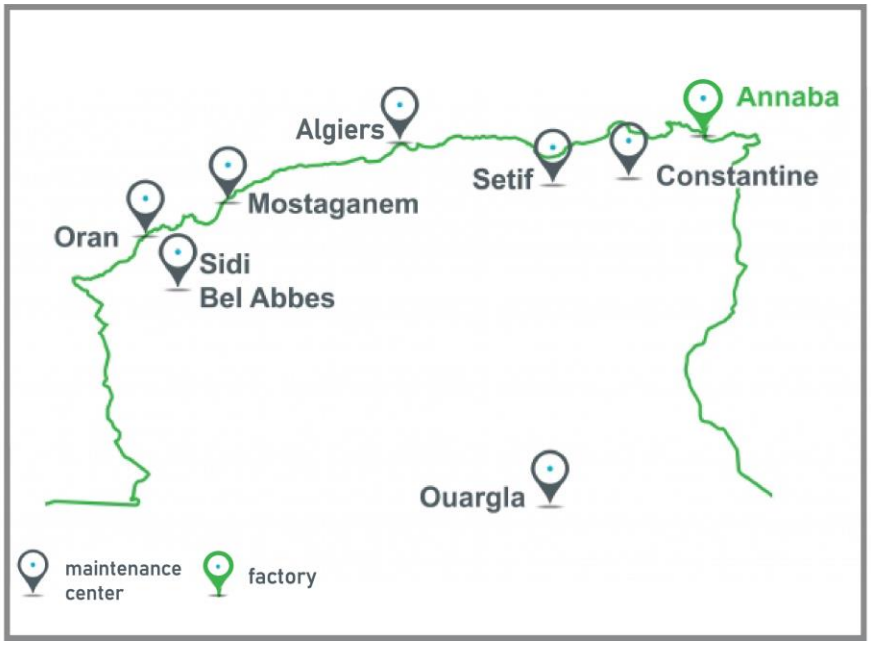

Figure 1-4: The distribution of sites.[1]

1.2.4 Annaba's factory:

The main activity of the Annaba's factory was based on the assembly of assemblies and sub-assemblies constituting the tram sets of the Citadis range. The Annaba workshops also have maintenance activities, shared with the 6 tram maintenance depots who are: Algiers, Constantine, Oran, Sidi Bel Abbes, Ouargla, Setif and future Mostaganem.

Their main objective is to complete several level 3 and 4 maintenance activities in repair and checking or repair operations following accidents and vandalism.

1.2.5 General description of the site:

• Location: ELHADJAR road, EL BOUNI ANNABA

• Overall area: 52,000m²

• Built area: 11,871m²

• Production capacity: 05 tram sets / month.

Figure 1-5: geographic position of the factory

Its main buildings are:

- Administrative Building
- Test Building
- Main Building
- Guardhouse
- Delivery Station and Electrical Substation
- Maintenance workshop
- Storage of oars
- Test track

Note:

The presentation of CITAL and more specifically the Annaba site were made in order to situate the company and its field of action, this helped us during our internship to ask the right questions to better understand the problem that we are facing.

1.3 STATE OF THE ART:

The railway train running along a track is one of the most complicated dynamical systems in engineering. Many bodies comprise the system, and so, it has many degrees of freedom. The bodies that make up the vehicle can be connected in various ways, and a moving interface connects the vehicle with the track. This interface involves the complex geometry of the wheel tread and the railhead and non-conservative frictional forces generated by relative motion in the contact area.

Streetcars are railway-based transportation vehicles that originally evolved from regular train networks into urban-based passenger transportation services when those railway lines became too embedded inside cities, making them unsuitable for transport of large steam, electric or diesel-powered trains. Modern streetcars (also known under names as tramcars, trams, trolleys or trolley cars) are usually traveling on ground level alongside regular car tracks, but with clear segregation so that cars, foot and bike traffic is not using parts of the road where tramway is laid (except on crossings).[2]

Today, over 380 cities around the world have purpose-built their tram systems that transport passengers in regular intervals and fixed city lines, enabling the much larger flow of population across large distances without impacting the flow of regular car transport. Many cities have elected to adopt tramways because they are much cheaper to build than digging entire underground subway network, and they can be added into already developed cities without the need of major overhauling of streets. Modern streetcars are operated by electricity (via suspended overhead cable network, or recently via ground delivery), and they are usually built to be light and usually between three to eight passenger carriages. Larger models can be found, especially in areas where city trams are also working on inter-city relations. In addition to working on tram tracks, some can operate on traditional railway tracks or even magnetic tracks.[3]

1.3.1 History:

History of trams began in first years of 19th century in South Wales, UK, where a small part of Swansea and Mumbles Railway located in urban areas was reconfigured to be used for trams. That very first model of the tram does not have many similarities with modern trams. It consisted of a railway car that was made from wheels and a single platform that featured no walls or seating positions. This simple platform was pulled by a team of two horses on a regular route where anyone could use them without the need to pre-hire the transport. This design from the UK quickly spread across the world and the urban areas where old railroad networks could be re-purposed for passenger use. Some of the first tram networks were in appeared in the United States (New York

in 1832, New Orleans in 1835), France (1839), Chile (Santiago, 1858), Egypt (Alexandria, 1850), Australia (Sydney, 1860) and Indonesia (Jakarta, 1869). In late 1800s trams became powered by small steam locomotives (although Paris trams used larger steam engines that were located below passenger carriage). They became very popular not only in Europe, North America in Asia but received complaints because of their smoke, noise and relatively low power that prevented them from pulling larger sets of carriages.[3]

While the majority of early tram networks were built in cities that were placed in level areas, some cities faced issues of extreme elevation, which caused them to adopt cable-operated tram lines. The first and most famous example of this drive system comes from San Francisco which introduced its cable-operated tram lines in 1873. Other cities that faced similar elevation problems quickly adopted this system (Dunedin in New Zealand in 1881, Melbourne in 1885, New York City, Los Angeles, Chicago, Dresden, London, and others. Even though cable-operated trams are effective, their integration, upkeep, and accident prevention mechanism costs are considerate.
1880 saw the appearance of the first fully electric tram. This marvel was created in Saint Petersburg, Russia by inventor Fyodor Piroshky. The basic operation principle of that first electric tram remains in use today – gathering of electricity from overhand cable network via pantograph or trolley pole (all attempts of building trams with built-in batteries failed). Just a year later in 1881, the first regular electric tram line was opened in Lochtefeld, then a suburb of Berlin. After that successful experiment and integration of electric trams in several other European cities, electric trams became a commonplace all around the world. However even though electric trams won the popularity battle, other power sources were also examined and used. This includes gas-powered trams that started being implemented in several cities between 1886 and 1908. Other power sources for trams can be petrol, compressed air, diesel motors and hydrogen cells. Some cities choose to implement those alternative power sources because of the higher costs of maintaining a strong electric network in specific areas (for example in hurricane-prone territories, rail networks with stronger elevations and more).[3]

1.3.2 Type of tramways:

Types of trams by their design:

- **Single-ended** – Tram that has operator position at just one end of the tram.
- **Double-ended** – Tram with two operating positions, one on each side of the tram. This approach makes tram more versatile (it does not need to run only in circular tracks), but it also increases its complexity and weight.

- **Low floor** – Modern design of trams that allow passengers to more easily and quickly enter or exit the tram. Disabled users with wheelchairs can much more easily use these trams because only a small platform is needed to serve them.
- **Ultra-low floor** – Recent technical improvement in which most of the motor systems are located in the roof, leaving the floor area very close to the ground. Because these trams have entry height of just 18cm (similar as sidewalk height), they can be very easily used by users with wheelchairs or baby carriages. On the other hand, their integration into city lines is more difficult because this tram type demands unique floor.
- **Articulated** – Trams that have articulated joints and a walking platform that connects adjoining passenger carriages. They are very popular all around the world, with some trams having up to 5 or six passenger compartments that are connected this way.
- **Double Decker** – Trams with 2nd floor. They are mostly used in Great Britain, Australia, Hong Kong and Alexandria.
- **Tram-train** – Trams that fulfill all technical requirements (power, wheel type, safety, etc.) that can operate on both city tram lines and regular gauge railway tracks. They are mostly used on longer lines that connect more than one urban area separated by a regular railway track.

1.3.3 Tramways in Algeria:

Algeria witnesses a remarkable expansion of tram networks. Since 2011, a total of six completely new built tram systems with modern low-floor vehicles have started regular operations with four other systems currently under construction.[4] They are disposed on the national territory as follows:

- Algiers tramway, inaugurated in 2011.
- Constantine tramway, inaugurated in 2013.
- Oran tramway, inaugurated in 2013.
- Sidi Bel Abbes tramway, inaugurated in 2017.
- Ouargla tramway, inaugurated in March 2018.
- Setif tramway, inaugurated on May 8, 2018.

The type of trams used in Algeria is the Alstom Citadis, which is a family of low-floor trams and light rail vehicles built by Alstom.

City	Picture	Model	Quantity	Order year
In service				
Algiers		Citadis 402	41	2010
Constantine		Citadis 402	47	2010
Oran		Citadis 302	30	2010
Sidi Bel Abbès		Citadis 402	30	2016
Ouargla		Citadis 402	23	2017
Sétif		Citadis 402	47	2016
Under construction				
Annaba	/	Citadis 402	30	2017
Batna	/	Citadis 402	30	2016
Mostaganem	/	Citadis 402	30	2017
Skikda	/	Citadis 402	20	2018
Tébessa	/	Citadis 402	20	2018

Table 1-1: Arrangement of tramways in Algeria.[4]

1.3.4 Alstom Citadis 302:

The frames are made up of 5 articulated modules resting on 3 bogies including 2 motors. The motor bogies are located under the end boxes, called motor 1 and 2 (M1 and M2). The carrying bogie is deployed under the central body known as the carrying nacelle (NP). Finally, between each power car and the carrying nacelle are interposed suspended boxes. C1 on the M1 side and C2 on the M2 side. The dissociation of a trainset is only possible in the workshop, for very exceptional maintenance operations (heavy repair following a serious accident, for example). The oars are equipped with their two supplied systems allowing the installation of a tow bar. These

systems are only used for emergency or workshop travel, provided by a rail-road machine or another trainset.[3]

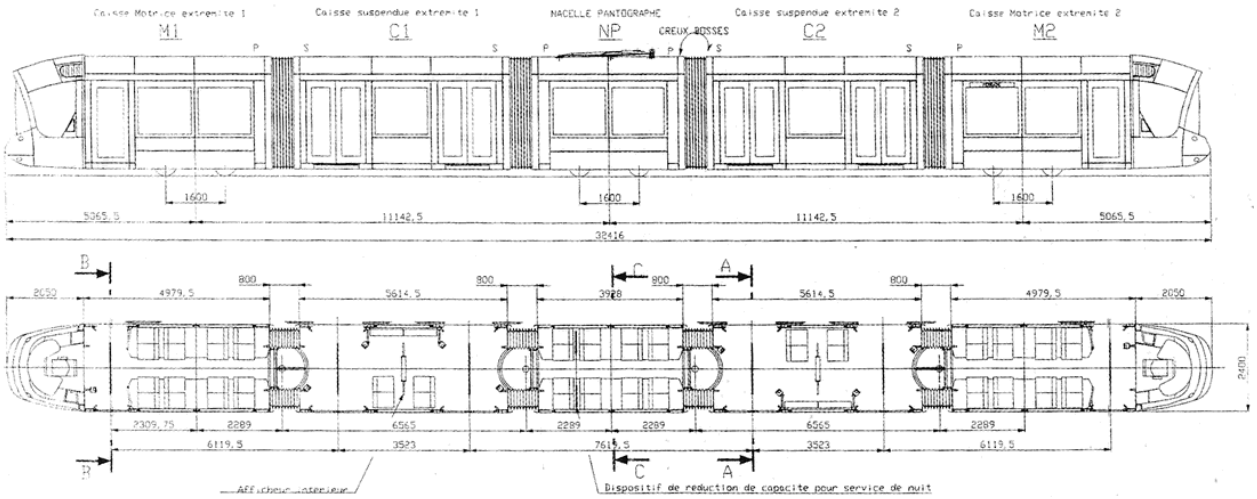

Figure 1-6: Diagram of the Citadis® 302 trains. [7]

Overall length	32 416 mm
Body width	2 400 mm
Maximum height above the rail	3 270 mm
Height from floor above rail	350 mm
Distance between bogie pivots	11 142 mm
Wheelbase of bogies	1 600 mm
Empty weight in running order	38,41 t
Mass under normal load	52,48 t
Number of motor bogies	2
Number of carrying bogies	1
Number of seats	56
normal load (Standard of 4 passengers per square meter)	201 passengers
Maximum charge (Standard of 6 passengers per square meter)	272 passengers
Maximum speed	70 km/h
Maximum power at the rim (traction)	688 kW
Supply voltage	750 V Direct Current
Average acceleration under normal load in level	1,10 $m.s^{-2}$ from 0 to 40 km/h
Minimum bending radius	25 m

Table 1-2: Alstom Citadis 302 main characteristics.[7]

1.3.4.1 Components:

- Under body:

- In motor modules M1 and M2, there are:

• Two motor bogies

• Two hydraulic centrals

• Four sandblasting compressors

- In carrying nacelle NP, there are:

• A carrier bogie

• A hydraulic power station

A) Bogies:

The bogie is a carriage located under a railway vehicle on which the axles (and therefore the wheels) are fixed; it is mobile with respect to the vehicle chassis. In general, each bogie has two axles and each axle contains two wheels. The term "bogie" is used in British English, while a "wheel truck", or simply "truck" is used in American English.

The running gear of the engine equipment is most often grouped together to constitute the BOGIE. It performs the following main functions:

- transmission of traction and braking forces
- support of the rail vehicle body
- stability on both straight and curved tracks
- providing ride comfort by absorbing vibration, and minimizing centrifugal forces when the train runs on curves at high-speed
- minimizing generation of track irregularities and rail abrasion

As an integral part of the machine, it must respect the constraints of the whole:

- mass, axle load
- gauge, in particular at track level
- satisfy performance in terms of effort and speed
- comply with life cycle cost objectives

In permanent contact with the track, the bogie must be the least aggressive possible in its regard, especially in curves. Conversely, it must withstand the stresses resulting from route - curves, switches and crossings - track defects without risks involving safety, comfort, noise, etc...

a) Motor bogie:

The motor bogies are of the Alstom Arpege 350M type, with an articulated welded steel frame. Their wheelbase is 1.6 meters. The diameter of the wheels (new) is 590 millimeters. The axles are wedged to run on a standard gauge track (1,432 millimeters). The body-bogie connection is ensured by connecting rods and the 4 supports of the secondary suspension. The primary suspension is provided by elastic wheels whose role is also to reduce rolling noise. The secondary suspension is provided by coil springs. Damping uses transverse and vertical shock absorbers between the body and the bogies, as well as anti-roll bars.[3]

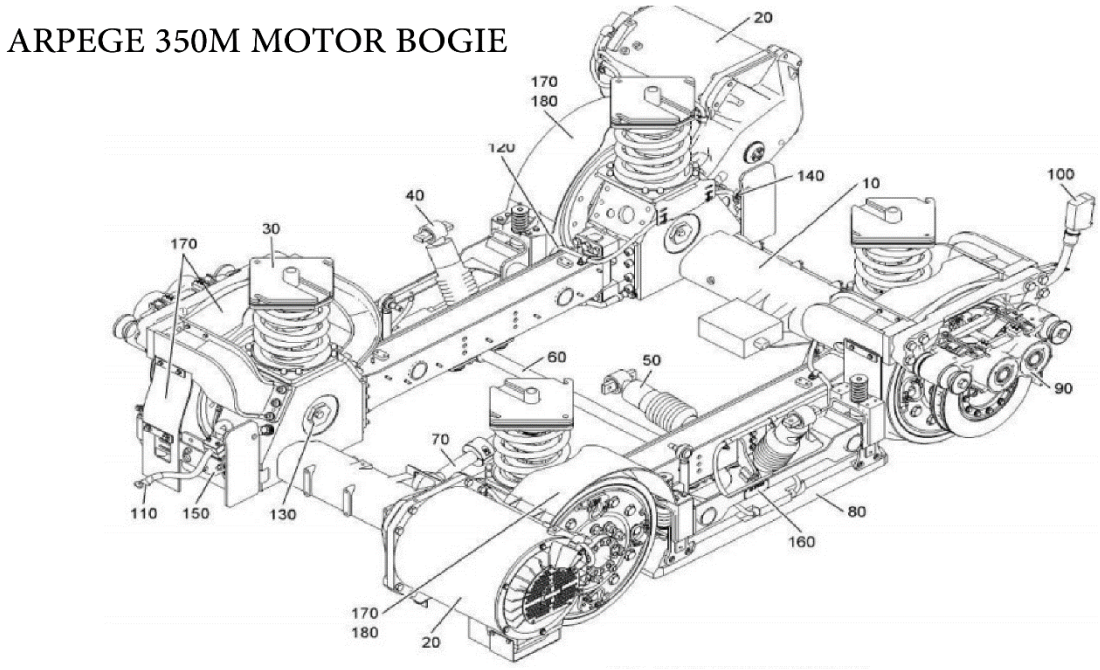

10- 12.5t engine frame assembly
20- traction engine
30- secondary suspension
40- vertical damper with bellows
50- transverse damper with bellows
60- anti-roll bar diam. 42
70- drag with sleeve
80- magnetic skate
90- overload passive disc brake
100- low voltage wiring
110- high voltage wiring
120- shunts
130- current return
140- motor shunt
150- sandblasting set
160- identification plate
170- fender engine assembly
180- motor bogie protection assembly

Figure 1-7: Motor bogie Alstom Arpege 350M components

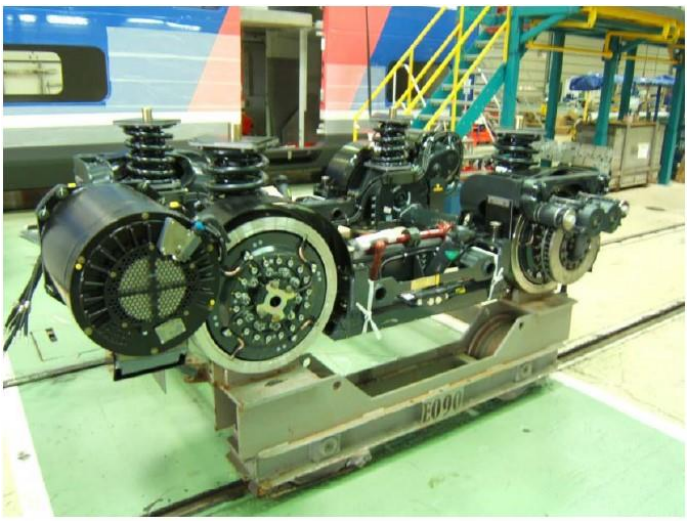

Figure 1-8: Picture of the motor bogie Alstom Arpege 350M

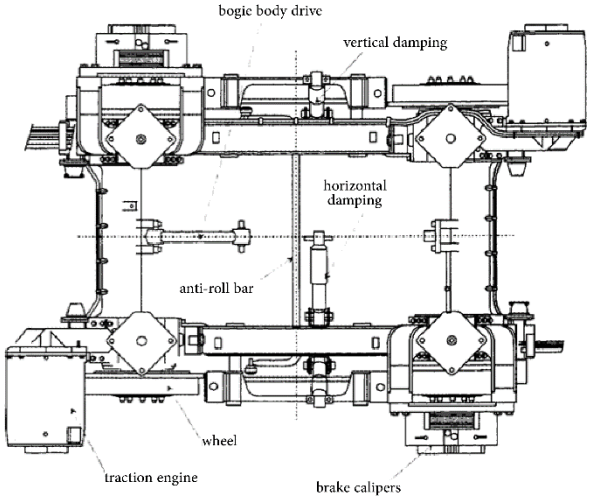

Figure 1-9: Above view diagram of the motor bogie Alstom Arpege 350M (Doc. Alstom).

The fight against slip phenomena is ensured by sandpits which have ejector pipes facing each wheel on the side of the end of the bogie. Only the forward ejectors in the direction of travel are active.

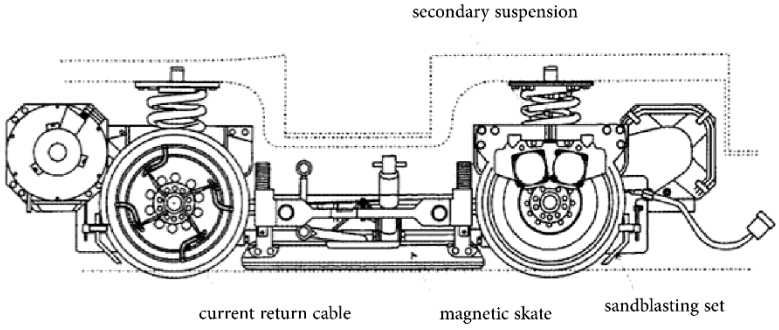

Figure 1-10: Side view diagram of the motor bogie Alstom Arpege 350M (Doc. Alstom).

There is a motor bogie for each M1 and M2 motor module.

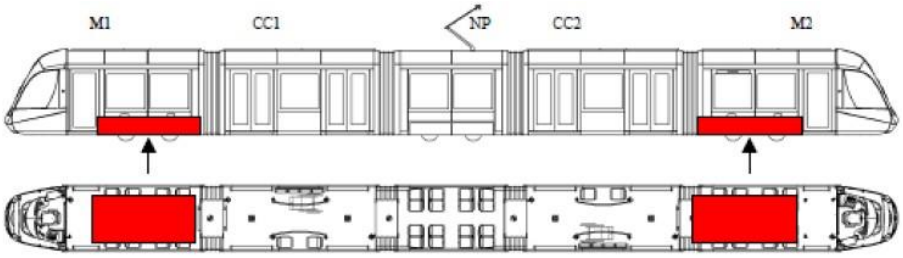

Figure 1-11: Implantation plan of motor bogies on the Alstom Citadis 302.

b) Carrier bogie:

The carrier bogie is of the Alstom Arpege 350P type, it has the same configuration and dimensions of the motor bogies except that it is motorless. It is generally used for more braking capacity and provides uniform load distribution and guidance along the tram.

The carrier bogie is fitted with a rail lubricator system intended to limit wear on the wheel flanges in curves. It also carries the SAE antenna and the speed and load measurement sensors of the train.[3]

Figure 1-12: Picture of the carrier bogie Alstom Arpege 350M

The carrying bogie is deployed under the central body known as the carrying nacelle (NP).

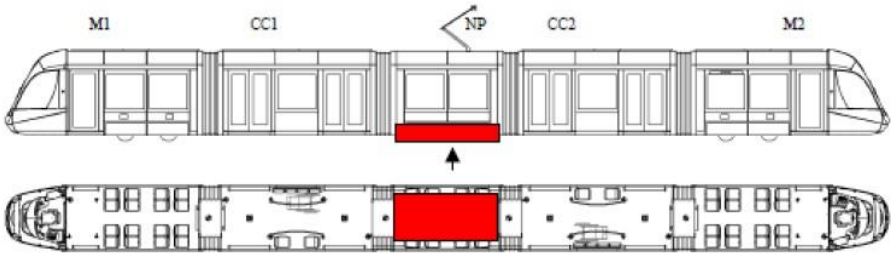

Figure 1-13: Implantation plan of carrier bogie on the Alstom Citadis 302.

B) Traction:

The traction of the trams is ensured by two motor bogies which are each equipped with 2 water-cooled three-phase asynchronous motors of type: Alstom 4 HGA 1433, with a mass of 335 kg and a power of 120 kW. Their maximum rotational speed is 4550 rpm. The transmission of the tractive effort is ensured by gears and a motor bridge forming a virtual bent axle.[6]

Figure 1-14: Picture of the Alstom 4 HGA 1433 motor.[6]

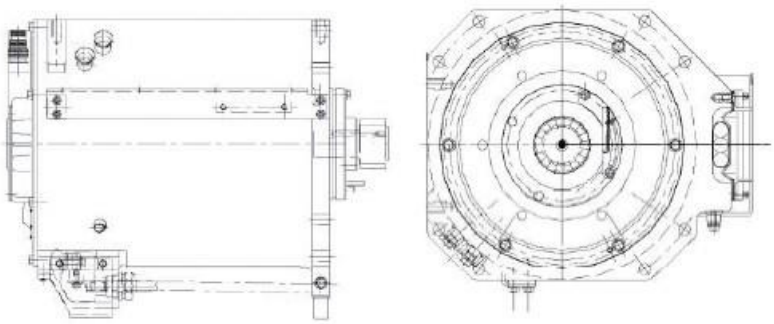

Figure 1-15: Side and front view plan of the Alstom 4 HGA 1433 motor.[6]

Traction motor type designation	4 HGA 1433
Technology	Asynchronous
Power rating	120 kW at 2600 rpm
Continuous torque	440 N.m
Mechanical transmission	Pinion
Cooling system	Water-cooled
Closed/Open	Closed
Outline: width x height x length (mm)	400 x 450 x 528
Weight (kg)	335

Table 1-3: Arpege 4 HGA 1433 motor main characteristics.[6]

C) Braking:

Three braking devices are implemented, independently or jointly, depending on the selected driving mode and the braking setpoint:

- An electrodynamic braking device,
- A friction brake device,
- A device of electromagnetic brake pads.

The braking of the vehicle is essentially ensured by electrodynamic braking acting on the drive axles. This braking is of the energy recovery type with the addition of a brake rheostatic. The distribution of energy dissipation between the regenerative brake and the brake rheostatic is performed automatically by the ETF traction box depending on the recovery capacity of the HV power line.

In addition, a friction brake (of the disc brake type) is mounted on the axles of the motor bogies and on the carrier bogie wheels.

The actuation of these disc brakes is electro-hydraulic of the indirect type (braking force provided by springs) on the motor bogies, and of the direct type (braking force provided by the hydraulic pressure) on the carrier bogie.

Finally, all the bogies are fitted with electromagnetic brake pads. These latter interfere only in emergency or safety braking.

The braking forces of the electrodynamic and friction brakes are enslaved to the load of the vehicle in service or emergency braking.

ETF traction boxes combine electrodynamic and friction brakes. They send a mechanical braking instruction to the brake electronics, for the friction brake, resulting from the conjugation.[3]

D) Sandblasting compressors:

The compressor allows the production of compressed air used for the implementation of the sandblasting, it is used in the case where there is slipping or jamming.

Figure 1-16: Sand-blasting compressor

E) Hydraulic power stations:

The control unit is a hydraulic component used in certain braking phases (service, emergency, back-up, immobilization and parking).

Figure 1-17: hydraulic central

- On the roof:

- In motor modules M1 and M2, there are:

• A low voltage electrical equipment box.

• A traction/braking equipment box.

• An engine cooling unit.

• A cabin air conditioning unit (in M1).

- In carrying nacelle NP, there are:

• A circuit breaker box.

• A pantograph.

• A lightning arrester.

- In suspended boxes, there are:

• A room air conditioning group.

• A braking rheostat.

• A battery compartment (in C1).

• A static converter (in C2).

A) Cabin air conditioning unit:

The role of the cabin air conditioning unit is to maintain and ensure, inside each driver's cabin, a constant temperature predefined and modifiable by the driver.

a) Low voltage electrical equipment box (LV):

It allows the raising and lowering of the pantograph and the electrical power supplies for the auxiliaries necessary for the preparation phase.

b) Engine cooling unit ECU:

Figure 1-18: picture of the engine cooling unit ECU

The engine cooling unit cools the traction motors of the same bogie.

c) Room air conditioning unit:

The role of the passenger room air conditioning unit is to maintain and ensure a constant temperature inside the passenger rooms.

Figure 1-19: picture of the room air conditioning unit.

B) Brake rheostat:

The braking rheostat makes it possible to dissipate the energy supplied by the motors, indeed in the braking phase the motors behave like generators and inject energy on the catenary but when this is no longer receptive the flow of energy is sent to the rheostats.

Figure 1-20: picture of the brake rheostat.

C) Battery box:

This network is mainly used to supply the functions which must remain available when the vehicle is unprepared (for example: garage lights).

Figure 1-21: Picture of the battery box.

D) CVS static converter:

The supply of auxiliary energy is ensured by a CVS static converter. From the high voltage 750V DC delivered by a pantograph, the static converter delivers, from various electrical modules, the medium and low voltage energy used on the train.

Figure 1-22: picture of the CVS static converter.

E) Circuit breaker box:

The circuit breaker box, located on the roof of the carrier nacelle NP, is the equipment that ensures electrical continuity against:

• On one hand, the equipment allowing the supply of the high voltage (pantograph, HV battery).

• And on the other hand, equipment requiring high voltage with mainly traction-braking boxes and static converters.

Figure 1-23: picture of the circuit breaker box.

F) Pantograph:

The pantograph is an articulated mechanical assembly, which captures the current on the catenary and routes it to the line of conduct. The control devices allow the raising or lowering of the pantograph.

Figure 1-24: picture of the pantograph's motor.

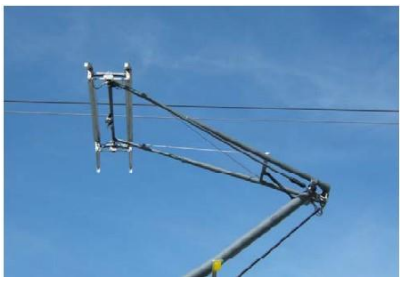

Figure 1-25: picture of the pantograph.

G) lightning arrester:

The lightning arrester protects the train against overvoltage of equipment supplied with a nominal voltage of 750V in direct current in the case of a storm.

1.3.5 Alstom Citadis 402:

The trams are made up of 7 articulated modules resting on 4 bogies including 3 motors. The motor bogies are located under the end bodies, called motor 1 and 2 (M1 and M2), and an intermediate body called the motor nacelle (NM). The carrier bogie is installed under one of the central bodies called the carrier nacelle (NP). Finally, between each engine and nacelles (engine and carrier) are interposed suspended boxes. C1 on the M1 side, central body (CC) between NM and NP, and C2 on the M2 side. The dissociation of a trainset is only possible in the workshop, for very exceptional maintenance operations (heavy repair following a serious accident, for example). The trains are equipped at both ends with systems for installing a tow bar. These systems are only used for emergency or workshop travel, provided by a rail-road machine or another trainset.[3]

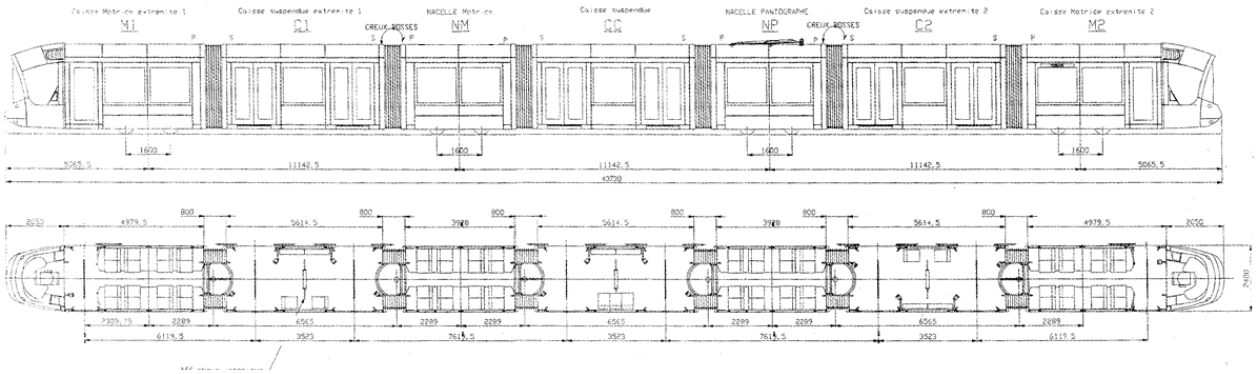

Figure 1-26: Diagram of the Citadis® 402 trains.[7]

Overall length	43 760 mm
Body width	2 400 mm
Maximum height above the rail	3 321 mm
Height from floor above rail	350 mm
Distance between bogie pivots	11 142 mm
Wheelbase of bogies	1 600 mm
Empty weight in running order	54,92 t
Mass under normal load	75,92 t
Number of motor bogies	3
Number of carrying bogies	1
Number of seats	71
normal load (Standard of 4 passengers per square meter)	287 passengers
Maximum charge (Standard of 6 passengers per square meter)	395 passengers
Maximum speed	70 km/h
Maximum power at the rim (traction)	880 kW
Supply voltage	750 V Direct Current
Average acceleration under normal load in level	1,15 $m.s^{-2}$ from 0 to 40 km/h
Minimum bending radius	25 m

Table 1-4: Alstom Citadis 402 main characteristics. [7]

1.3.5.1 Components:

The components of the Alstom Citadis 402, which is used in most of Algeria's tram networks, are exactly the same of the Alstom Citadis 302 and which were detailed previously in this paper. The main difference between these two models is the number of modules in a tram and the position of those components on it. Thus, it is useless to represent them again. However, there is a difference in the number of bogies of the two models, therefore we are going to represent the implantation of the bogies on Alstom Citadis 402 type tramway.

As precised previously, the tram is based on 4 Arpege bogies:

- 3 motor bogies of the ARPEGE 350M type supporting the M1, M2 and NM elements.
- 1 ARPEGE 350P type carrier intermediate bogie supporting the NP element.

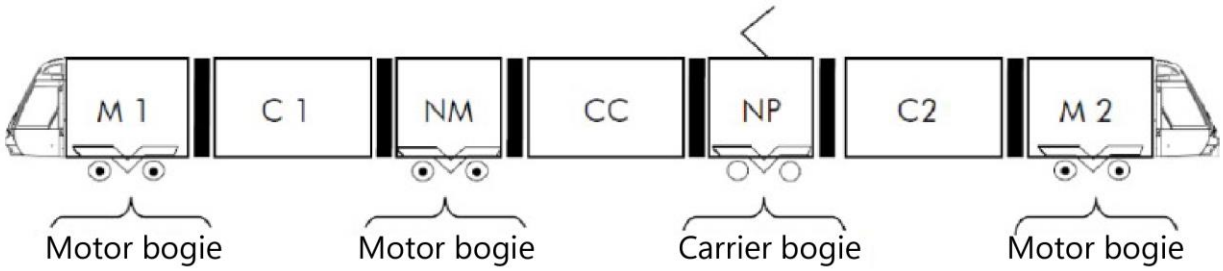

Figure 1-27: Implantation plan of motor and carrier bogies on the Alstom Citadis 402.

1.3.6 The motor bridge:

An axle-engine frame is made up of an engine axle and a side member rigidly fixed to the motor bridge. Each frame - drive axle acts as an axle and half - bogie frame, the axle forming the transverse part of the 1/2 bogie frame.

Each motor is rigidly attached to an axle and drives the driveline without coupling. The bridge is equipped with 2 hubs on which the elastic iron wheels are fixed.

The load-bearing structure of the motor bridge consists of:

- A resistant beam in 1 part, called bridge body.
- 2 side casings, bolted to the axle body, along which the electrical cables will be routed,
- 2-wheel hubs receiving:

- For each, an elastic wheel whose rim is bolted to the hub,
- For one of the two, a brake disc.

Figure 1-28: The Texilis Arpege bridge

1.3.7 The gear reducer:

A gear reducer is a mechanical system of gears in an arrangement such that input speed can be lowered to a slower output speed but have the same or more output torque. The operation of a gear reducer involves a set of rotating gears that are connected to a shaft with a high incoming speed,

which is sent to a set of rotating gears where the speed or torque is changed. How many gears are in a gear reducer assembly is dependent on the speed requirements of the application.

Figure 1-29: Example of a two-stage reduction gear box

The use of a gear reducer occurs when the drive gear is smaller and has fewer teeth than the driven gear. This is unlike the condition where the drive gear is larger with more teeth than the driven gear, which is referred to as overdrive.

Gear reducers are an essential component in cars, trucks and also railway machinery where the high rotational speed of the engine is converted such that the slower motion of the wheels can interpret and use the power safely.

1.3.7.1 The Process of a Gear Reducer:

- Gear ratio:

The gear ratio is a way of measuring how different sizes of gears interact to transfer energy. The essential aspect of this calculation is the measurement of a circle, which is a major part of gears. The determination of the gear ratio can be understood by examining the circumference of a circle. A gear that makes two rotations to turn a larger gear once has a ratio of 2:1, which means that the output speed has been cut in half. This example simplifies more complex gear reducers with several gear pairs in a series for converting revolutions per minute (RPMs) to torque.

- Gear reducer torque:

Torque is a rotational force that is received by the gear reducer and changed into a different force and speed with the amount of power remaining the same. Gear reducers are a gear or series of gears designed to reduce the torque of a motor, which increases in direct proportion to the

reduction of rotations per unit of time or revolutions per minute. This is accomplished by base mounted or shaft mounted gear reducers.

Gears are used to multiply or divide torque, which is determined by the size of the gears. The ratio of the gear sizes increases or decreases torque, which is the foundational aspect of the operation of a gear box.

- Drive gear:

Drive gears or gear drives are designed to change the speed, torque, or direction of a rotating shaft. In their simplest form they are a small gear that drives a larger gear connected to the output shaft. They are essential for providing variable output speed from a constant power source.

- Driven Gear:

The driven gear is connected to the output shaft and transfers the reduced power to the application. They are the larger of the gear set regardless of how many gears there are in the series and come in a variety of shapes.

1.3.8 The Texilis Arpege bridge gear reducer:

The interior of the shell of the Texilis Arpege bridge lodges the gear reducer of the tramway. This reducer is a two-stage type gear reducer made of six helical gears driven by the motor gear of the traction engine which is of the same type. The following figure represents the cut view of the bridge with the different gears constituting the reducer:

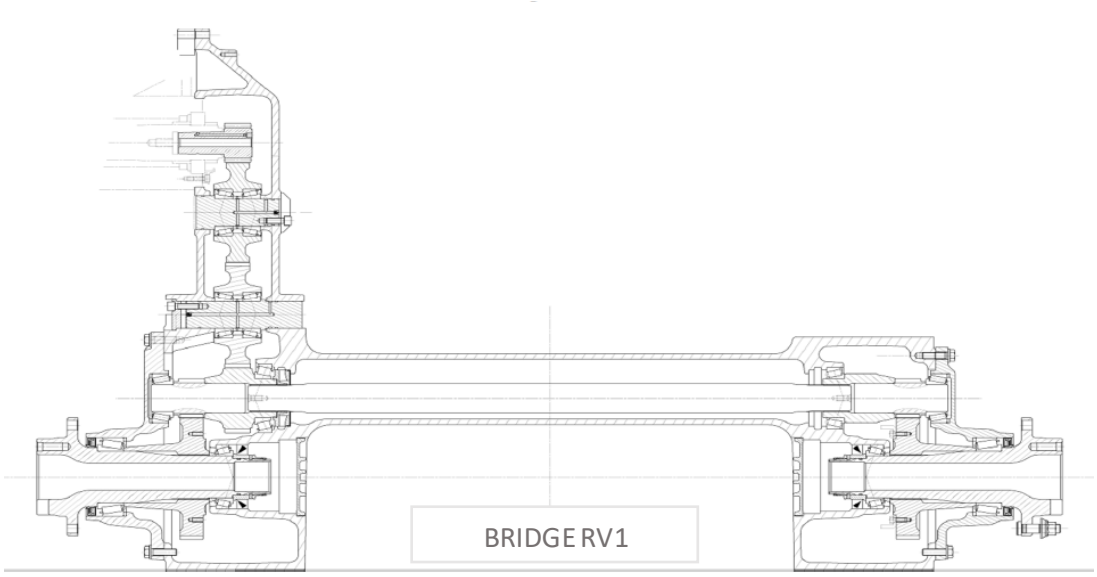

Figure 1-30: Cut view of the Texelis Arpege bridge.[5]

The bridge above is divided into two sides, the left side on this figure and in which movement come from the motor gear, is called: “Motor side”; The opposite side which is the right one, is called: “brake side” because of that braking system is mounted on this side of the bridge.

The 3D assembly of the gears train without the shell is presented in the following figure:

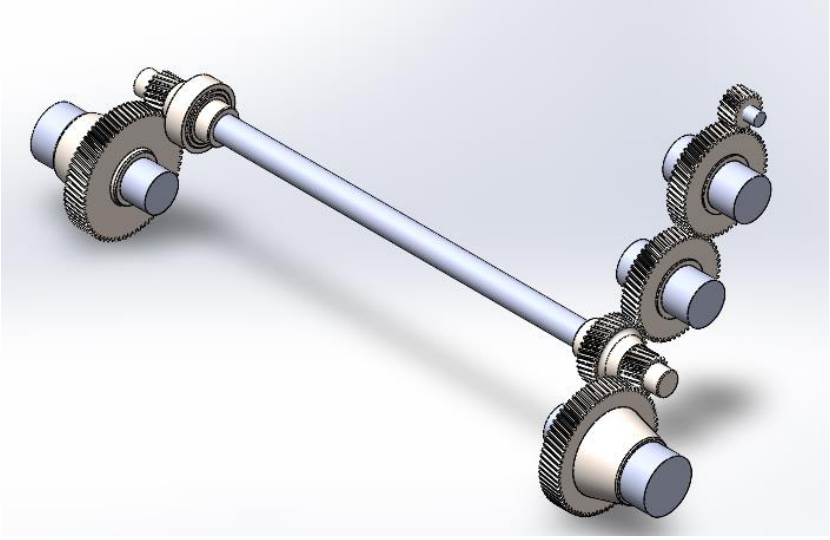

Figure 1-31: 3D perspective view of the gears of the bridge gear reducer.

The gear reducer is constituted of seven gears, with five of them on the motor side and two on the brake side. The different gears along their general design and characteristics are presented in the following table:

Gear designation	Design	Manufacturing process	Number of teeth	Exterior diameter (mm)
Motor side				
Motor gear	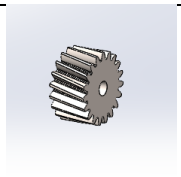	Casting	19	37.5
Gear ‘58’	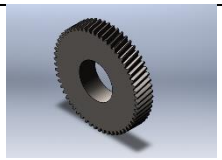	Casting	58	214
Gear ‘57’		Casting	57	210
Sintered gear	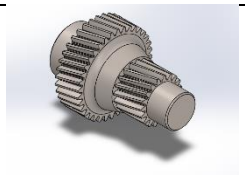	Casting	36	140.5
		Sintering	19	79.5
Crown gear	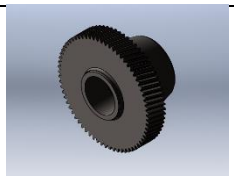	Casting	69	255
Brake side				
Sintered gear	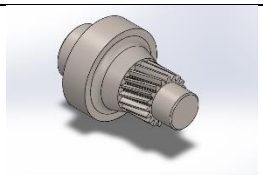	Sintering	19	79.5
Crown gear	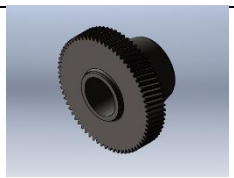	Casting	69	255

Table 1-5: *Gears of the Texilis Arpege bridge and their general characteristics.*

The drive shaft is cylindrical in shape, with a diameter of: 54 mm and a length of: 1000 mm. it transmits the rotational movement from the motor side to the brake side by connecting the two sintered gears on the side of the 36-toothing using the splines located at its ends.

Figure 1-32: 3D perspective view of the drive shaft

1.3.8.1 Gear ratios:

the gear ratios of the two stages of the reducer as long as the global gear ratio are given by the maintenance manual of the bridge as follows :[5]

- First stage (19/58/57/36) : $r_1 = 1.895$
- Second stage (19/69) : $r_2 = 3.632$
- Global ratio : $r_g = r_1 \cdot r_2 = 6.881$

1.3.8.2 Angular position of the gears:

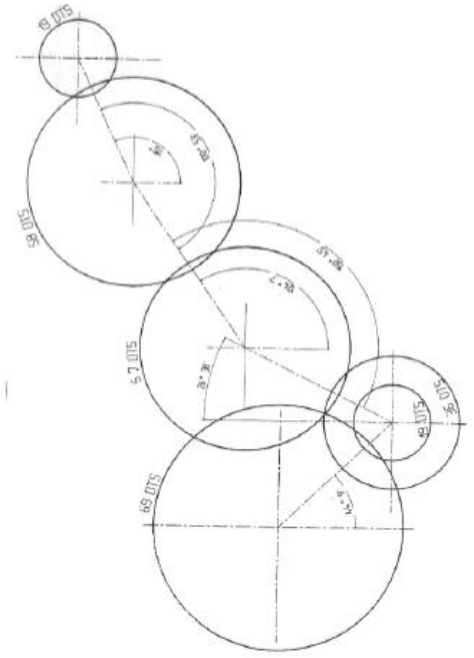

Figure 1-33 : Angular position of the gears.[5]

1.4 PROBLEMATIC:

The establishment of the functioning mode of the different mechanisms of the tramway and more precisely the motor bogies and the motor bridge above, allows us to understand the mechanical aspect of those components and by that to focus on the mechanical part presenting the failure.

This failure is a breakage defect which occurs within the reducer of the motor bridge. The part presenting this defect is the sintered gear on the motor side of the reducer. The defect is a significant tooth breakage phenomenon which can be noticed in the following figures:

Figure 1-34: Tooth breakage defect (early phase) Figure 1-35: Tooth breakage defect (advanced phase)

The sintered gear being geared to the crown gear, at a certain level of deterioration, it causes also the breakage of teeth of the crown.

Figure 1-36: Tooth breakage defect on the crown gear

Gear Failure occurs in different modes. There are Many modes of gear failure, for example fatigue, impact, wear, or plastic deformation. Of these, one of the most common causes of gear failure is tooth breakage. According to the literature, tooth breakage failure can be caused by only two causes which are: Overload breakage or Fatigue breakage.[9]

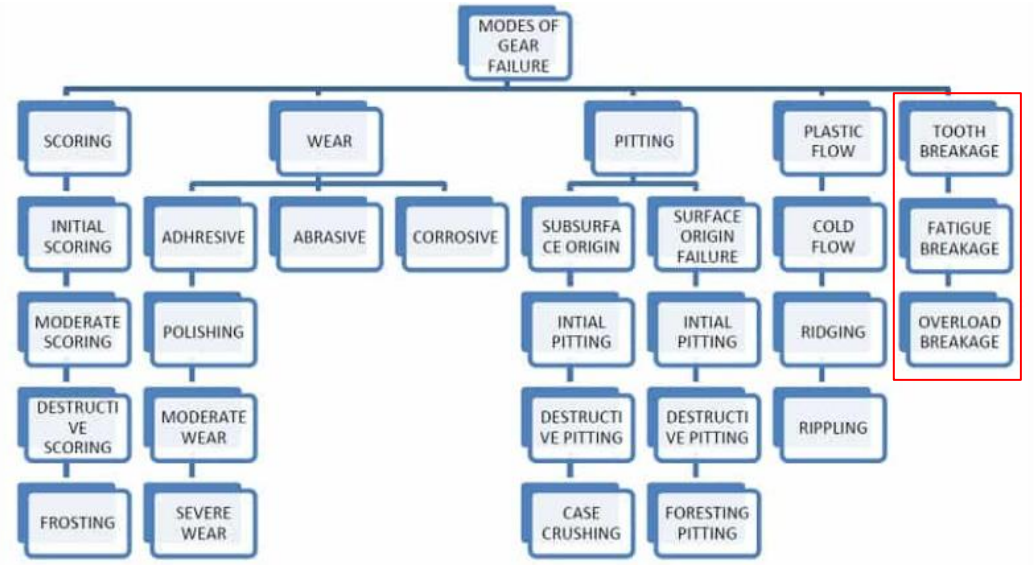

Figure 1-37: Gear failure modes.[9]

The frequency of breakages rising regularly during events which welcome a large number of people and which are accessible by tramway, thus where the tramway carries a large number of passengers, the cause of overload breakage is relatively intended to be the main factor of the tooth breakage failure. This reasoning is the main opinion we had from the majority of CITAL's Annaba factory engineers, and which we will pursue analyzing in this paperwork.

That after gathering all the technical data we need by ourselves due to their unavailability at the enterprise level. Whence, the methodology followed in the next chapters for the treatment of this project.

1.5 CONCLUSION:

In this chapter we presented the functioning principle of tramway guidance equipment and interface equipment. By that we were able to acquire knowledge on the functioning of the tramway in general and on the bridge in particular.

We then set up the problematic in order to better identify it and guide our approach in the management of this project.

In the next chapter, we begin our analysis.

Chapter 2

Reliability analysis of field failure data of the tramway guidance equipment

2.1 INTRODUCTION:

The goal of maximum production and long run availability under the given operative condition can be achieved by making the system failure free as far as possible by proper maintenance, planning and control. Due to increasing complexity of modern engineering systems, which involve high risks, the concept of reliability has become a very important factor in the overall system design [1]. So, during the last 25 years reliability concepts have been applied in various technological fields. An adequate use has been made in the area of electrical and electronics. Reliability techniques have also been applied to a number of industrial and transportation problems.[2]

Provision of reliable rolling stock and infrastructure equipment is an important part in achieving high levels of safety. [3] Therefore, the railway industry uses different methods and tools to improve the performance of different subsystems in order to ensure safety and reliability, which are the important factors for passengers and cargo transportation. Hence, reliability analysis is required to identify the bottlenecks in the system and find the components or subsystems with low reliability for a desired level of performance[4]. The purpose of this chapter is to present a case study describing reliability analysis of field failure data of tramway guidance equipment, the motor and carrier bogie, particularly the bridges over a period in CITAL Company of Algeria.

2.2 WHAT IS RIALIBILITY:

Reliability is a special attribute that describes the dependability of a component. This means that the component consistently performs a desired function under certain conditions for a certain period of time in order to meet business goals and customer needs. Theoretically, reliability can be described as:

$$\textit{Reliability} = 1 - \textit{Probability of Failure} \quad \text{(2.1)}$$

Thus, the lower the probability of failure the greater the reliability of the system. However, there are many factors that can contribute to the uncertainty involved with any new design and capital project including variations in materials, manufacturing plants, shipping, storage, and use.[5]

Another way of thinking about reliability is the quality of the component over time. A common term used in a reliability engineering context is mean time between failures (MTBF).

2.2.1 Mean Time Between Failures:

2.2.1.1 Introduction:

MTBF it is one of the first and most basic measurements one can use to measure reliability. MTBF is the average time an asset will function before it fails. MTBF is a simple measurement to pinpoint these poorly performing assets.[6]

2.2.1.2 The Definition Mean Time Between Failure:

MTBF is a metric that describes the average time it takes for a specific component to failure. MTBF does not measure the time when a component is waiting for repair or being repair; rather, it measures the time only when the component is operating. This is an important parameter to consider in the decision-making process when investing in new equipment. The higher the MTBF the higher the reliability of the product.[6]

$$\boldsymbol{MTBF} = \frac{\sum \boldsymbol{numbers\ of\ good\ function\ between\ n\ failures}}{\boldsymbol{Number\ of\ good\ working\ times}} \text{..... (2.2)}$$

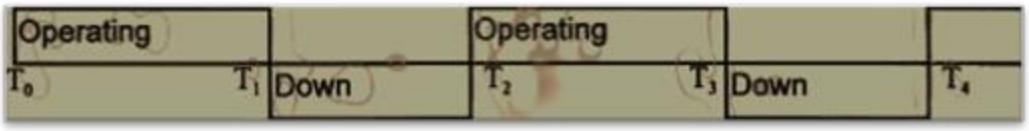

Figure 2-1: The operating profile of the system.

2.2.2 Failure rate:

Failure rate can be defined as the anticipated number of times that an item fails in a specified period of time. It is a calculated value that provides a measure of reliability for a product. This value is normally expressed as failures per million hours, but can also be expressed as a FIT (failures in time) rate or failures per billion hours. For example, if a component has a failure rate of two failures per million hours, then it is anticipated that the component fails two times in a million-hour time period.

$$\lambda(t) = \frac{number\ of\ failures}{duration\ of\ use} \text{..... (2.3)}$$

For equipment (repairable system), the failure rate is often translated by a curve called "bathtub curve" highlighting 3 periods as the figure 2-2 shows:

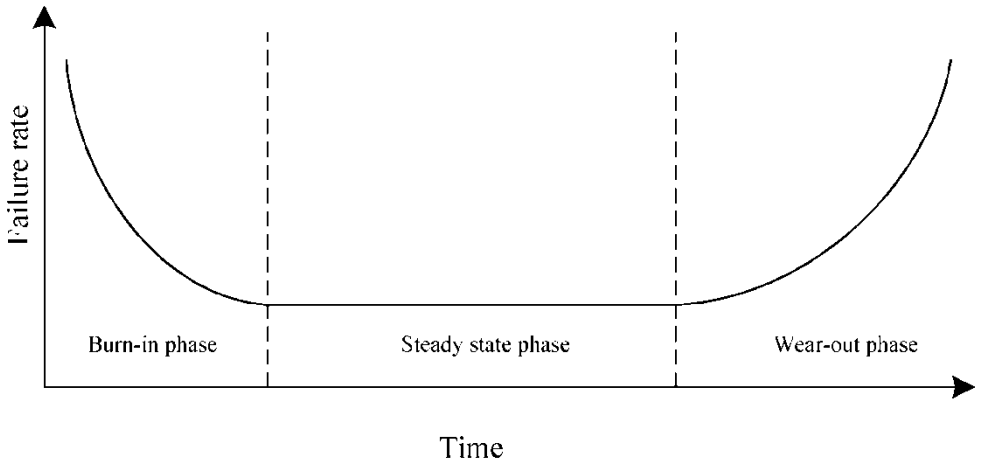

Figure 2-2: Bathtub Curve.[7]

2.2.3 The Time of Reliability:

The time that is related to the definition of reliability can be:

- A number of cycles performed: automatic machine.
- A distance covered: rolling stock.
- A tonnage produced: production equipment.

Its estimation is generally established:

- From a time interval with extrapolation to the period of operation or duration of life (for an entity).
- From a sample with extrapolation to the whole population (for a component).

2.2.4 Reliability Indicator Parameters:

Reliability is a complex concept, and many definitions can be interpreted under it. Is a system reliable when it does not produce a bad quality product? Or is this terminology used for providing information about the condition of a machine? However, it can be stated that both approaches aim at providing quality product for the customers, as well as smooth operation for the production including maintenance and other components of production. According to[8], there are 4 major categories for the mostly used indicators in production reliability:

2.2.4.1 Faultlessness:

These indicators are created in order to examine the smooth operation of the production system. These are usually time-bounded/calculated ratio: failure rate, mean operation time, probability of failure, probability of faultless operation and mean time between failures.

2.2.4.2 Reparability:

It includes all the indicators which are calculated when a job breaks down and needs to be repaired. These indicators are usually time-bounded or a calculated ratio: mean repair time, mean downtime, recovery intensity, probability of recovery, mean time to repair.

2.2.4.3 Durability:

This category reflects on the durability of the jobs, such as: mean operation time, mean lifespan, q-percent operation.

2.2.4.4 Storability:

This category stands for the storability of the product. This is also an important factor for the customer, as it also has an effect on the perception of quality: mean storage life, percentage of storage time.

2.2.5 Mathematical expressions of reliability:

2.2.5.1 Reliability law:

$$R(t) = e^{-\int_0^t \lambda(t)dt} \ldots\ldots (2.4)$$

2.2.5.2 Distribution function:

$$F(t) = 1 - R(t) = 1 - e^{-\int_0^t \lambda(t)dt} \ldots\ldots (2.5)$$

2.2.5.3 Probability density:

$$f(t) = \frac{dF(t)}{dt} = \lambda(t)e^{-\int_0^t \lambda(t)dt} \ldots\ldots\ldots (2.6)$$

2.2.5.4 Mathematical expectation:

$$E(t) = MTBF = \int_0^\infty t\, f(t)dt \ldots\ldots (2.7)$$

2.2.6 Association of equipment:

2.2.6.1 Serial system:

A system is said to be a serial system from a reliability point of view if the system fails when only one of its elements fails**.**

Figure 2-3: Serial system.[9]

$$R_s(t) = \prod R_i(t) \ldots\ldots (2.8)$$

for i ∈ {1, n} and $R_i(t)$ reliability of component (i)

2.2.6.2 Parallel system:

A system is said to be a parallel system from a reliability point of view if when one or more of its elements fail, the system does not fail.

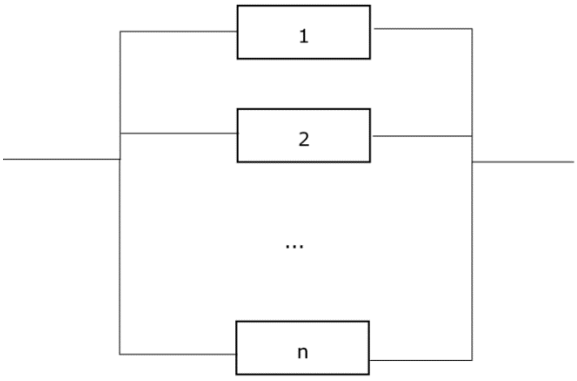

Figure 2-4: Parallel system.[9]

$$R_s(t) = 1 - \prod(1 - R_i(t)) \ldots\ldots (2.9)$$

for i ∈ {1, n} and $R_i(t)$ reliability of component (i)

2.2.7 Probability Laws Used in Reliability:

2.2.7.1 Introduction:

It is always possible to associate a probability with a random variable and thus define a probability law. When the number of trials increases indefinitely, the observed frequencies for the phenomenon studied tend towards the probabilities and the observed distributions towards probability distributions or probability laws. A probability law is a model representing "at most", a frequency distribution of a random variable[10]. We can distinguish two types:

2.2.7.1.1 Discrete Distribution Law:

Discrete Law Distribution is a type of probability distribution that shows all possible values of discrete random variable along with the associated probabilities. In other words, a discrete probability distribution gives the likelihood of occurrence of each possible value of a discrete random variable[11]. A law is said to be discrete if it takes its values in N, i.e. integer values such as for example the one which counts the number of failures. There are two conditions that a discrete probability distribution must satisfy**:**

- $0 \leq P(X = x) \leq 1$. This implies that the probability of a discrete random variable, X, taking on an exact value, x, lies between 0 and 1.

- ∑P (X = x) =1. The sum of all probabilities must be equal to 1.

2.2.7.1.2 Continuous Distribution Law:

Continuous Law Distribution is a probability distribution in which the random variable X can take on any value (is continuous). Because there are infinite values that X could assume, the probability of X taking on any one specific value is zero. Therefore, we often speak in ranges of values (p(X>0) = 50). The probability that X falls between two values (a and b) equals the integral (area under the curve) from a to b[12].

2.2.8 Types of Reliability's Distribution Laws:

2.2.8.1 Discrete Distribution Laws:

2.2.8.1.1 Hyper geometric Distribution:

The hyper geometric distribution models probability of successes in Bernoulli trials from population N containing m success without replacement[10].

The reliability function is defined by:

$$p = \frac{m}{N} \ldots\ldots \text{(2.10)}$$

The PDF to the hyper geometric distribution is:

$$f(k,n,m,N) = \frac{\left(\binom{m}{k}\binom{N-m}{n-k}\right)}{\left(\binom{N}{n}\right)} \ldots\ldots \text{(2.11)}$$

2.2.8.1.2 Uniform Distribution:

A probability distribution follows a uniform distribution when all the values taken by the random variable are equiprobable. If n is the number of different values taken by the random variable. [10]

The reliability function is defined by:

$$P(X = x_i) = \frac{1}{n} \ldots\ldots \text{(2.12)}$$

n: the number of different values taken by the random variable.

2.2.8.1.3 Bernoulli Discrete Distribution:

In the theory of probability and statistics, a Bernoulli trial is a random experiment with exactly two possible outcomes, "success" and "failure", in which the probability of success is the same every time the experiment is conducted Independent repeated trials of an experiment with exactly two possible outcomes are called Bernoulli trials. Call one of the outcomes "success" and the other outcome "failure". Let P be the probability of success in a Bernoulli trial, and q be the probability of failure. Then the probability of success and the probability of failure sum to one, since these are complementary events: "success" and "failure" are mutually exclusive and exhaustive.[13]

We have:

$$P = 1 - q \quad and\ q = 1 - p \quad so: \quad P + q = 1 \ \ldots\ldots (2.13)$$

2.2.8.1.4 Binomial Discrete Distribution:

First described by Isaac Newton in 1676 and first demonstrated by the Swiss mathematician Jacob Bernoulli in 1713, the binomial distribution is one of the most frequently encountered probability distributions in applied statistics.[14]

In mathematics, a binomial distribution of parameters n and p is a probability distribution that corresponds to a random experiment with two possible outcomes, generally referred to as "success" and "failure" respectively, the probability of success being p.

The probability distribution function (PDF) is:

$$P(K) = P(X = K) = C_k^n P^k q^{n-k} \ldots\ldots (2.14)$$

And:

$$C_k^n = \frac{n!}{k!(n-k)!} \ldots\ldots (2.15)$$

With:

- (n≥0): number of trials.
- (0≤p≤1): Probability of success

And: $$1 - p = q \ldots\ldots (2.16)$$

2.2.8.1.5 Poisson Discrete Distribution:

The Poisson distribution is a discrete function, meaning that the variable can only take specific values in a (potentially infinite) list. Put differently, the variable cannot take all values in any continuous range. For the Poisson distribution, the variable can only take whole number values (0, 1, 2, 3, etc.), with no fractions or decimals.[15]

The probability that x is equal to k is:

$$P(x = n) = e^{-\lambda} \frac{\lambda^n}{n!} \ldots\ldots (2.17)$$

λ: Law parameter (positive constant).

2.2.8.2 Continuous Distribution Law:

2.2.8.2.1 The Chi-square Law:

The Chi-square law, or Pearson's law, is not used to model reliability directly, but essentially to calculate confidence limits in confidence interval estimates. It is characterized by a positive parameter α called degrees of freedom and defined only for positive values.[10]

$$Pr(x^2 < \alpha) = \frac{1}{2^{\frac{n}{2}}\Gamma(\frac{n}{2})} \int_0^{\alpha} t^{\frac{n}{2}-1} e^{-\frac{t}{2}} dt \ldots\ldots (2.18)$$

2.2.8.2.2 Gamma Continuous Distribution:

The gamma law is the law of the time of occurrence of the α^{th} event in a Poisson process. Let {T} be the vector representing the inter-event times (the times between successive failures of a system). If these durations are independently random variables and identically distributed according to an exponential law of parameter β, then the cumulative time of occurrence of these failures follows a Gamma law of parameter (α, β).[12]

The probability density function:

$$f(t) = \frac{\beta^{\alpha} t^{\alpha-1} e^{-\beta t}}{\Gamma(\alpha)} \quad t \geq 0, \alpha \geq 1 \text{ and } \beta \geq 0 \ldots\ldots (2.19)$$

2.2.8.2.3 *Beta Continuous Distribution:*

The beta law is a family of continuous probability laws, defined on [0,1], parameterized by two shape parameters, typically denoted α and β. It is a special case of the Dirichlet distribution, with only two parameters.[16]

2.2.8.2.4 Normal Distribution:

Normal distribution, also known as the Gaussian distribution, is a probability distribution that is symmetric about the mean, showing that data near the mean are more frequent in occurrence than data far from the mean.[17]

$$f(t) = \frac{1}{\sigma\sqrt{2\pi}} exp\left[\frac{1}{2}\left(\frac{t-\mu}{\sigma}\right)^2\right] = \frac{1}{\sigma}\phi(\frac{t-\mu}{\sigma}) \ldots\ldots (2.20)$$

Where ϕ is the standard normal pdf with $\mu = 0$ and $\sigma^2 = 1$

2.2.8.2.5 The exponential distribution:

The exponential distribution is one of the widely used continuous distributions. It is often used to model the time elapsed between events.

Most natural phenomena are subject to the aging process. There are phenomena where there is no degradation or wear. These are generally accidental phenomena. For these phenomena, the probability for an object to be still alive or not to fail before a given time knowing that the object is in good condition at a time t, does not depend on t. For example, for a crystal glass, the probability of being broken within five years does not depend on its date of manufacture or its age. By definition, a lifetime is said to be wear-free if the probability of survival at time t does not depend on t.[18]

Hypothesis:

- The failure rate λ(t) is independent of the age of the system.
- For the system operating on demand, the failure at the nth demand is independent of those at the n-1 demand.
- For the system operating continuously, this represents a constant λ(t).

The exponential distribution is expressed as follows:

- Reliability:

$$R(t) = e^{-\lambda t} \quad \ldots\ldots (2.21)$$

Where λ is the intensity.

- Probability density:

$$f(t) = \lambda e^{-\lambda t} \ldots\ldots (2.22)$$

- The distribution function:

$$F(t) = 1 - e^{-\lambda t} = \int_0^t \lambda e^{-\lambda t} dt \ldots\ldots (2.23)$$

- Failure rate:

$$\lambda = \frac{f(t)}{R(t)} = constant \ldots\ldots (2.24)$$

2.2.8.2.6 The Weibull Distribution:

It is well known that the Weibull distribution is the most popular and the most widely used distribution in reliability and in analysis of lifetime data. It was introduced by the Swedish physicist Weibull. It has been used in many different fields like material science, engineering, physics, chemistry, meteorology, medicine, pharmacy, economics and business, quality control, biology, geology, and geography.

The expression Weibull's law covers in fact a whole family of laws, some of them appearing in physics as a consequence of certain hypotheses. This is in particular the case of the exponential law (β = 1) and the normal law (β = 3).[19]

A) Mathematical expressions of reliability:

The three-parameter Weibull distribution is specified by the cumulative distribution function (CDF):

$$R(t) = 1 - F(t) = e^{-\left(\frac{t-\gamma}{\eta}\right)^{\beta}} \quad \ldots\ldots (2.25)$$

Where η, γ and β are scale, position and shape parameters, respectively. The corresponding probability density function (PDF) is:

$$f(t) = \frac{\beta}{\eta}.\left(\frac{t-\gamma}{\eta}\right)^{\beta-1}.e^{-\left(\frac{t-\gamma}{\eta}\right)^{\beta}} \quad with \quad t \geq \gamma \ldots\ldots (2.26)$$

The failure rate is defined by:

$$\lambda(t) = \frac{\beta}{\eta}\left(\frac{t-\gamma}{\eta}\right)^{\beta-1} \ldots\ldots (2.27)$$

Mean time between failures (MTBF) is:

$$E(t) = MTBF = \lim_{x\to\infty} \int_0^{\infty} t\, f(t)dt \ldots\ldots (2.28)$$

$$E(t) = MTBF = \gamma + \eta\Gamma\left(1 + \frac{1}{\beta}\right) = A\eta + \gamma \ldots\ldots (2.29)$$

Standard deviation is:

$$\sigma = B.\eta \ldots\ldots (2.30)$$

B) <u>The three-parameter Weibull distribution:</u>[20]

a) β The Form Parameter:

It's dimensionless; we have many cases to the β value:

- β>1, the failure rate is increasing, characteristic of the old age zone:
    a. 1< $\boldsymbol{\beta}$ < 2,5: fatigue
    b. 2,5< β < 4: wear, corrosion
- If β=1, the failure rate is constant, characteristic of the mature zone.
- If β<1, the failure rate is decreasing, characteristic of the youth zone.

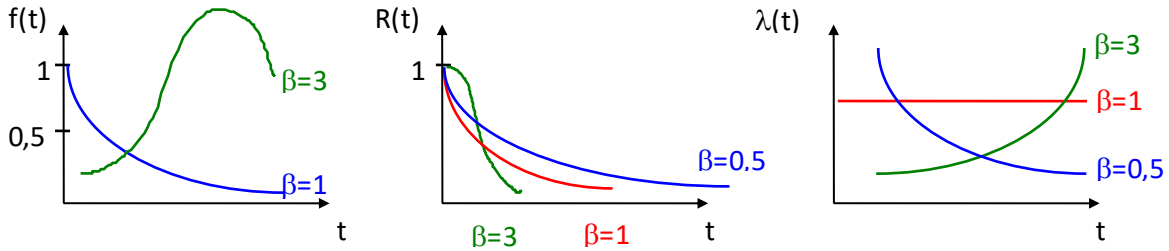

Figure 2-5: Variation of the failure rate the reliability and the distribution function with different value of form parameter.

b) η Scale parameter:

That is expressed in the unit of time:

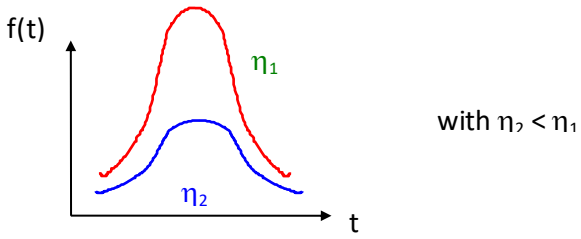

Figure 2-6: The distribution function variation with two different value of scale parameter

c) γ *Position parameter:*

$-\infty < \gamma < +\infty$, which is expressed in the unit of time:

- $\gamma>0$: total survival over the time interval $[0, \gamma]$.
- $\gamma=0$: failures start at the time origin.
- $\gamma<0$: failures started before the time origin;

This shows that the commissioning of the equipment under study preceded the history of TBFs:

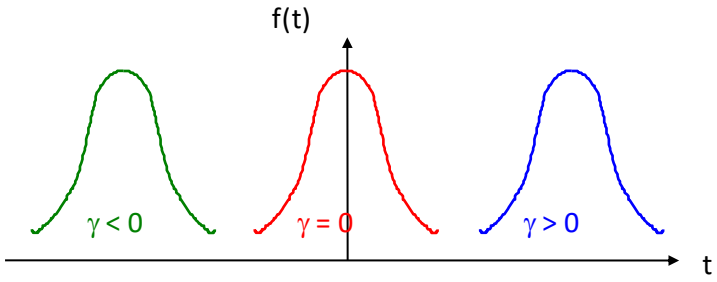

Figure 2-7: probability density curve

2.2.9 Reliability Modeling:

2.2.9.1 Introduction:

After collecting life data for the analysis, it is apparent that a suitable and valid reliability model is essential to the feasibility of model estimation and analysis. As a result, various reliability models have been generated for data analysis; for example, the frequently used Exponential distribution, Weibull distribution, Normal distribution, lognormal distribution, Gamma distribution and so on.

Before the 1980s, most products were assumed to follow exponential distribution, which has the simplest mathematical form with tractable statistical properties. Products following an exponential lifetime distribution have the so-called no-memory property. However, it is found out later that the assumptions of the exponential distribution must always be taken into consideration in order to have more accurate predictions of the underlying failure mechanism.

Hence, different models should be utilized under complex situations when the assumption of constant random failure rate is restrictive. Among these statistical models, the Weibull distribution (Weibull, 1951), named after the Swedish Professor Waloddi Weibull, is perhaps the most frequently used life time distribution for lifetime data analysis mainly because of not only its flexibility of analyzing diverse types of aging phenomena, but also its simple and straight forward mathematical forms compared with other distributions.

The two-parameter Weibull distribution is recognized as an appropriate model and the most widely used is given by:

$$R(t) = 1 - F(t) = e^{-\left(\frac{t}{\eta}\right)^{\beta}} \quad \ldots\ldots (2.31)$$

2.2.9.2 Overview about the Weibull Distribution:

Research related to the theory of Weibull model has been discussed in Barlow and Proschan (1981), Nelson (1982), Lawless (1982), Mann et al. (1974), Bain (1974), etc. More than one thousand references to the applications of Weibull distribution is also listed in the report by Weibull (1977). However, a rather practical problem lies in that most industrial components or products will generally experience three main life phases:

1. The infant mortality region, when the sample is newly introduced and has a high failure rate;
2. The constant failure rate region, when the product is stable and with low failures;
3. The wear-out region, when the failure rate is significantly increased.

Typically, Reliability Data focus on lifetimes. In the industrial cases, these data are cycles until failure, which is a surrogate for time. Engineering examples include extremely complex systems, such as aircraft engines, as well as relatively simple parts such as metal braces. Often, engineers must build reliability models on the relatively simple components in order to develop a reasonable model for the complex system. The most common distributions used by reliability engineers to model reliability data are the lognormal, the exponential, and the Weibull. Of these three, the Weibull tends to dominate, especially since the exponential is a special case. The lognormal distribution transforms highly skewed data to the normal distribution. The exponential distribution has a constant hazard function, which is associated with true random failure behavior, i.e., there is no specific failure mechanism associated with the failure. The biggest value of the Weibull distribution is its ability to model the times to failure for specific failure mechanisms.[2]

To conclude, we like incorporating the Weibull distribution into our data analysis of tramway guidance equipment, the motor and carrier bogie, particularly the bridges over a period in CITAL

Company of Algeria. Because it is can accurately model the time-to-failure of real-world events also it is sufficiently flexible despite having only two parameters to model a variety of data sets.

2.3 CASE STUDY:

The three-parameter Weibull distribution is specified by the cumulative distribution function (CDF):

$$R(t) = 1 - F(t) = e^{-\left(\frac{t-\gamma}{\eta}\right)^{\beta}} \quad \ldots\ldots (2.32)$$

Where η, γ and β are scale, position and shape parameters, respectively.

The corresponding probability density function (PDF) is:

$$f(t) = \frac{\beta}{\eta}.\left(\frac{t-\gamma}{\eta}\right)^{\beta-1}.e^{-\left(\frac{t-\gamma}{\eta}\right)^{\beta}} \quad with:\ t \geq \gamma \quad \ldots\ldots (2.33)$$

It is a 3-parameter reliability law which allows taking into account the periods where the failure rate is not constant (youth and old age). This law allows:

1. An estimation of the MTBF.
2. The calculation of λ (t) and R (t) and their graphical representation.

$$R(t) = e^{-\left(\frac{t-\gamma}{\eta}\right)^{\beta}} \quad \ldots\ldots (2.34)$$

$$\lambda(t) = \frac{\beta}{\eta}\left(\frac{t-\gamma}{\eta}\right)^{\beta-1} \quad \ldots\ldots (2.35)$$

The shape parameter β can orientate a diagnosis, because β can be characteristic of certain failure modes. So, to start our reliability analysis of tramway guidance equipment, the motor and carrier bogie, particularly the bridges over a period in CITAL Company we determine Weibull's parameters using graphical and numerical method using EXCEL.

2.3.1 Numerical method:

The procedure that we have been following is summarized in the following steps:

1. The preparation of the needed data to plot the points cloud, which are the operating time (TBF) and the distribution function (F_i).
2. Plot the points cloud.
3. Plot of the Weibull line.
4. Determination of the equations of the Weibull distribution.

2.3.1.1 Preparation of data, operating time and the distribution function (t_i, Fi):

2.3.1.1.1 Methods of approximating the values of the distribution function:

For our reliability studies, we have a certain number of real data on the TBF; TBF whose distribution function we want to study. These data represent a sample $n = 116$ of the population we want to study.

First, they must be classified in ascending order of duration in hours, and days so we organized them in first time in an Excel file. according to the most suitable unit. The middle ranks or the median-rank regression methods are most commonly used today.

The estimate of the density function for a time t_i is given by:

$$f(t_i) = \frac{i}{n+1} \quad \ldots\ldots (2.36)$$

However, it is not the density function that interests us but the distribution function F(ti). This distribution function can be estimated according to several methods, two of which are particularly applicable to reliability laws (exponential and Weibull): these are the methods of median ranks and average ranks. The choice between the two methods depends on the size "n" of the sample.

- *If* $n \leq 20$ *we use the median ranks method and:* $F(t_i) = \frac{i-0,3}{n+0,4} \ldots\ldots (2.37)$
- *If* $n > 20$ *the medium rank method is used and:* $F(t_i) = \frac{i}{n+1} \quad \ldots\ldots (2.38)$

In our case: n=120, so: $n > 20$.

So, to summarize all data that we need to calculate these two parameters:

First, we made an excel file from 3 sheets:

1. The first sheet we placed several data that the CITAL Company like intervention date, date of delivery on site, operating date, number of intervention and the incident date.
2. The second sheet:

❖ we calculated the operating time (TBF) such as:

$$TBF = T_{in} - T_o \ldots\ldots (2.39)$$

considering that:

T_{in}: The incident date when the failure happened.

T_o: The exploitation date when the tramway started.

❖ We classified the TBFs in ascending order of duration in hours, and minutes.

❖ We calculated also the distribution function $F(t_i)$ by the medium rank method.

❖ We put other parameters like the order (i) the number of interventions, the time of intervention.

3. The last sheet we represented all the plots and results of our study.

The couple of $F(t_i)$ and t_i are presented in the Appendix in table number (Table b-1).

2.3.1.2 Plot the points cloud:

We used Excel to represent the cloud points plot:

To plot this points cloud we did some mathematics development starting by the three-parameter distribution function F(t):

$$F(t) = 1 - e^{-\left(\frac{t}{\eta}\right)^{\beta}} \quad \ldots\ldots (2.40)$$

$$\Rightarrow \ln\left(1 - F(t)\right) = -\left(\frac{t}{\eta}\right)^{\beta} \quad \ldots\ldots (2.41)$$

$$\Rightarrow -\ln\left(1 - F(t)\right) = \left(\frac{t}{\eta}\right)^{\beta} \quad \ldots\ldots (2.42)$$

$$\Rightarrow \ln\left(-\ln\left(1 - F(t)\right)\right) = \beta \ln\frac{t}{\eta} \ldots\ldots (2.43)$$

$$\Rightarrow ln\left(-ln\left(1 - F(t)\right)\right) = \beta\, ln\, t - \beta\, ln\, \eta \quad \ldots\ldots (2.44)$$

In the end we have an equation $Y = ax + b$ such as we were able to calculate the couple (X,Y)

$$X = ln(t_i) \ldots\ldots (2.45)$$

$$Y = ln(-ln(1 - F(t))) \ldots\ldots (2.46)$$

Then we put the couple (X,Y) in the Excel file then we plot the cloud point using the equations (2.46) , (2.45) and (2.43) as the figure (2-8) shows:

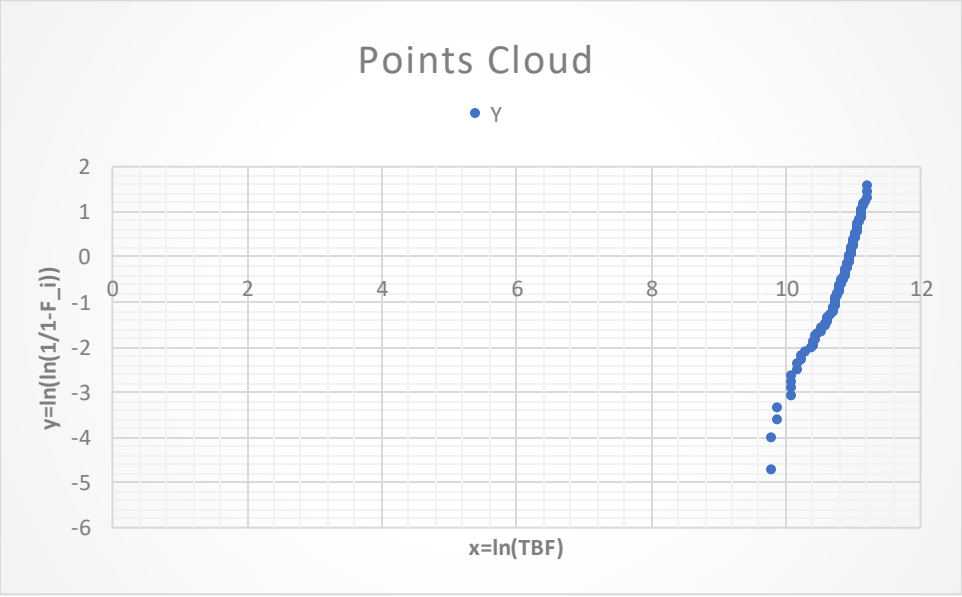

Figure 2-8: The points cloud

To make the plot clear more we have expanded the scale:

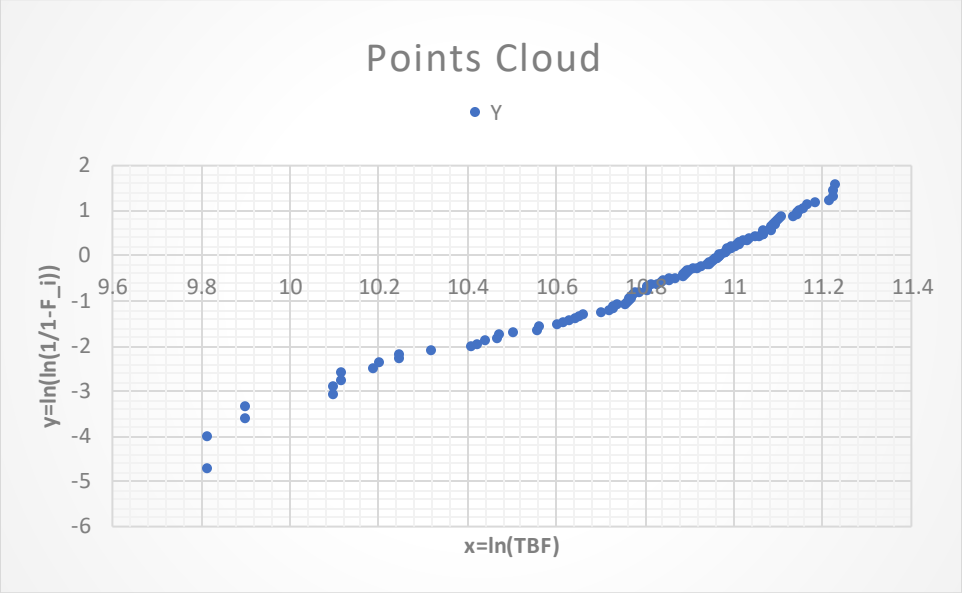

Figure 2-9: the points cloud with expanded scale

2.3.1.3 Plot of the Weibull line:

After the plot of the cloud, we traced the Weibull line and we found the following equation:

$$Y = 3{,}6985X - 40{,}555 \ldots\ldots \text{(2.47)}$$

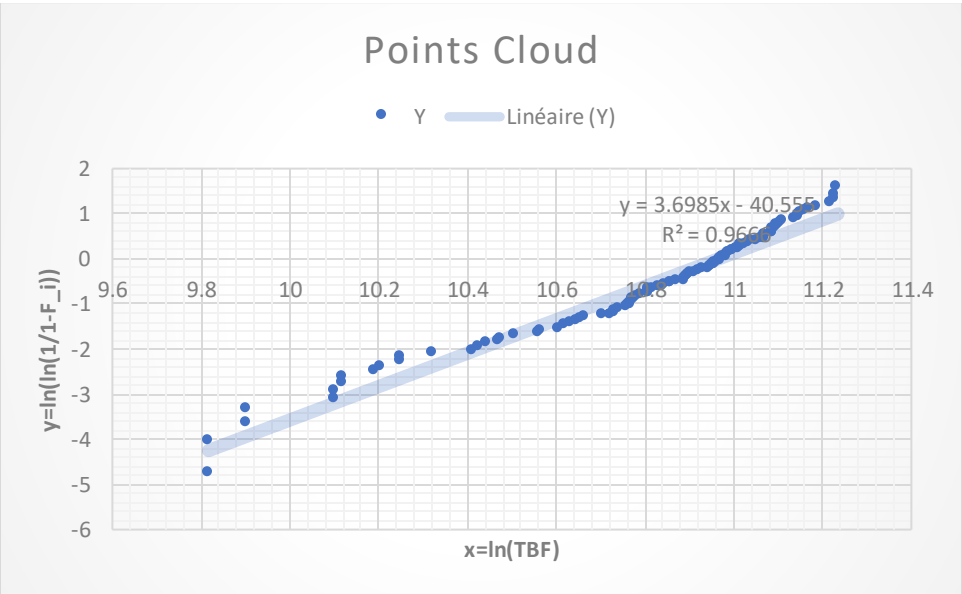

Figure 2-10: Weibull Line.

By identification between the two equations (2.47) and (2.46):

$$\Rightarrow ln\ (-ln(1 - F(t))) = \beta\ ln\, t - \beta\ ln\, \eta \ \ldots\ldots \text{(2.48)}$$

We could determine the shape parameter β:

$$\beta = 3.6985$$

And the scale parameter η:

$$\beta \ln \eta = 40{,}555 \Rightarrow \ln \eta = \frac{40{,}555}{3{,}6985} \Rightarrow \eta = e^{\left(\frac{40{,}555}{3{,}6985}\right)} \Rightarrow \eta = 57830hrs \ldots\ldots (2.49)$$

The parameters of the Weibull distribution are then:

$$\begin{Bmatrix} \gamma = 0 \\ \beta = 3.6985 \\ \eta = 57830 \end{Bmatrix}$$

2.3.1.4 Determination of the equations of the Weibull distribution:

$$R(t) = e^{-\left(\frac{t}{57830}\right)^{3,6985}} \ldots\ldots (2.50)$$

$$\lambda(t) = 6{,}3955 \times 10^{-5} \left(\frac{t}{57830}\right)^{2,6985} \ldots\ldots\ldots (2.51)$$

$$f(t) = \frac{\beta}{\eta} . \left(\frac{t-\gamma}{\eta}\right)^{\beta-1} . e^{-\left(\frac{t-\gamma}{\eta}\right)^{\beta}} \text{ with } t \geq \gamma$$

$$f(t) = 6{,}3955 \times 10^{-5} \left(\frac{t}{57830}\right)^{2.6985} e^{-\left(\frac{t}{57830}\right)^{3.6985}} \ldots\ldots (2.52)$$

2.3.1.5 Calculation of the MTBF:

To determine the value of the MTBF we have the appendix table that give the values of A and B for the value of shape parameter $\beta = 3.6985$:

$$A = 0.9011$$

$$B = 0.278$$

Finally, the Mean Time Between Failure is:

$$MTBF = A\eta + \gamma = 0.9011 \times 57830 = 52111 \ldots\ldots (2.53)$$

$$MTBF = 52111 \text{ (Hrs)}$$

So, we can calculate the reliability and the failure rate of the bridge for: t=MTBF=52111(Hrs)

$$R(t = MTBF) = e^{-\left(\frac{52111}{57830}\right)^{3,6985}} = 0.5064 \ldots\ldots (2.54)$$

$$\lambda(t = MTBF) = 6{,}3955 \times 10^{-5} \left(\frac{52111}{57830}\right)^{2,6985} = 0{,}0000482 \ldots\ldots (2.55)$$

We were able to plot the Reliability R(t) and the failure rate $\lambda(t)$ for period of time:

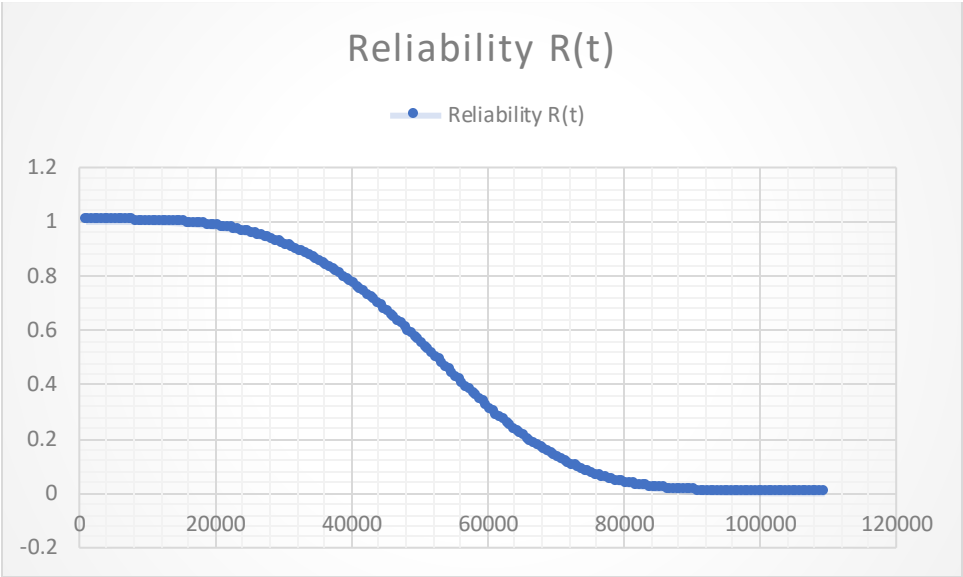

Figure 2-11: Reliability plot of the bridge

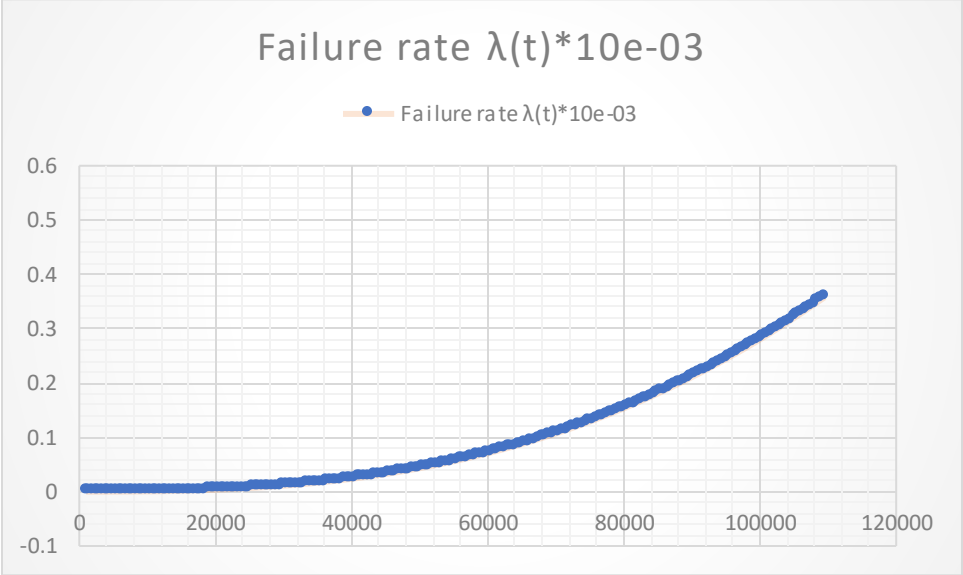

Figure 2-12: Failure Rate of the bridge

2.3.2 Graphical method:

The procedure that we have been following is summarized in the following steps and it is similar to the numerical method using the Weibull paper:

1. The preparation of the needed data to plot the points cloud, which are the operating time (TBF) and the distribution function (Fi) using the middle ranks or the median-rank regression methods.
2. Plot the points cloud using the weibull paper.

3. Plot of the Weibull line.
4. Determination of the equations of the Weibull distribution.
5. Calculating the MTBF.

2.3.2.1 Preparation of data the operating time and the distribution function (t_i, Fi):

2.3.2.1.1 Methods of approximating the values of the distribution function:

For our reliability studies, we have a certain number of real data on the TBF; TBF whose distribution function we want to study. These data represent a sample $n = 116$ of the population we want to study.

We did the same steps that we used in the numerical method:

1. We placed several data that the CITAL Company like intervention date, date of delivery on site, operating date, number of intervention and the incident date.
2. We placed the distribution function F (ti) and the TBF and other parameter we need to make our study (see the appendix):

❖ we calculated the operating time (TBF) such as:

$$TBF = T_{in} - T_o$$

considering that:

T_{in}: The incident date when the failure happened.

T_o: The exploitation date when the tramway started.

❖ We classified the TBFs in ascending order of duration in hours, and minutes.

❖ We calculated also the distribution function F (t_i) by the medium rank method.

❖ We put other parameters like the order (i) the number of interventions, the time of intervention.

2.3.2.2 Plot of the points cloud:

2.3.2.2.1 Weibull paper:

This Weibull paper is used to read graphically the parameters of a Weibull distribution in the case where the parameter is null. Indeed, the distribution function associated with a Weibull distribution of parameters $\beta, \gamma = 0 \; and \; \eta$

2.3.2.2.2 Scales used on the Weibull paper:

- Upper axis: natural scale in X
- Intermediate axis: logarithmic scale (reading of the parameter η)
- Low axis: logarithmic scale (each value of t is associated with its neperian logarithm $\ln(t)$

- Left ordinate: the values of F(t) are placed in percentage in $\ln(-\ln(1-F(t))$scale
- Ordinate on the axis $X=-1$(reading of the parameterβ: these are the values $\ln(-\ln(1-F(t))$

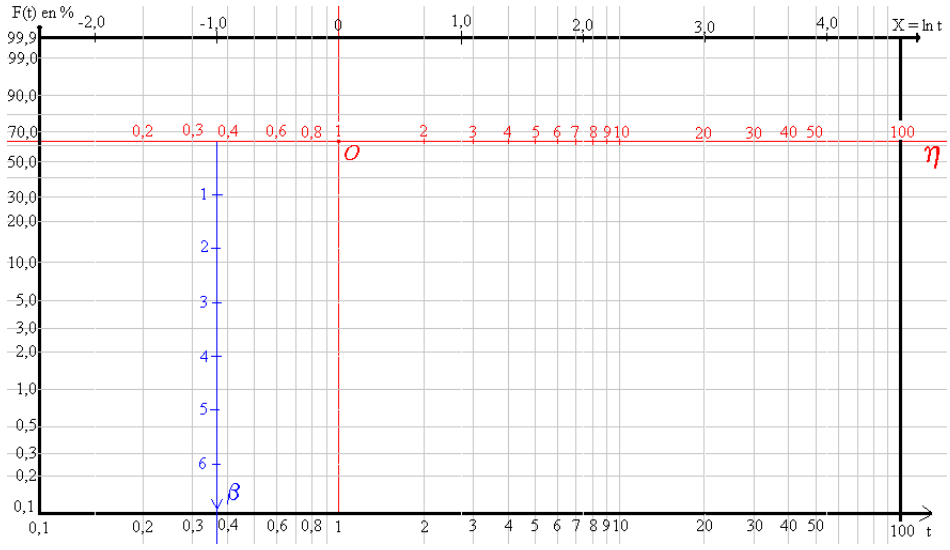

Figure 2-13: Weibull paper [21]

2.3.2.3 Plot of the Weibull line:

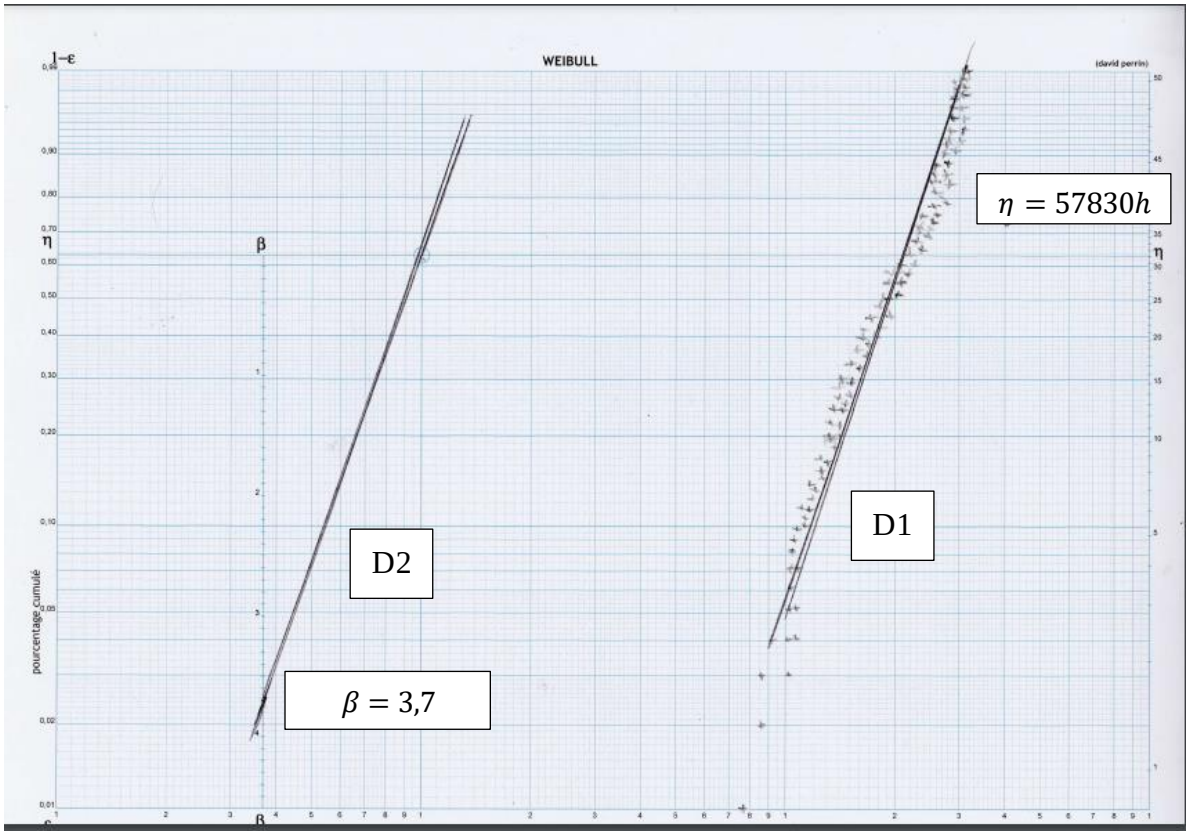

Figure 2-14: Plot of the Weibull line

Comments:

- The direct obtaining of a line D1 without rectification indicates that γ=0 (positional parameter)
- The line D1//D2, passing through the origin intersects the "b" axis at a point β=3.7 this is the value of the shape parameter
- The line D1 intersects the time axis at t=η=57830 hours. This is the parameter of the Weibull distribution

2.3.2.4 Determination of the equations of the Weibull distribution:

$$R(t) = e^{-\left(\frac{t}{57830}\right)^{3,7}} \ldots\ldots (2.56)$$

$$\lambda(t) = 5,2111 \times 10^{-4}\left(\frac{t}{57830}\right)^{2,7} \ldots\ldots (2.57)$$

$$f(t) = 5,2111 \times 10^{-4}\left(\frac{t}{57830}\right)^{2,7} e^{-\left(\frac{t}{57830}\right)^{3,7}} \ldots\ldots (2.58)$$

2.3.2.5 Calculating the MTBF:

To determine the value of the MTBF we have the appendix table that gives the values of the A and B for the value of shape parameter $\beta = 3,7$:

$$A = 0,9011$$

$$B = 0,278$$

Finally, the Mean Time Between Failure is:

$$MTBF = A\eta + \gamma = 0,9011 \times 57830 = 52111 \ldots\ldots (2.59)$$

$$MTBF = 52111 \text{ (Hrs)}$$

So we can calculate the reliability the failure rate of the bridge for t=MTBF=52111 (Hrs)

$$R(t = MTBF) = e^{-\left(\frac{52111}{57830}\right)^{3,7}} = 0,5064 \ldots\ldots (2.60)$$

$$\lambda(t = MTBF) = 5,2111 \times 10^{-4}\left(\frac{52111}{57830}\right)^{2,7} = 0,0000482 \ldots\ldots (2.61)$$

2.3.3 Results and discussion:

From the results obtained and after determination of the Weibull parameters, such as the shape parameter $\beta = 3,7$and the scale parameter $\eta = 57830$graphically with the help of the paper of WEIBULL and numerically with the help of Excel $\eta = 57830$ we notice that the mechanism in this case the couple gear-crown is according to the curve in bathtub in the period of old age, the defect develops according to a nonlinear curve and the parameter of form since β is situated between $3 < \beta < 4$ that means that the mechanism is in a state of wear or corrosion.

The study allowed us to calculate the reliability of the mechanism, we arrived at a result:

$$R(t = MTBF) = e^{-\left(\frac{52111}{57830}\right)^{3,7}} = 0{,}5064$$

2.4 RELIABILITY, AVAILABILITY, MAINTAINABILITY (RAM) ENGINEERING*:*

2.4.1 Assessment of RAM parameters:

DuJulio and Leet (1988) have presented space station synergetic RAM-Logististics analysis, this study emphasizes to analyze the maintenance activities and processes that can be accomplished on-orbit within the known design and support constraints of the space station. Wood **(**1989) has developed equations for the availability of a system with exhaustible spares. Terje and Grundt (1989) discussed how catastrophic events should be treated when assessing availability. Bluvband (1990) has presented a technique for tracking the systems availability growth during development and testing so that decision regarding proposed changes can be evaluated**.** Cockerill (1990) has presented a RAM (Reliability, Availability, and Maintainability) analysis of a turbine-generator system. McFadden (1990) has proposed the techniques for developing the database for reliability, availability and maintainability improvement program for an industrial plant or commercial building. Nurie (1990) has discussed that good testability and higher fault coverage tests provide high quality. Without adequate fault coverage, bad parts pass the acceptance test and are installed in the final product, resulting in a product with very low reliability. Mi (1991) has presented a methodology for system, which consists of an independent subsystem connected in series. Prince and Haire (1991) presented some Markov models to evaluate the impact of maintenance system availability on the overall plant. Kumar et al. (1992) have presented some results from an analytic study of reliability and availability of the crystallization system in sugar plants.[21]

2.4.2 Reliability, Availability, Maintainability (RAM) engineering:

RAM analysis is a well-known method of estimating the production availability of a system by assessing failure modes, frequencies and consequences, all the while paying attention to the effect on production. The intention is to find out if the estimated production availability meets the requirements, and to identify the most cost-efficient parameters to help pave the way for an optimum solution in terms of profit.

In this context, the complex of RAM factors constitutes a strategic approach for integrating reliability, availability and maintainability, by using methods, tools and engineering techniques

(Mean Time to Failure, Equipment down Time and System Availability values) to identify and quantify equipment and system failures that prevent the achievement of the productive objectives. The application of such methodologies requires a deep experience and know-how together with the possibility of acquiring and processing data in operating conditions.

2.4.2.1 The definition of Maintainability:

Maintenance involves the different stages of the life cycle of industrial equipment, it allows to ensure a continuity of the production and to reduce the maximum of failures, which occur during the life cycle of the production chain and thus guarantees productivity gains. Its role is appreciable and essential during all the phases of product definition: value analysis, design and feasibility studies, construction and manufacturing, exploitation, disposal.

Maintainability concerns the maintenance action as such. By maintainability, we are looking for the optimization of the intervention time in order to increase the production time by decreasing the delays due to:

- Time for waiting for replacement parts
- Time to complete the documents
- Time to prepare the action

The maintainability can be characterized by its MTTR (Mean Time To Repair), Its index is the MTTR and is calculated as follows:

$$MTTR = \frac{\sum Total\ time\ of\ breaks}{Number\ of\ failures} \ldots\ldots (2.62)$$

Repair rate μ is equal to the unit of time on the MTTR:

$$\mu = \frac{1}{MTTR} \ldots\ldots (2.63)$$

2.4.2.2 The definition of the availability:

The ability of an asset to perform required function under given conditions, at a given time or during a given interval of time, assuming that the supply of the necessary external means is assured. This ability depends on the combination of reliability, maintainability and maintenance logistics. The necessary external means other than maintenance logistics do not affect the availability of the good.

For an equipment have a good availability, it must:

- Have as little downtime as possible.
- Be rapidly repaired if it breaks down.

Availability therefore combines the notions of reliability and maintainability. Increasing availability involves:

- The extension of the MTBF (action on reliability)
- The notion of MTTR (action on maintenance)

2.4.3 Continuous of case study using RAM Engineering:

2.4.3.1 The maintainability:

The maintainability of the bridge can be characterized by its MTTR (Mean Time To Repair), Its index is the MTTR and is calculated as follows:

$$MTTR = \frac{\sum Total\ time\ of\ breaks\ of\ the\ bridge}{Number\ of\ failures} \ldots\ldots (2.64)$$

We placed before the time and the number of the intervention in our Excel file:
So we just applied the equation (2.58) to calculate the maintainability of our bridge:

$$MTTR = \frac{4114}{116} = 35.4655 \ldots\ldots (2.65)$$

$$MTTR = 35hrs$$

Repair rate μ of our bridge is equal to the unit of time on the MTTR:

$$\mu = \frac{1}{35} = 0{,}0286 \ldots\ldots (2.66)$$

2.4.3.2 Availability:

To quantify the Availability, we have two types of Availability to calculate:

2.4.3.2.1 Inherent availability Ai:

The designer has designed and manufactured the product by giving it a certain number of intrinsic characteristics, i.e., characteristics that take into account the conditions of installation, use, maintenance and environment, which are supposed to be ideal.
The calculation of the intrinsic availability Ai uses 3 parameters:

- **TBF**: time of good working order.
- **TTR**: technical repair time.
- **TTE**: technical operating time.

$$A_i = \frac{TBF}{TBF + TTR} \ldots\ldots (2.67)$$

2.4.3.2.2 Operational availability Do:

It is the availability from the user's point of view. This takes into account the actual operating and maintenance conditions. The calculation of Ao uses the same parameters except that these 3

parameters are no longer based on ideal operating conditions but on real conditions (operating history). So, to start our work we have the expression of the availability A(t) is given by:

$$A = \frac{MTBF}{MTBF+MTTR} \ldots\ldots (2.62)$$

We know that: $MTBF = 52111 \quad and \quad MTTR = 35$

we replaced these two expressions in the equation (2.62), we found:

$$A = \frac{52111}{35+52111} \ldots\ldots (2.63)$$

We replaced to have the value of the availability:

$$A = 0{,}9993 \ldots\ldots (2.64)$$

2.5 CONCLUSION:

The reliability study is the indispensable tool for a company to reduce the probable failures of its equipment.

The case study (gear-crown), allowed us to analyze the reliability according to the model of WEIBULL, the reliability was at 50% and the failure rate was at 0,0000482

These results lead us according to the parameter of form β which is located between $3 < \beta < 4$ to make assumptions that these failures of wear are the origin of several factors, thus to know the main problem we must treat each factor using the mechanical aspects so that we can fix one or more assumption and to validate them in order to solve the problem of break of the bridge. As an example, we can say that an overload of the torque (gear-crown) on the engine side one of the factors that can be treated also the problem of modulus or the incorrect using of the material and the heat treatment and so one.

As far as maintenance is concerned, we strongly recommend that maintenance managers apply conditional preventive maintenance by using a verification system after each number of hours of use.

Chapter 3

Material characterization

3.1 INTRODUCTION:

It is primordial to know the mechanical characteristics of the material which the gears are made of, in order to collect the necessary data to proceed the technological study on the gears, especially the gears which present the breakage defect, namely the sintered gear and the crown gear. In this chapter a presentation of the characterization techniques used in this study will be established, along results obtained.

3.2 MATERIAL CHARACTEIZATION:

Characterization, when used in materials science, refers to the broad and general process by which a material's structure and properties are probed and measured. Material characterization enables researchers to determine the structure of a material, how this structure relates to its macroscopic properties, and how it will behave in technological applications. Definitions of what is considered "material characterization" vary, as the term is also used to refer to any materials analysis process, including bulk thermal analysis and density testing. Most of these material characterization techniques can be categorized as either microscopy, macroscopic testing or spectroscopy.

3.2.1 Microscopy:

Microscopy is a category of characterization techniques which probe and map the surface and sub-surface structure of a material. These techniques can use photons, electrons, ions or physical cantilever probes to gather data about a sample's structure on a range of length scales. Some common examples of microscopy techniques include:

- Optical microscopy
- Scanning electron microscopy (SEM)
- Transmission electron microscopy (TEM)
- Field ion microscopy (FIM)
- Scanning probe microscopy (SPM)
    - Atomic force microscopy (AFM)
    - Scanning tunneling microscopy (STM)
- X-ray diffraction topography (XRT)

3.2.2 Macroscopic testing:

A huge range of techniques are used to characterize various macroscopic properties of materials, including:

- Mechanical testing, including: tensile, compressive, torsional, creep, fatigue, toughness and hardness testing
- Differential thermal analysis (DTA)
- Dielectric thermal analysis (DEA, DETA)
- Thermogravimetric analysis (TGA)
- Differential scanning calorimetry (DSC)
- Impulse excitation technique (IET)

3.2.3 Spectroscopy:

Spectroscopy is a category of characterization techniques which use a range of principles to reveal the chemical composition, composition variation, crystal structure and photoelectric properties of materials. Some common examples of spectroscopy techniques include:

3.2.3.1 Optical radiation:

- Ultraviolet-visible spectroscopy (UV-vis)
- Fourier transform infrared spectroscopy (FTIR)
- Spark spectroscopy (SS)
- Thermoluminescence (TL)
- Photoluminescence (PL)

3.2.3.2 X-ray:

- X-ray diffraction (XRD)
- Small-angle X-ray scattering (SAXS)
- Energy-dispersive X-ray spectroscopy (EDX, EDS)
- Wavelength dispersive X-ray spectroscopy (WDX, WDS)
- Electron energy loss spectroscopy (EELS)
- X-ray photoelectron spectroscopy (XPS)
- Auger electron spectroscopy (AES)
- X-ray photon correlation spectroscopy (XPCS)

3.2.3.3 Mass spectrometry

- Modes of mass spectrometry:
    - Electron ionization (EI)
    - Thermal ionization mass spectrometry (TI-MS)
    - MALDI-TOF
- Secondary ion mass spectrometry (SIMS)

3.2.3.4 Nuclear spectroscopy:

- Nuclear magnetic resonance spectroscopy (NMR)
- Mössbauer spectroscopy (MBS)
- Perturbed angular correlation (PAC)

3.3 FRICTION AND WEAR

Wear is inherent to mechanical systems. It is the result of friction between two organs moving relative to each other. It depends on the materials present, the pressure exerted, the nature of the contact and the duration.

In the more or less long term, depending on the previous parameters, friction causes local heating and it is the rise in temperature produced that will accelerate the degradation.

Concretely, wear, with its 2 components (erosion and abrasion), leads to micro-deterioration of the surface by tearing of particles. This impairment results in a dimensional, geometric and structural modification leading mainly to an increase in functional play. By accelerating the degradation by wear of the components present, these alterations can go as far as rupture, passing through dangerous intermediate phases such as increased vibrations.

Wear therefore leads to a loss of material from the surfaces in contact. This mode of failure is inexorable when two surfaces in contact have a relative movement. Tribology is the experimental science that studies these phenomena.

It appears on case-hardened or tempered teeth, inside the metal, between the treated and untreated part. Possible causes are an insufficient thickness of the treated layer or too sudden transition in hardness between treated and untreated layer.

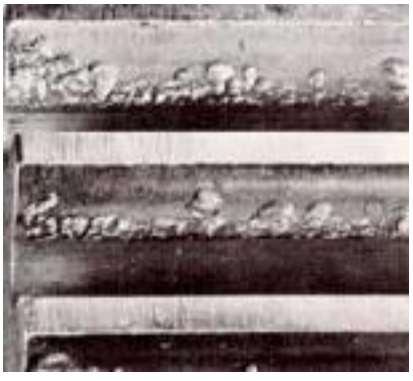

Figure 3-1: appearance of wear on gear teeth

3.3.1 Dynamics of wear and laws of degradation:

The wear is progressive but not constant. It is broken down into 3 phases, each with a different appearance:

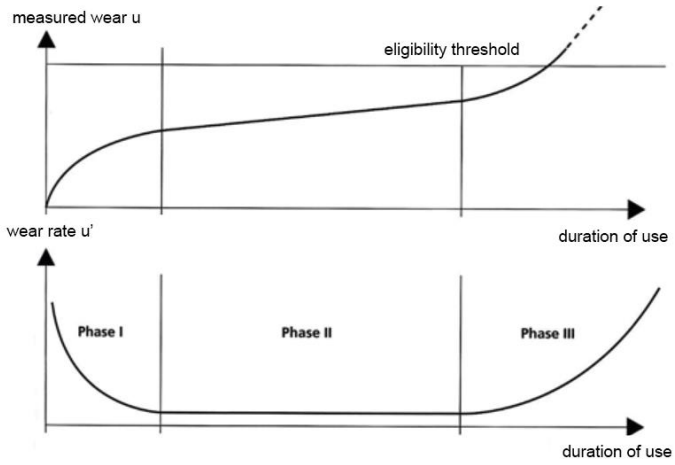

Figure 3-2: wear and wear rate function of duration of use

From 2 initial surfaces:

• **Phase** I: this is the running-in period during which wear is relatively rapid. On microscopic examination, the surfaces show irregularities which are leveled off until a bearing surface corresponding to a balance between material hardness and pressure is obtained. This inevitable phase can be reduced over time by pre-running before use.

• **Phase II:** representative of natural wear, stable and linear over time. Wear is reported mainly on one of the contact surfaces. It is slowed down by lubrication (oil or grease); hence an extension of this use phase.

• **Phase III:** period of accelerated degradation. During this phase, the wear of the surfaces present accelerates under the action of several combined phenomena: amplification of the functional games (vibrations, chattering, shocks, etc.), alteration of the surface treatments intended to increase the hardness superficial, aging of the material by structural modification by the effect of repeated heating. This phase, called the catastrophic wear phase, consists of particulate emissions. This debris causing plowing of the softest surface and rapid degradation. The analysis of lubricants highlights this succession of phases by characterizing the number and the increasing size of the metal particles released.

3.3.2 Wear prevention:

There are 4 ways to prolong phase II of normal wear and operation: greasing and lubrication, use of anti-friction materials, heat treatments and surface coatings, technological rules.

3.3.2.1 Greasing and lubrication:

Greasing and lubrication are the simplest means of application and also the most economical. However, they require permanent and continuous attention and, in some cases, require access to the parts to be lubricated.

By placing a film with a low coefficient of friction between the moving parts, greasing and lubrication provide 4 functions:

• reduction of friction and therefore limitation of erosion,

• evacuation of particles promoting abrasion,

• removal of heat caused by friction,

• insulation from the surrounding environment which can induce corrosion

3.3.2.2 Anti-friction materials:

There are several kinds. The most common are copper alloys: bronze (copper-tin), brass (copper-zinc), nickel silver (copper-nickel-zinc). With sometimes an addition of cadmium and/or antimony, these alloys have a relatively low coefficient of friction, thus reducing the phenomenon of wear.

Ceramics which are oxides, carbides or nitrides, have qualities of hardness, resistance to extreme temperatures and chemical resistance. They are an effective way to fight against abrasion, wear at all temperatures and corrosion.

Sintered materials, the most commonly used of which are copper- or iron-based sinters, can be impregnated with oil. Then qualified as self-lubricating, the particles that compose them expand during the heating created by friction and expel the oil they contain. During cooling, by reverse effect, they suck the oil into their structure.

Composite materials allow so-called dry friction thanks to their excellent resistance to seizing. They are now more and more resistant to mechanical stresses. They can thus be used for the production of complex parts. A composite material can be made up of a material having excellent mechanical characteristics at the core for the resistance and rigidity of the part and at the periphery of another material improving the behavior in the face of friction.

Plastics such as PTFE (polytetrafluoroethylene), PA (polyamides), polyimides, Teflon, PVCU (rigid polyvinyl chloride), allow, among other things by their ease of implementation and their low cost, the construction of all kinds of parts such as gears, pump vanes, axles, etc.

3.3.2.3 Surface treatments and surface coatings:

Surface treatments and coatings essentially aim to increase the surface hardness of a part. Surface treatments such as cementation, surface hardening, nitriding, hard chromization, induction heating are thermal processes that are relatively simple to implement and of very suitable efficiency.

Other treatments, rather mechanical, such as sandblasting, shot-blasting, micro blasting, hammering, burnishing also offer an increase in fatigue resistance by slowing down the formation of cracks.

Pure and simple machining, because it creates surface hardening, also improves wear resistance.

Surface coatings such as sulfurization, plating, allow to obtain surfaces of greater plasticity without altering the resistance to wear. Although generally more complex than the previous treatments, they offer the advantage of allowing the deposition of pure metals (aluminum or titanium which also act against ageing; tantalum, chromium, cadmium, etc.) as well as that of alloys or metal-metalloid compounds (titanium nitride, silicon carbide, alumina, manganous sulfate, etc.). In addition, many types of support can benefit from it: steels, light alloys, copper alloys, but also materials as different as glass or plastics.

A metal surface can also be coated with anti-friction materials such as PTFE, nylon or even Teflon.

3.3.2.4 Technological rules:

The importance of the friction is all the less great as the materials present are more difficult to weld one into the other. This is called friction torques based on the compatibility of metals.

The technological rules preside over the designs and also take into account the orientation of the machining grooves which can favor the elimination of particles, the shapes of the parts, the cooling of the part supposed to store the most heat, etc. These rules, which are generally simple and very effective, are often overlooked.

For example, to reduce the phenomenon of wear, it is necessary to make rub the most different possible structures, or even, to cross the lines of machining.

3.4 CHARACTERIZATION OF THE SINTERED GEAR:

Due to lack of material and time requirements, two types of characterization were performed on the sintered gear, which are:

- Spark spectroscopy, in order to determine the chemical composition of the material.

- Brinell hardness testing, in order to determine the hardness of the material.

3.4.1 Spark spectroscopy:

Spectroscopy, a field of study that uses light absorption and emission patterns to characterize matter, is divided into a range of specialty areas. Spark Spectroscopy is one of the most useful, with high sensitivity and fast analysis times making it the technique of choice for a variety of applications.

3.4.1.1 The fundamentals of Spark Spectroscopy:

As the name suggests, Spark Spectroscopy relies on electromagnetic radiation created by a spark. This spark is generated by creating a reaction between a sample and a counter-electrode, which excites atoms and ions and forces them to move to a higher energy state. When the atoms and ions return to their ground state, they release what's known as a discharge plasma. This plasma is ignited and emits a unique emission spectrum that can be used to detect and quantify individual elements present in the sample.

Figure 3-3: Spark spectroscopy fundamental reaction

As well as detecting metals and semimetals, Spark Spectroscopy can be used to identify non-metals such as oxygen, nitrogen, carbon, sulphur and phosphorous. With specialized instruments, these can be detected and quantified based on distinctive wavelength signatures.

3.4.1.2 Applications of Spark Spectroscopy:

Spark Spectroscopy is a versatile technique used across a wide range of industries and sectors. Compared to other techniques, Spark Spectroscopy offers excellent accuracy and low cost of operation.

3.4.1.2.1 Quality control for metal production and processing:

The ability to quickly detect a wide range of metals makes Spark Spectroscopy especially useful in the metal production and processing sector. The technique is used during quality control processes and to detect and quantify metals such as iron, cobalt, aluminum, magnesium, copper, nickel, lead, titanium and zinc in secondary raw materials. Information is used to determine the value of a product and its suitability for different applications.

3.4.1.2.2 Environmental analysis:

Trace elements can have a significant impact on soil quality, making Spark Spectroscopy a valuable tool used by environmental scientists. The most advanced spark emission spectrometers offer a spectral range as high as 780nm, making them capable of detecting even the smallest concentrations.

3.4.1.2.3 Water quality monitoring:

As well as analyzing soils, Spark Spectroscopy is used to monitor the quality of water sources and detect contaminants such as heavy metals. With some spark emission spectrometers offering results in as little as 10 seconds, the technique is ideal for in-field sampling and analysis.

3.4.1.3 Spectrometer:

The equipment we used to process the chemical composition characterization of the sintered gear is the ARUN technology metal scan: PolySpec Neo.

The PolySpek Neo is the new multi-CCD, multi-optic desktop spectrometer from ARUN Technology, the originators of CCD based metals analysis. Almost 30 years of CCD - OES know-how have gone into the design of the new PolySpek Neo. Up to four separate optical systems can be incorporated to cover the emission spectrum required for metallurgical work, which conventionally lies between 130 and 680 nanometers. Particular combinations of the optical systems are available for specific single matrix or multi-matrix applications. The optical systems have been tailored to provide different dispersions over different wavelength ranges, with the optimal resolution in the ultraviolet region of 130 to 200 nanometers. Less resolution is required in the infrared region between 470 and 680 nanometers where only a few key emission lines need to be resolved. Neither optical fibers, nor vacuum pumps are used in the PolySpek Neo and only the ultraviolet optical section (if required) is Argon (optionally Nitrogen) purged.

Figure 3-4: PolySpec Neo spectrometer

The PolySpek Neo is capable of analyzing almost any element in any metal. For many metals and their alloys, the spectrometer offers standard calibrations. Currently available calibrations for the PolySpek Neo are:

- Iron & Steel alloys
- Cast Iron
- Aluminum and its alloys
- Zinc and its alloys
- Copper and its alloys
- Nickel and its alloys
- Cobalt and its alloys
- Titanium and its alloys
- Magnesium and its alloys
- Lead and its alloys
- Tin and its alloys.

With all results showing directly in a material composition table on the computer screen, as PolySpec Neo is controlled with an external PC as supports a keyboard-mouse operation via USB connection and propose a series of different programs to choose from depending on the material we are analyzing.

3.4.1.4 Process:

The process of the analysis is relatively simple. It requires at first to cut out a sample in the form of a medal so that it can be integrated under the tungsten electrode.

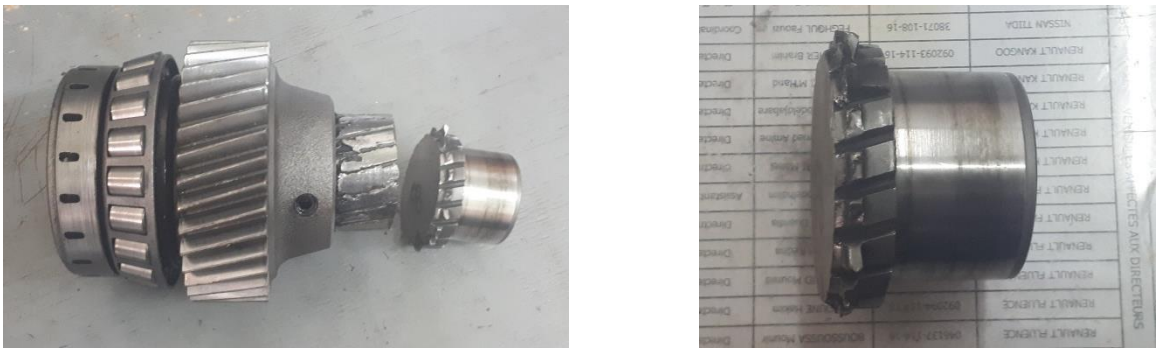

Figure 3-5: Sample cut.

It is then sufficient to fix it under the tip of the electrode and to choose the type of program to be carried out according to the type of metal to be analyzed and start the analysis.

Figure 3-6: traces of spark spectrometry

3.4.1.5 Results and comments:

The results of the different chemical components ratios analysis are displayed on the table of the spectrometer computer screen as it follows:

Material	C	Si	Mn	S	Cr	Ni	Mo	Ti
%	0.17	0.23	0.94	0.045	1.05	1.09	0.11	0.11

Table 3-1: Chemical composition analysis results

From where we can determine the material of the sintered gear and which is:

17Cr4Ni4Mn4

We notice that this steel has a low alloys density.

3.4.2 Brinell hardness testing:

Hardness is a characteristic of a material, not a fundamental physical property. It is defined as the resistance to indentation, and it is determined by measuring the permanent depth of the indentation.

More simply put, when using a fixed force (load) and a given indenter, the smaller the indentation, the harder the material. Indentation hardness value is obtained by measuring the depth or the area of the indentation using one of over 12 different test methods.

The **Brinell hardness test method** as used to determine Brinell hardness, is defined in ASTM E10. Most commonly it is used to test materials that have a structure that is too coarse or that have a surface that is too rough to be tested using another test method, e.g., castings and forgings. Brinell testing often use a very high-test load (3000 kgf) and a 10mm diameter indenter so that the resulting indentation averages out most surface and sub-surface inconsistencies.

The Brinell method applies a predetermined test load (F) to a carbide ball of fixed diameter (D) which is held for a predetermined time period and then removed. The resulting impression is

measured with a specially designed **Brinell microscope** or **optical system** across at least two diameters – usually at right angles to each other and these results are averaged (d). Although the calculation below can be used to generate the Brinell number, most often a chart is then used to convert the averaged diameter measurement to a Brinell hardness number.

Common test forces range from 500kgf often used for non-ferrous materials to 3000kgf usually used for steels and cast iron. There are other Brinell scales with load as low as 1kgf and 1mm diameter indenters but these are infrequently used.

Typically, the greatest source of error in Brinell testing is the measurement of the indentation. Due to disparities in operators making the measurements, the results will vary even under perfect conditions. Less than perfect conditions can cause the variation to increase greatly. Frequently the test surface is prepared with a grinder to remove surface conditions.

The jagged edge makes interpretation of the indentation difficult. Furthermore, when operators know the specifications limits for rejects, they may often be influenced to see the measurements in a way that increases the percentage of "good" tests and less re-testing.

Two types of technological remedies for countering Brinell measurement error problems have been developed over the years. **Automatic optical Brinell scopes**, such as the **B.O.S.S. system**, use computers and image analysis to read the indentations in a consistent manner. This standardization helps eliminate operator subjectivity so operators are less-prone to automatically view in-tolerance results when the sample's result may be out-of-tolerance.

Brinell units, which measure according to ASTM E103, measure the samples using Brinell hardness parameters together with a **Rockwell hardness method**. This method provides the most repeatable results (and greater speed) since the vagaries of optical interpretations are removed through the use of an automatic mechanical depth measurement.

Using this method, however, results may not be strictly consistent with Brinell results due to the different test methods – an offset to the results may be required for some materials. It is easy to establish the correct values in those cases where this may be a problem.

Brinell hardness testing machine:

The Brinell hardness test method often presents some challenges for users. Poor operating conditions, inexperienced users, tedious high-volume testing and demanding applications contribute to reduce accuracy and repeatability.

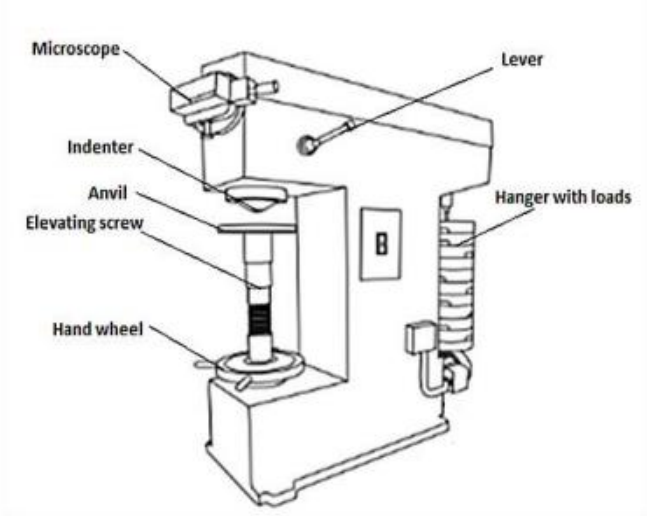

Figure 3-7: Brinell testing machine diagram

A well-structured Brinell hardness number reveals the test conditions, i.e., "70 HB 10/500/30" which means that a Brinell Hardness of 70 was obtained using a 10mm diameter hardened steel ball with a 500 kilogram load applied for a period of 30 seconds. Highly hardened steel cannot be tested by a hardened steel ball because the ball will get flattened and become permanently deformed. The appreciable error in BHN occurs at indentation diameter less than 2.9mm and for softer materials inaccuracy is at diameter greater than 6mm. On tests of extremely hard metals a tungsten carbide ball is substituted for the steel ball (up to 444-627 HB) and a special hardened and burnished steel ball called the "Hulked" ball may be used up to 500 HB.

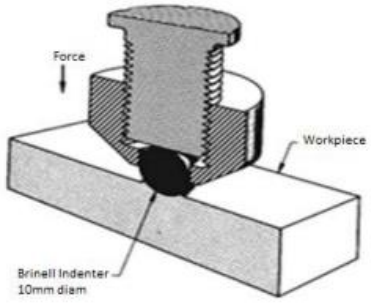

Figure 3-8: Brinell hardness test indenter illustration

Compared to the other hardness test methods, the indenter used in Brinell makes the deepest and widest indentation, so that test averages the hardness over a wider number of materials which will accounts for multiple grain structures and any irregularities in the uniformity of the material.

The Brinell hardness number is defined as the ratio of test load to the surface area of indentation:

$$HBW = \frac{2P}{\pi D[D - \sqrt{(D^2 - d^2)}]} \quad \ldots\ldots (3.1)$$

Where:

P: Load (Kg)

HBW: Brinell hardness number (Kg/mm^2)

D: diameter of the ball (mm)

d: diameter of the indentation (mm)

3.4.2.1 Process:

The process of the Brinell hardness testing is detailed in the following steps:

1. Select the load P based on the type of material selected.
2. The sample is placed on the supporting table, then the hand wheel below the table is turned in clockwise direction until the gap between the surface of the specimen and the indentor is 5 mm.
3. The motor is switched on. The hand lever is pulled into load position. The load is applied for a period of 10 to 15 seconds.
4. The hand lever is pulled back into unload position. The diameter of the impression is measured through a microscope attached to the apparatus.
5. Repeat the experiment at other positions of the test piece.
6. Calculate the value of HB.

The following figure shows the Brinell test traces on the shaft of the sintered gear where hardness was measured:

Figure 3-9: Brinell hardness test traces

3.4.2.2 Results and comments:

The hardness was measured at 447 HB on the shaft which corresponds according to the conversion table (see appendix) to 54.7 HRC.

Plus that, the sintered gear and the crown undergo a heat treatment at heart of a quenching at 850°C and a tempering at 250°C and the teeth undergo a thermochemical treatment, namely carburizing of a hardened layer ranging from 0.5 to 1.5 mm.

3.5 CONCLUSION:

In this chapter, we could determine two very important material characteristics of the sintered gear that are the hardness of the material and its chemical composition.

the determination of these two parameters is a key step to determine other parameters needed to proceed the verification calculations on the bridge and more precisely the sintered gear and that by using charts and the appropriate documentation.

In the next chapter this verification calculations will be presented along all the data needed and determined from the results of this chapter

Chapter 4

Verification of the surface pressure and the tensile strength of the sintered gear and crown couple of the bridge

4.1 INTRODUCTION

Gear is most essential element of power transmission prefer for short distance. It is very economical and very effective way of power transmission .it is used almost all engineering purpose for power transmission. A gear is a machine element designed to transmit force and motion from one mechanical unit to another.[1]According to the vision report of the gear industry[2], are mostly used in in automotive, aerospace or marine industry. Their application ranges from simple, e.g. in household appliances, to complex example.in industrial or power generating plants. Complete understanding of their performance can contribute to improved design, manufacturing and maintenance process of gears. All of that can help in reducing failures of gears that make up about 10% of all failures of rotating machinery.[3]

Gears can and do fail in service for a variety of reasons. In most cases, except for an increase in noise level and vibration, total gear failure is often the first and only indication of a problem. Many modes of gear failure have been identified, for example fatigue, impact, wear or plastic deformation. For these, Contact fatigue is one of the most common wear modes for gear tooth surfaces [4] and, generally, two types of surface contact fatigue exist in gears pitting and spalling [5]. Recently, there has been considerable effort in trying to investigate gear failures and most of the causes fall into spalling or pitting occurrence and subsequent wear, damage and failure. This is especially true for example carburized gears where fatigue induced defects initiate at subsurface instead of surface[6],[7] which aids pitting and cracking process and the rolling contact surface fatigue can lead to final failure [8]. Failure analysis of a gear in the gearbox showed that the teeth failed because of a crack initiated from pitting and spalling region[9]. This pitting and spalling were a consequence of gear misalignment. Premature failure of an industrial mixer timing gears was found to be the result of surface hardness deficiencies of the gear leading to severe pitting and final failure.[10]

These Failures are most commonly caused by excessive wear and damage of gear teeth. Extreme loading, insufficient lubrication and/or gear shafting misalignment, include also poor design of the gear set, inadvertent stress raisers or subsurface defects in critical areas, and the use of incorrect materials and heat treatments. In this chapter we are going to represent the verifications of the two most important criteria for calculating spur gears at surface pressure and at failure to know the main problem of the failure is present in the fretted gear on the gearbox of the bridge, if it is incorrect using of material which means the verification of its resistance is it enough to can handle the overload on the tramway?

4.2 THE DATASHEET OF THE BRIDGE:

Now, to build the datasheet of our bridge we have to use the data given by CITAL Company:

4.2.1 The common data:

Pressure angle: $\alpha = 20°$.

4.2.2 The geometric data:

The gearbox is composed of two sides:

4.2.2.1 Motor side:

we have three couples of gears:

4.2.2.1.1 Motor gear-wheel gear 58 teeth:

Gear designation	Teeth number	Outside diameter (mm)	Width (mm)
Motor gear	19	79,5	40
Wheel gear '58'	58	214	40

Table 4-1: Motor gear and wheel gear '58' data

4.2.2.1.2 Wheel gear 57 teeth- sintered gear (36 teeth side):

Gear designation	Teeth number	Outside diameter (mm)	Width (mm)
Wheel gear '57'	57	214	40
sintered gear (36 teeth side)	36	140,5	42

Table 4-2: Wheel gear '57' and sintered gear (36 teeth side) data

4.2.2.1.3 Sintered gear (19 teeth side)-crown gear:

Gear designation	Teeth number	Outside diameter (mm)	Width (mm)
Sintered gear (19 teeth side)	19	79,5	42
Crown gear	69	255	40

Table 4-3: Sintered gear (19 teeth side) and crown gear data

4.2.2.2 Brake side:

we have here just one couple*:*

4.2.2.2.1 Sintered gear (19 teeth side)-crown gear:

Gear designation	Teeth number	Outside diameter (mm)	Width (mm)
Sintered gear (19 teeth side)	19	79,5	42
Crown gear	69	255	40

Table 4-4: Sintered gear (19 teeth side) and crown gear data (Brake side)

4.2.3 Technical data of the engine:

Traction motor type designation	4 HGA 1433
Technology	Asynchronous
Power rating	120 kW at 2600 rpm
Continuous torque	440 N.m
Mechanical transmission	Gear
Cooling system	Water-cooled
Closed/Open	Closed
Outline: width x height x length (mm)	400 x450 x528
Weight (kg)	335

Table 4-5: Technical data of the engine

4.2.4 Characteristics of the used material:

4.2.4.1 General overview:

Low alloy steel (0.17% Carbon, 1.2% Chromium) for case hardening. Commonly used material for the manufacture of mechanical parts, it has a high impact and deformation resistance, and is not recommended for welding. Preferred use in low temperature environment. Areas of application: general and specialized mechanical industry is used for high loaded parts in the vehicle and mechanical engineering with high demands on toughness and core strength (e.g. gear parts, drive pinions).[11]

4.2.4.2 Chemical analysis:

As described in the previous chapter, we have:

Material	C	Si	Mn	S	Cr	Ni	Mo	Ti
%	0.17	0.23	0.94	0.045	1.05	1.09	0.11	0.11

Table 4-6: Chemical composition of the used material (17Cr4Ni4Mn4)

4.2.4.3 Mechanical Properties:

Variant	Condition	Dimension [mm]	Yield strength min [MPa]	Tensile strength [MPa]	Elongation A_5[%]	Hardness (HB)	Density [kg/m^3]
Sintered Gear	QT	50<100 $D_1 = 79.5$	750	1420	10	447	7800
Crown gear		>200 $D_2 = 255$	750	1180	10	447	7800

Table 4-7: Mechanical Properties of the used material (17Cr4Ni4Mn4)

4.2.4.4 Other properties (typical values):

Variant	Young Module [GPa]	Poisson's ration	Shear Module [GPa]	Density [kg/m^3]	Specific heat capacity 50/100°C [J/kg.°K]	Thermal conductivity ambient temperature [W/m°K]	Electrical resistivity Ambient temperature [$\mu\Omega m$]
Sintered gear	210	0.3	80	7800	460-480	40-45	0.20-0.25
Crown gear	210	0.3	80	7800	460-480	40-45	0.20-0.25

Table 4-8: Other properties of the used material (17CrNi4Mn4)

The kinematic chain of the bridge:

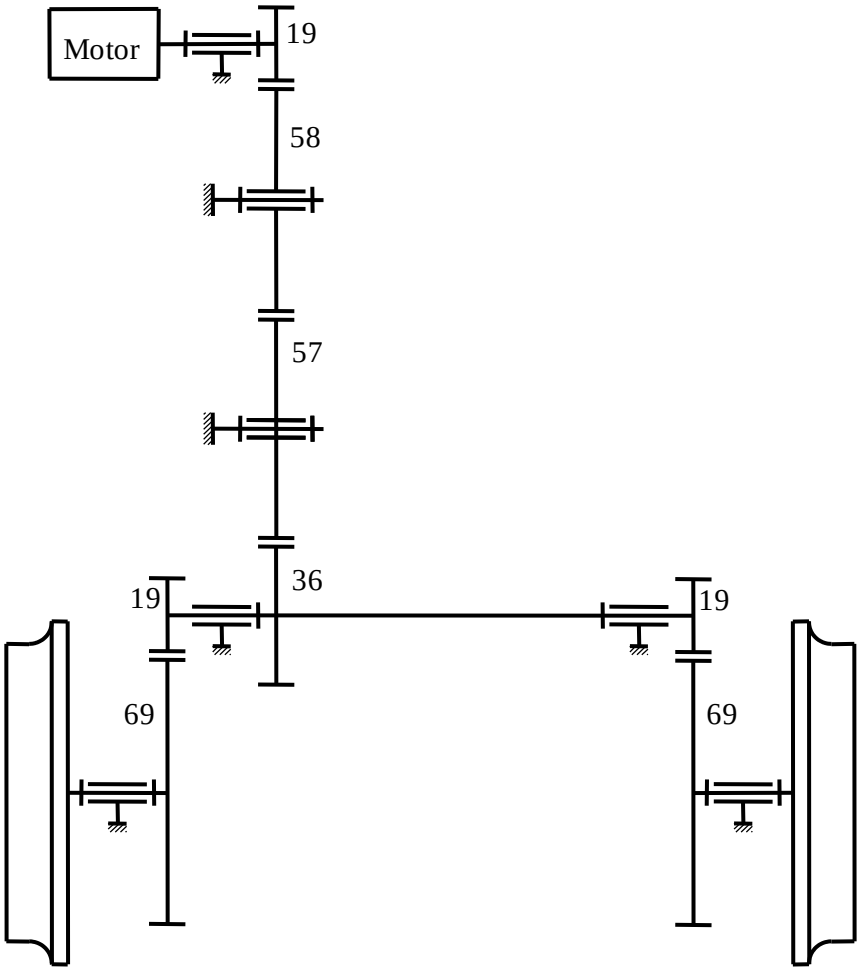

Figure 4-1: The kinematic chain of the bridge

Description:

The set of components of the bridge allowing the movement of this one is called "kinematic chain". To make it simple, this chain consists of the engine, the gearbox which contains 4 pairs of gears: the engine gear which meshes with the 58 teeth wheel, the 57 wheel with the 36 teeth sintered gear and the 19 teeth sintered gear with the crown wheel in both (engine side and brake side), finally we have wheels in both engine and brake side, the pivot link is the only link is presented in this chain.

Note: *All wheel axles in the chain are in the same vertical plane.*

4.3 Sizing of the cinematic chain:

After building the datasheet of our bridge we can start the sizing. Calculation of the pitch angle and the modulus of a cylindrical helical gear are presented in the following:

4.3.1 Leading Helix Angle

Figure 4-2 shows the head circle development of a gear in the reduction gearbox of the streetcar. The inclined lines in bold lines are the traces of the head thickness. These lines are also the development of the head helix.

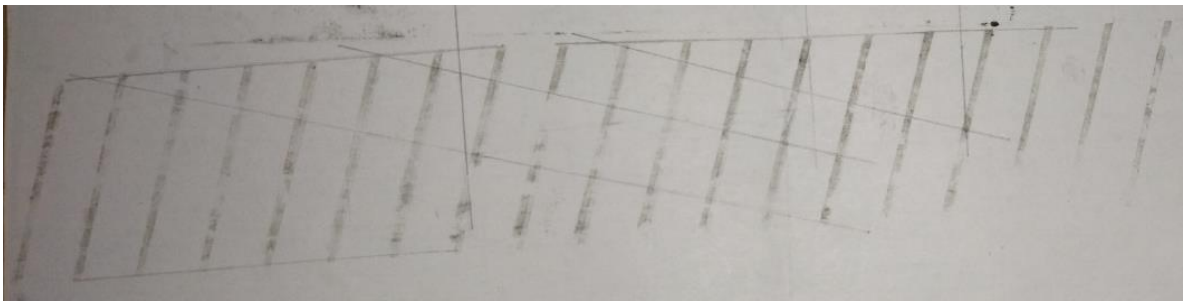

Figure 4-2: Development of the head circle of a gear of the streetcar gearbox

Their inclination with reference to the axis of the part is the head helix angle. To determine this angle, we construct a triangle ABC rectangular at B (Figure 4-3). We have:

$$\mathrm{tg}\beta_a = \frac{BC}{AB}$$

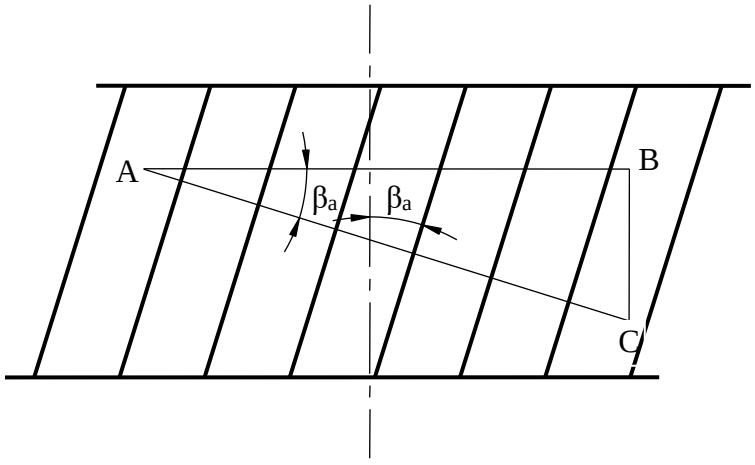

Figure 4-3: Method for determining the head helix angle

We determine the angle βa by constructing AC perpendicular to the expanded helix.
We construct three triangles considering three different helices, which gives βa1, βa2, βa3. We then take their average. Their values are:

$$\beta_{a1} = 15{,}3575° \;\; ; \;\; \beta_{a2} = 15{,}7808° \;\; ; \;\; \beta_{a3} = 15{,}5000°$$

Which gives:

$$\beta_a = 15{,}5461°$$

4.3.2 The pitch angle:

Knowing the rated power of the engine and the characteristics of the gear, we calculate the modulus by the relation:

$$m_n \geq 10^3 \sqrt{\frac{11P\cos\beta}{k\sigma_p Z\omega}} \ldots\ldots (4.1)$$

With:

- The practical failure strength is given by: $\sigma_p[\text{Mpa}] = \frac{\sigma_{\text{failure}}}{s}$ (s is the security coefficient)
- Tooth width coefficient is: $k[mm] = \frac{b}{m_n}$ (b is the tooth width [mm]).
- β (°) is pitch helix angle.
- $\omega = \frac{\pi N}{30}$ Is angular velocity [rad/s].
- P : Puissance (W) au pignon endommagé
- Z : Nombre de dents de ce pignon.

It comes:

$$m_n^3 = 10^3 \frac{11P\cos\beta}{\frac{b}{m_n}\sigma_p Z\omega} \ldots\ldots (4.2)$$

Then:

$$m_n^2 = 10^3 \frac{11P\cos\beta}{b\,\sigma_p Z\omega} \ldots\ldots (4.3)$$

This gives:

$$m_n = \sqrt{10^3 \frac{11P\cos\beta}{b\,\sigma_p Z\omega}} \ldots\ldots (4.4)$$

Knowing the head diameter (da) and assuming that the gear is without offset (offset coefficient x=0), the modulus can also be given by the relation:

$$m_n = \frac{d_a\cos\beta}{Z+2\cos\beta} \ldots\ldots (4.5)$$

We have then:

$$10^3 \frac{11P\cos\beta}{b\sigma_p Z\omega} = \left(\frac{d_a \cos\beta}{Z+2\cos\beta}\right)^2 \ldots\ldots (4.6)$$

So:

$$10^3 \frac{11P}{b\sigma_p Z\omega} = \left(\frac{d_a}{Z+2\cos\beta}\right)^2 \cos\beta \ldots\ldots (4.7)$$

Developing this equation, we have:

$$11x10^3 P(Z + 2\cos\beta)^2 = b\sigma_p Z\omega d_a^2 \cos\beta \ldots\ldots (4.8)$$

$$Z^2 + 4\cos^2\beta + 4Z\cos\beta = \frac{b\sigma_p Z\omega d_a^2}{11x10^3 P}\cos\beta \ldots\ldots (4.9)$$

Hence the second-degree equation in $\cos(\beta)$:

$$4\cos^2\beta + Z\left(4 - \frac{b\sigma_p \omega d_a^2}{11x10^3 P}\right)\cos\beta + Z^2 = 0 \ldots\ldots (4.10)$$

We put:

$$x = \cos\beta \;;\; A = 4 \;;\; B = Z\left(4 - \frac{b\sigma_p \omega d_a^2}{11x10^3 P}\right) \;;\; C = Z^2$$

The 2nd degree equation is therefore:

$$Ax^2 + Bx + C = 0 \ldots\ldots (4.21)$$

The discriminant value is: $\Delta = B^2 - 4AC$

The solutions are: $x_{1,2} = \frac{-B \pm \sqrt{\Delta}}{2A}$

We use a MATLAB program to calculate these solutions.

The solutions where $x < 0$ or $x > 1$ are denied

The damaged gear and the 36-tooth gear are mounted on the same drive shaft. Their rotational speeds are therefore the same. The drive train (Figure 4-1) can be used to calculate the transmission ratio. We note by Ni the speed of rotation of the gear i. Let N5 be the speed of the sintered gear.

We know that for an ordinary gear train, the transmission ratio is expressed by the following expression:

$$r = \frac{No}{Ni} = (-1)^n \frac{Product\ of\ driving\ wheels}{Product\ of\ driven\ wheels} \ldots\ldots \qquad (4.30)$$

With:

- No: output speed
- Ni: input speed

- n: Number of outside contacts

Let's apply this expression to shaft.

- The number of external contacts between gear 19 and wheel 36 is 3.

The transmission ratio between the motor and the drive shaft is:

$$r = \frac{N_o}{N_i} = (-1)^3 \frac{19x58x57}{58x57x36} = -\frac{19}{36}$$

- The sign (-) means that the drive shaft rotates in the opposite direction to the motor.

In arithmetic value, the speed of the drive shaft is:

$$N_o = 2600x\frac{19}{36} \cong 1372{,}2 \text{ tr/mn}$$

We have: $N_o = N_4 = N_5 = 1372{,}2$ tr/min

The angular velocity is therefore: $\omega = \frac{N_5}{30} = \frac{\pi.1732{,}22}{30} = 143.7 \text{ rd/s}$

On the other hand, the driving power is distributed between the two wheels. So we have :

$$P = \frac{\text{driver power}}{2} = \frac{120000}{2} = 60000W$$

The solution to be retained is the one corresponding to: $\beta < \beta_a = 15, 5461°$.

The safety coefficient s is not known. It is determined by respecting the condition $\beta < \beta_a$.

Figure 4-4: Pitch helix angle function of safety coefficient

To do this, we choose it using the graph β=f(s).

From this graph, we have:

$$S_{min} = 1{,}7255 \; ; S_{max} = 1{,}7786$$

The average value is: $S_{moy} = \frac{s_{min} + s_{max}}{2} = \frac{1{,}7255 + 1{,}7786}{2} \cong 1{,}7521$

For this value, the helix angle from the function β = f(s) is: β = 10,990°

4.3.3 The real modulus for this value:

The primitive helix angle being known, we determine the real modulus by calculating first the primitive diameter, we have:

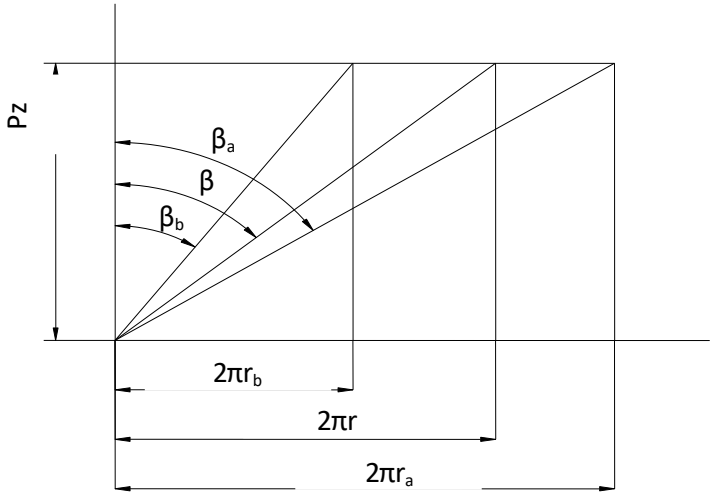

Figure 4-5: The helical pitch Pz of the helical cylinder

From this figure we can notice that the helical pitch Pz is the same for all helices on the helical cylindrical gearing. We then have:

$$tg\beta_b = \frac{2\pi r_b}{P_z} \; , tg\beta = \frac{2\pi r}{P_z} \; , tg\beta_a = \frac{2\pi r_a}{P_z} \ldots\ldots (4.32)$$

$$P_z = \frac{2\pi r_b}{tg\beta_b} = \frac{2\pi r}{tg\beta} = \frac{2\pi r_a}{tg\beta_a} \ldots\ldots (4.43)$$

$$tg\beta_b = \frac{r_b}{r} tg\beta \;\; and \;\; tg\beta_a = \frac{r_a}{r} tg\beta$$

From these equations we can calculate the pitch diameter:

$$r = r_a \frac{tg\beta}{tg\beta_a} \qquad \Rightarrow \qquad d = d_a \frac{tg\beta}{tg\beta_a}$$

The numerical application gives: $d = 79{,}5 \frac{tg10{,}9651^\circ}{tg15{,}5461^\circ} = 55{,}499 mm$

The real modulus calculated is: $m_n = \frac{d cos\beta}{Z} = \frac{55{,}368 x cos 10{,}9651^\circ}{19} = 2{,}867 mm$

Common standard modulus	
Principal serial	1 ; 1,25 ; 1,5 ; 2 ; 2,5 ; 3 ; 4 ; 5 ; 6 ; 8 ; 10 ; 12 ; 16 ; 20
secondary serial	1,125 ; 1,375 ; 1,75 ; 2,25 ; 2,75 ; 3,50 ; 4,50 ; 5,50 ; 7 ; 9 ; 11 ; 14 ; 18
Exceptional serial	0,75 ; 3,25 ; 3,75 ; 6,50

Table 4-9: The common standard modulus

The second highest normalized modulus is:

$$m_n = 3{,}0 \text{ mm (principal serial)}$$

The final pitch diameter is therefore:

$$d = \frac{m_n}{\cos\beta} Z = \frac{3}{\cos 10{,}9961°} x19 = 58{,}065 \text{ mm}$$

The projection height is:

$$h_a = \frac{d_a - d}{2} = \frac{79{,}5 - 58{,}066}{2} = 10{,}718 \text{ mm}$$

As: $h_a = m_n (1 + x)$

The offset coefficient is equal to :

$$x = \frac{h_a}{m_n} - 1 = \frac{10{,}717}{3} - 1 = 2{,}573$$

This is an **erroneous offset factor**. The value of the primitive helix angle is therefore not appropriate. Let's increase it. To do this, let's decrease the safety coefficient s.

4.3.4 The choice of the safety coefficient:

From the graph $\beta = f(s)$, the primitive helix angle increases as the security coefficient decreases, but it must remain less than that of the leading helix $\beta_a = 15{,}5461°$.

We also note that for $s \geq s_{moy}$. The primitive helix angle is not suitable. We choose a portion of the graph $\beta = f(s)$ respecting $\beta < \beta_a$ and $s < s_{moy}$. The curve below shows the variation of β for $s = 1{,}728$ to $1{,}754$.

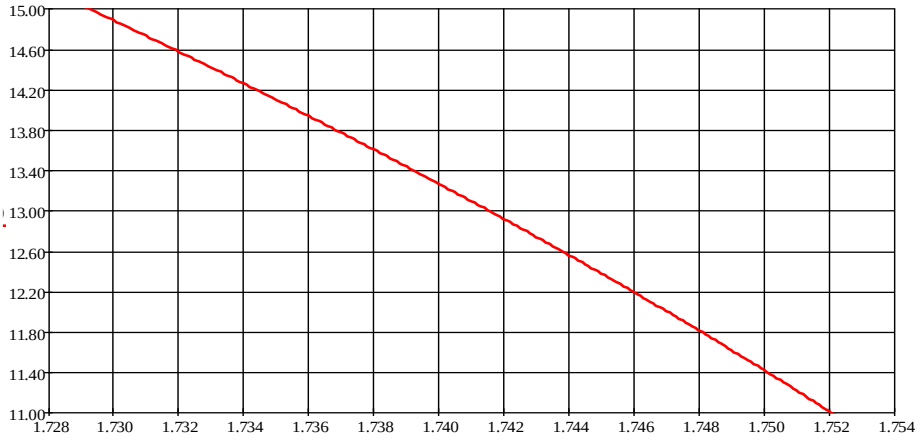

Figure 4-6: Retained safety coefficient

The following table gives the values of the safety factor s that may be appropriate. Using the standard secondary series modulus of 3,5 and the standard exceptional series modulus of 3,75. s can be taken as 1,646 or 1,647.

Safety coefficient	Angle bêta (°)	Real modulus m_n (mm)			Offset Coefficient	Observation
		Calculated	Normalized	Serial		
1,730	1,730	3,862	4	Principal	–0,892	Refused
1,732	1,732	3,784	4	Principal	–0.878	Refused
1,734	1,734	3,703	3,75	Exceptional	–0,202	Retained
1,736	1,736	3,621	3,75	Exceptional	–0,188	Retained
1,738	1,738	3,537	3,75	Exceptional	–0,174	Retained
1,739	1,739	3,494	3,50	Secondary	0,590	Retained
1,740	1,740	3,450	3,50	Secondary	0,597	Retained
1,742	1,742	3,361	3,50	Secondary	0,611	Retained
1,744	1,744	3,270	3,50	Secondary	0,624	Retained
1,746	1,746	3,176	3,25	Exceptional	1,512	Refused

Table 4-10: The values of the safety factor s that may be appropriate

Retained modulus:

The sizing of gears couples with the modulus of 3,75 mm showing that, in several cases the offset coefficient is inacceptable. The table below shows that the modulus of 3.75 mm with the helix angle of 13.6009° lead, in general, to unacceptable offset coefficients. The modulus and the primitive helix angle to be retained are therefore:

$$m_n = 3{,}5 \text{ with } s = 1{,}739 \; and \; \beta = 13{,}4325°.$$

Couple of gears	β = 13,6009° ; m_n = 3,75 mm		β = 13,4325° ; m_n = 3,50 mm	
	x_1	x_2	x_1	x_2
19x58	–0.174	–2.303	0,590	–0.244
57x58	–1.789	–2.303	0,270	–0.244
36x57	–0.786	–1.789	0,565	0,270
19x69	–0,174	–2.495	0,590	–0,042

Table 4-11: Comparison between couple of gears at the value of the offset coefficient with $m_n = 3{,}75$ and $m_n = 3{,}5$

4.3.5 Calculation of geometric elements:

4.3.5.1 Calculation of the minimum width coefficient:

For a helical cylindrical gear**:** $k = \frac{b}{m_n} = \frac{47}{3{,}5} = 13{,}43$

For the rest of the calculations, we take: k=14

4.3.5.2 Apparent modulus (mm):

We know that:

$$m_t = \frac{m_n}{cos\beta} \ldots\ldots (4.55)$$

We replace the value of: $m_n = 3{,}5 \; and \; \beta = 13{,}4325$

So:

$$m_t = \frac{3{,}5}{cos\,(13{,}4325)}$$

$$m_t = 3,\ 5984 \text{ mm}$$

Now we have the different geometric elements for the sintered gear summarized in the below table:

Characteristic element	**formulas**	**gear** $Z_1 = 19$
Apparent pressure angle (°)	$\alpha_t = tg^{-1}(\frac{tg(\alpha_n)}{cos\beta}) = tg^{-1}(\frac{tg(20)}{cos\,(13{,}4325)})$	$\alpha_t = 20{,}5162°$
Pitch diameter (mm)	$d_1 = m_t.Z_1 = 3{,}5984 * 19$	$d_1 = 68{,}370mm$
Base diameter (mm)	$d_{b1} = d_1.\cos(\alpha_t) = 68{,}384 * \cos(20{,}52162)$	$d_{b1} = 64{,}034mm$
Projection height (mm)	$h_{a1} = (1 + x_1).m_n = (1 + 0{,}4471) * 3{,}5$	$h_{a1} = 5{,}0648mm$
Depth of cavity (mm)	$h_{f1} = (1{,}25 - x_1).m_n = (1{,}25 - 0{,}4471) * 3{,}5$	$h_{f1} = 2{,}8102mm$
Tooth height (mm)	$h_1 = h_{a1} + h_{f1} = 5{,}0648 + 2{,}8102$	$h_1 = 7{,}8750\ mm$
Head diameter (mm)	$d_{a1} = d_1 + 2.h_{a1} = 68{,}370 + 2 * 5{,}0648$	$d_{a1} = 78{,}5mm$
Foot diameter (mm)	$d_{f1} = d_1 - 2.h_{f1} = 68{,}370 - 2 * 2{,}8102$	$d_{f1} = 62{,}750mm$

Table 4-12: Geometric elements of sintered gear 19 teeth

paparent functioning pressure angle	$inv\alpha'_t = inv\alpha_t + \frac{2(x_1 + x_2)}{Z_1 + Z_2} tg\alpha_n$	$inv\ \alpha'_t = 0{,}0195$ $\alpha'_t = 21.8036°$
Apparent function modulement (mm)	$m'_t = m_t\left(\frac{\cos\alpha_t}{\cos\alpha'_t}\right)$	$m'_t = 3{,}6297mm$
Cutting coefficient	$K = \frac{Z_1 + Z_2}{2\,cos\,\beta}\left(1 - \frac{cos\,\alpha_t}{cos\,\alpha'_t}\right) + (x_1 + x_2)$	K =0,0330
Projection height after cutting (mm)	$h_a = m_n(1 + x - k)$	$h'_a = 4{,}9493mm$
Head diameter after cutting (mm)	$d'_{a1} = d_1 + 2h'_a$	$d'_{a1} = 78{,}2689\ mm$
Operating diameter (mm)	$d'_1 = m'_t.Z_1$	$d'_1 = 68{,}9650\ mm$

Table 4-13: Functioning elements of the couple sintered gear-crown

4.3.5.3 Determination of the total conduct ratio:

$$\varepsilon_\gamma = \varepsilon_\alpha + \varepsilon_\beta \text{ ..... } (4.66)$$

4.3.5.3.1 *Apparent conduct ratio:*

It is given by the relation:

$$\varepsilon_\alpha = \frac{1}{\pi \cos\alpha_t}\left[\sqrt{\frac{Z_1^2}{4}\sin^2\alpha_t + y_1^2 + Z_1 y_1} + \sqrt{\frac{Z_2^2}{4}\sin^2\alpha_t + y_2^2 + Z_2 y_2} - \left(\frac{Z_1 + Z_2}{2}\right)\sin\alpha_t\right] \text{ ..... } 4.17)$$

y1 and y2 are the coefficients of reduced projections. Their values are :

$$y_1 = 1 + x_1 = 1 + 0{,}59 = 1{,}59$$

$$y_2 = 1 + x_2 = 1 - 0{,}042 = 0{,}958$$

The conduct ratio is :

$$\varepsilon_\alpha = \frac{1}{\pi \cos 20.5162}\left[\sqrt{\frac{19^2}{4}\sin^2 20.5162 + 1{,}59^2 + 19*1{,}59} + \sqrt{\frac{69^2}{4}\sin^2 20.5162 + 0{,}958^2 + 69*0{,}958} - \left(\frac{19 + 69}{2}\right)\sin 20.5162\right]$$

$$\varepsilon_\alpha = 1{,}9716$$

4.3.5.3.2 *Recovery ratio:*

It is given by the relation:

$$\varepsilon_\beta = \frac{k}{\pi} sin\,\beta = 1{,}0352$$

The total conduct ratio is:

$$\varepsilon_\gamma = \varepsilon_\alpha + \varepsilon_\beta = 3{,}007$$

4.4 Verification of the condition of resistance to surface pressure by the ISO method of the sintered gear and the crown:

4.4.1 The maximum contact pressure σ_H[MPa]:

It represents the maximum contact pressure according to the Hertz Theory; it is called the functioning surface pressure and its expression is:

$$\sigma_H = \sigma_{HB}\sqrt{K_A \cdot K_V \cdot K_{H\beta} \cdot K_{H\alpha}} \text{ ..... } (4.18)$$

With:

K_A:*The application factor*

K_V:*The dynamic factor*

$K_{H\beta}$*: The load's longitudinal distribution factor*

$K_{H\alpha}$*: The load's transversal distribution factor*

And:

σ_{HB} [MPa] is the surface pressure calculated in the contact point its expression is given by:

$$\sigma_{HB} = \sigma_{HO} . Z_B . Z_\beta \ldots\ldots (4.19)$$

With:

Z_B:The Inclination factor

Z_β:The high contact factor

And:

σ_{HO} [MPa] is the reference (basic) surface pressure is given by:

$$\sigma_{HO} = Z_H \cdot Z_E \cdot Z_\varepsilon \sqrt{\frac{F_t \cdot (u+1)}{b \cdot d_1 \cdot u}} \ldots\ldots (4.20)$$

With:

Z_H: The geometric factor

Z_ε: The conduct factor

Z_E:The elasticity factor

Where:

- $F_t\,[N]$: Tangential force (nominal) at the reference cylinder
- $u = \frac{Z_2}{Z_1}$: The ratio between the numbers of teeth.
- $b[mm]$: The width of the teeth
- $d_1[mm]$: Pitch diameter of the fretted gear

All factors representing in the three expression of different pressure surface, we are considering them in our calculation for verifying the condition of the resistance showing below:

$$\sigma_H \leq \sigma_{HP}$$

We define the safety factor with:

$$S_H = \frac{\sigma_{HP}}{\sigma_H} \ldots\ldots (4.21)$$

With:

σ_{HP} [MPa]: it is the allowable contact (Hertz) pressure is given by the relation:

$$\sigma_{HP} = \frac{\sigma_{Hlim}}{S_{Hmin}} \cdot Z_n \cdot Z_L \cdot Z_R \cdot Z_V \cdot Z_w \cdot Z_X \ldots\ldots (4.22)$$

Where:

σ_{Hlim} [MPa]: is the nominal reference stress (contact pressure)

S_{Hmin}: is the minimum safety coefficient (puncture formation)

4.4.2 Calculation of coefficients:

4.4.2.1 Elasticity factor Z_E:

It is defined with the following expression:

$$Z_E = \sqrt{\frac{1}{\pi\left(\frac{1-{\nu_1}^2}{E_1}+\frac{1-{\nu_2}^2}{E_2}\right)}} \text{ ..... (4.23)}$$

In our case we have:

$$E_1 = 210\ GPa\ , E_2 = 210\ \ GPa\ ;\ \nu_1 = \nu_2 = 0{,}3$$

So this simplification gives the following new expression:

$$Z_E = 0{,}59\sqrt{\frac{E_1 E_2}{E_1 + E_2}} \text{ ..... (4.24)}$$

The numerical application gives:

$$Z_E = 0{,}59\sqrt{\frac{210}{2}}$$

$$Z_E = 191{,}1819\ MPa$$

4.4.2.2 Geometric factor Z_H:

It is given by the following expression:

$$Z_H = \sqrt{\frac{2\cdot cos\ (\beta_b) cos(\alpha'_t)}{sin\ (\alpha_t)\cdot\ cós^2\ (\alpha_t)}} \text{ ..... (4.25)}$$

With:

- $\alpha_t(°)$: is the apparent pressure angle.
- $\alpha'_t(°)$: is the functioning pressure angle.
- $\beta_b(°)$:is the basic helix angle it is given by the relation:

$$tan\,\beta_b = cos\,\alpha_t\, tan\,\beta \text{ ..... (4.26)}$$

With:

- $\beta(°)$:is the pitch helix angle

So, the basic helix angle is: $\beta_b = 12{,}6095$

Then the geometric factor is: $Z_H = 2{,}3584$

4.4.2.3 Conduct factor Z_ε:

This factor was introduced to take into account the improvement brought by large driving ratios: we have different case depending on ε_β:

- If $\boldsymbol{\varepsilon_\beta \geq 1}$: $\boldsymbol{Z_\varepsilon = \sqrt{\frac{1}{\varepsilon\alpha}}}$
- Else $\boldsymbol{\varepsilon_\beta \leq 1}$: $\boldsymbol{Z_\varepsilon = \sqrt{\frac{4-\varepsilon_\alpha}{3}(1-\varepsilon_\beta) + \frac{\varepsilon_\beta}{\varepsilon_\alpha}}}$

We have: ε_α =1,6512

So, we're using the relation:

$$Z_\varepsilon = \sqrt{\frac{1}{\varepsilon\alpha}} \ldots\ldots (4.27)$$

$$Z_\varepsilon = 0{,}7782$$

4.4.2.4 The inclination factor Z_β:

This factor was introduced following tests showing a certain advantage to a helical gearing due to the load distribution on the contact generators:

$$Z_\beta = \sqrt{cos(\beta)} = \sqrt{cos(13{,}4325)}\, Z_\varepsilon = \sqrt{\frac{1}{\varepsilon\alpha}} \ldots\ldots (4.28)$$

$$Z_\beta = 0{,}9862$$

4.4.2.5 The single contact factor Z_B:

Z_B For helical spur gears, we will not be able to determine it so it will be taken equal to 1.

$$Z_B = 1$$

4.4.2.6 Application factor K_A:

The application factor takes into account all forces from the outside, introduced into the gear in addition to the nominal tangential force T. These overloads depend on the nature of the leading and driven machines, the masses and inertia of the connections with the driving or driven element. The AGMA gives a list completes of the application factor showing in tables page 332 of [12]:

In our case we take:

$$K_A = 1{,}75$$

4.4.2.7 Dynamic factor K_V:

The dynamic factor or the speed factor, a majority of the tangential force T taking into account the phenomena of the pitch defects of the various consecutive profiles on the pitch circle, the flexion of the teeth under overload and the variation of the oil film thickness.

We used simplified method which is available under the following conditions:

- $\beta = 13{,}4325 < 30°$
- $1{,}2 < \varepsilon_\alpha = 1{,}9716 > 1{,}9$

  ε_α Being close to 1.9, we will make the calculations as if it is in the interval.
- Steel gear
- linear load $\frac{TK_A}{b} = \frac{1{,}2214 \times 10^4 \times 1{,}75}{47}$ = 454,779, greater or equal to 100 N/mm
- $c_{kv} = \frac{VZ_1}{100}\sqrt{\frac{u^2}{u^2+1}} = 0{,}8999 \leq 10\ \left(\frac{m}{s}\right)$

With:

- V [m/s]: Tangential velocity.
- Z_1 :Teeth number of the fretted gear
- $u = \frac{Z_2}{Z_1}$: Teeth ratio

The tangential velocity is given by:

$$V = \frac{\omega_5 d_1}{2} \ldots\ldots (4.29)$$

Where: $\omega_5 = \frac{\pi \times N_5}{30}$

We take for this reducer the quality 9 from the page 341of [13]:

We have: linear load $\cong 500$:

$$f_F = 0{,}73$$

From the graph:

$$K_{350}\, N = 0{,}18$$

Then the dynamic factor is:

$$K_V = 0{,}73 \times 0{,}18 + 1 = 1{,}131$$

$$K_V = 1{,}131$$

4.4.3 Longitudinal load distribution factor $K_{H\beta}$:

It is given by the expression:

$$K_{H\beta} = 2 \cdot \frac{b}{b_{cal}} \ldots\ldots (4.31)$$

Where:

$$\frac{b_{cal}}{b} = \sqrt{\frac{2 \cdot \frac{F_m}{b}}{F_{\beta y} \cdot C_\gamma}} \ldots\ldots (4.32)$$

With:

- $F_m[N]$: Average tangential load at the reference cylinder and is given by: $F_m = K_A K_V F_t$.
- $F_{\beta y}[\mu m]$: Misalignment after running-in.
- $C_\gamma \left[\frac{N}{mm \cdot \mu m}\right]$: Average value of the meshing stiffness per unit of tooth width.

$$F_t = \frac{60P}{\pi N_5 d_1} = \frac{60 \times 60000}{\pi \times 1372{,}2 \times 68{,}370 \times 10^3} = 12{,}214\ kN$$

$$F_m = 2 \times 1{,}131 \times 68{,}370 \times 12{,}214 = 27{,}638\ kN$$

According to the page 355 [12] we have:

$$q = c_1 + \frac{c_2}{Z_{V1}} + \frac{c_3}{Z_{V2}} + c_4 x_1 + \frac{c_5 x_1}{Z_{V1}} + c_6 x_2 + \frac{c_7 x_2}{Z_{V2}} + c_8 {x_1}^2 + c_9 {x_2}^2 \ldots\ldots (4.33)$$

With:

c_1=0,0473; c_2=0,15551; c_3=0,25791; c_4=-0,00635; c_5=-0,11654; c_6=-0,00193; c_7=-0,24188 ; c_8=0,00529 ; c_9=0,00182.

And: $Z_{V1} = \frac{Z_1}{\cos^3 \beta}$; $Z_{V2} = \frac{Z_2}{\cos^3 \beta}$

We calculate: the mesh stiffness by:

$$C_\gamma = c'(0{,}75\varepsilon_\alpha + 0{,}25) \ldots\ldots (4.34)$$

$$C_\gamma = 18{,}4795(0{,}75 \times 1{,}6512 + 0{,}25) = 27{,}5049$$

With: $c' = \frac{1}{q}$=18, 4795

From the graph from the page 346[13]:

$$F_{\beta y}\left(C_\gamma, \frac{F_m}{b}\right) \quad \Longrightarrow \quad F_{\beta y} = (18\mu m)$$

Then:

$$\frac{b_{cal}}{b} = \sqrt{\frac{2 \times \frac{27{,}638 \times 10^3}{42}}{18 \times 27{,}5049}} = 1{,}4653$$

$$K_{H\beta} = 2 \cdot \frac{b_{cal}}{b} = 2{,}9306$$

$$K_{H\beta} = 2{,}9306$$

4.4.3.1 Transverse load distribution factor $K_{H\alpha}$:

This factor takes into account all the deformations and displacements essential for the distribution of the load over the width of the teeth.

It is given by the relation:

$$K_{H\alpha} = C_1 + C_2\left(\sqrt{\frac{2(\frac{b_{cal}}{b}-1)}{\frac{b_{cal}}{b}}}\right)\left(\frac{C_\gamma(V-1{,}865)(b)}{F_{th}}\right)\ldots..\ (4.35)$$

So, we have to calculate:

First, the determining tangential force on the reference cylinder:

$$F_{th} = F_t \cdot K_A \cdot K_v \cdot K_{H\beta}\ldots..\ (4.36)$$

$$F_{th} = 12{,}214\ \times 1{,}75 \times 1{,}131 \times 2{,}9306$$

$$F_{th} = 80{,}996\ kN$$

$$K_{H\alpha} = 0{,}9 + 0{,}4\left(\sqrt{\frac{2(0.6825-1)}{0.6825}}\right)\left(\frac{27{,}5049(4{,}9124-1{,}865)(42)}{80{,}996\times 10^3}\right) = 0{,}9304$$

$$K_{H\alpha}\ = 0{,}9304$$

4.4.3.2 Duration factor Z_N:

The duration factor accounts for the fact that a higher Hertz pressure can be allowed if only a limited endurance (number of cycles) is required:

First the average hours of operation:

$$H = 3 \times 265 \times 17 = 18615\ (\text{Hrs})$$

The rotational speed of the fretted gear:

N_5= 1372,2 tr/min; so we have the cycle number: $N_L = N_5.H = \ N_L = N_5 H = \ 1{,}5326 \times 10^9$

From the page 360[12]:

$$10^7 \leq N_L \leq 10^9\ldots..\ (4.37)$$

So:

$$Z_{NT} = \left(\frac{10^9}{N_L}\right)^{0{,}057} = 0{,}9760$$

$$Z_{NT}\ = 0{,}9760$$

4.4.3.3 Viscosity factor Z_L:

The kinematic absolute viscosity of the oil (*TRANSMISSION RS FE 80W-140)* is given by:

$$\nu_{40}\ = 252\frac{mm^2}{s}$$

$C_{ZL} = 0{,}91\ (\sigma_{Hlim} > 1200\ MPa)$, from where:

$$Z_L = C_{ZL} + \frac{4(1-C_{ZL})}{\left(1{,}2+\frac{134}{\nu_{40}}\right)^2}\ldots..\ (4.38)$$

$$Z_L\ = 1{,}030$$

4.4.3.4 Speed factor Z_V:

Hardness of the (17Cr4Ni4Mn4) was estimated at: 62 HRC ; From the graph page 98 [14] :

$$\sigma_{Hlim} = 1460\ {}^{N}/_{mm^2}$$

$$Z_V = C_{ZV} + \frac{2(1-C_{ZV})}{\sqrt{0{,}8+\frac{32}{V}}} \ldots\ldots (4.39)$$

We take $\sigma_{Hlim} \geq 1200$ so the value of $C_{ZL} = 0{,}91$

$$C_{ZV} = C_{ZL} + 0.02 = 0{,}91 + 0{,}02 = 0{,}93$$

$$Z_V = 0{,}93 + \frac{2(1-0{,}93)}{\sqrt{0{,}8+\frac{32}{4{,}9124}}} = 0{,}982$$

$$Z_V = 0{,}982$$

4.4.3.5 Roughness factor Z_R:

We have: $Z_R = \left(\frac{3}{R_{Z10}}\right)^{C_{ZR}}$ ..... *(4.40)*

With:

$C_{ZR} = 0{,}08$ ($\sigma_{Hlim} \geq 1200\ N/mm^2$)

$$R_{Z10} = 100 \Rightarrow Z_R = \left(\frac{3}{100}\right)^{0{,}08} = 0{,}755$$

$$Z_R = 0{,}755$$

4.4.3.6 Hardness ratio factor Z_W:

The hardness of the (17Cr4Ni4Mn4) is 447 HB according to [14].

$$130 < HB < 470$$

Thus: $Z_W = 1{,}2 - \left[\frac{HB-130}{1700}\right]$ ..... *(4.41)*

$$Z_W = 1{,}014$$

4.4.3.7 Dimension factor Z_X:

Value can be adopted if the steel is properly selected and if the heat treatment and the depth of the hardened layer are appropriate

$$\boldsymbol{Z_X = 1}$$

4.4.4 Checking conditions:

$$\sigma_{HB} = \sigma_{HO}.Z_B \cdot Z_\beta = Z_H \cdot Z_E \cdot Z_\varepsilon \cdot Z_B \cdot Z_\beta \sqrt{\frac{T_0(u+1)}{b \cdot d_1 \cdot u}} \ldots\ldots (4.42)$$

$$\sigma_{HO} = 2{,}3584 \times 191{,}1819 \times 0{,}7782 \sqrt{\frac{1{,}2214 \times 10^3 (3{,}6316 + 1)}{42 \times 68{,}370 \times 3{,}6316}} = 734{,}4746\ MPa$$

$$\sigma_{HB} = \sigma_{HO} . Z_B . Z_\beta = 734{,}4746 \times 1 \times 0{,}9862 = 724{,}3589\ MPa$$

$$\sigma_H = 724{,}3589 \sqrt{2 \times 1{,}1314 \times 2.9306 \times 0{,}9304} = 1{,}7993 \times 10^3 MPa$$

$$\sigma_{HP} = \frac{1460}{1{,}7255} \times 0{,}9760 \times 1{,}0300 \times 0{,}9818 \times 0{,}7554 \times 1{,}014 \times 1$$

$$\sigma_{HP} = 639{,}3476\ MPa$$

We have: $\boldsymbol{\sigma_H < \sigma_{HP}}$

Hence, **the condition of resistance to surface pressure is not satisfied.**

At this stage, the verification of the tensile strength is unnecessary. It will be done when the surface pressure resistance criterion is verified. Therefore, it is necessary to increase the modulus, or to use a stronger (harder) material, or to make an analysis of the critical operating conditions of the streetcar to evaluate the load actually applied on the gears of the reducer.

4.5 CONCLUSION:

In this chapter, we have studied the conditions of resistance of the couple sintered gear-crown, where we have the damaged gear teeth are practically sheared off at their root.

As mentioned in the introduction, two criteria exist. If one of them is not verified, it is useless to verify the other, but it is necessary to improve the operating parameters.

We started with the verification of the condition of resistance to the surface pressure. We found that this condition is not satisfied. We can put the following assumptions:

- The material has insufficient resistance.
- The modulus is not sufficient.
- Conditions of the underestimated

Therefore, it is necessary to review these conditions to achieve normal operation.

General conclusion

This work deals with the damage of the gears in the drive train of the streetcar of Algiers site of the company CITAL. It was conducted by studying:

In the second chapter, reliability analysis using the Weibull law.

According to the parameter of form β which is located between $3 < \beta < 4$, the system is according to the curve in bathtub in the period of old age which means the present of the wear in just 50% of its reliability these result lead us to make some assumption that the main problem is in the:

- The material of insufficient resistance
- The modulus is not sufficient
- Conditions are underestimated

In the third chapter, we characterized the material which the sintered gear is made of and determined its composition and hardness in order to proceed the calculations of resistance.

In the final chapter, the resistance of the material used for the sintered gear has been studied and it has been shown that the criterion of surface pressure is not satisfied. This confirms the assumptions we made in the 2nd chapter on:

And according to the chapter three that is showing the material and its process of manufacturing which is the sintering process can lead us to make another assumption about this process is it the best mode that we can use to resist the external load of the rolling stock.

So to close our work we propose solutions to fix the problem of this failure:

For the reliability analysis is the indispensable tool for a company to reduce the probable failures of its equipment so, we strongly recommend that maintenance managers apply conditional preventive maintenance by using a verification system after each number of hours of use.

For the resistance of our material, we propose to increase the modulus and resizing from the beginning with taking into account the actual overload conditions, or use another material can resist any overload in the streetcar also we can recommend to change the sintering process by other process like forging process, another thing concerning the heat treatment and thermochemical treatment which has not been checked, to foresee a hardening heat treatment and a carburizing up to 1.5mm of hardened layer.

Bibliography

[2] Simon Iwnicki, Maksym Spiryagin, Colin Cole and Tim McSweeney. Handbook of railway vehicle dynamics second-edition. CRC Press, Boca Raton, FL, 2017.

[5] SAVMER0012-G ARPEGE – « Manuel entretien et reparation » JT+RLT FR CITAL.

[6] Alstom Motors General Catalogue - MAYA transmission Co., LTD.

[8] Catalog : Bogie Arpege 350 m 1600 pont moteur CITAL.

[10] X. Yu and A. M. Khambadkone, 'Reliability Analysis and Cost Optimization of Parallel-Inverter System', *IEEE Trans. Ind. Electron.*, vol. 59, no. 10, pp. 3881–3889, Oct. 2012.

[11] F. Corvaro, G. Giacchetta, B. Marchetti, and M. Recanati, 'Reliability, Availability, Maintainability (RAM) study, on reciprocating compressors API 618', *Petroleum*, vol. 3, no. 2, pp. 266–272, Jun. 2017.

[12] S. M. Rezvanizaniani, J. Barabady, M. Valibeigloo, M. Asghari, and and U. Kumar, 'Reliability Analysis of the Rolling Stock Industry: A Case Study', *Int. J. Perform. Eng.*, vol. 5, no. 2, p. 167, Feb. 2009.

[17] Gábor Á., Ferenc B., János E., and János K., 'KOCKÁZAT ÉS MEGBÍZHATÓSÁG A MENEDZSMENTBEN RISK AND RELIABILITY IN MANAGEMENT', p. 15.

[19] A. O'Connor, 'Probability Distributions Used in Reliability Engineering', p. 215.

[27] L. Bütikofer, B. Stawarczyk, and M. Roos, 'Two regression methods for estimation of a two-parameter Weibull distribution for reliability of dental materials', *Dent. Mater.*, vol. 31, no. 2, pp. e33–e50, Feb. 2015.

[28] S. Saraswat and G. S. Yadava, 'An overview on reliability, availability, maintainability and supportability (RAMS) engineering', *Int. J. Qual. Reliab. Manag.*, vol. 25, no. 3, pp. 330–344, Mar. 2008.

[29] Leng, Yang. Materials Characterization: Introduction to Microscopic and Spectroscopic Methods. Wiley. (2009)

[33] R. Basan and T. Marohnic, 'Multiaxial fatigue life calculation model for components in rolling-sliding line contact with application to gears', *Fatigue Fract. Eng. Mater. Struct.*, vol. 42, Mar. 2019.

[34] Y. Ding and N. F. Rieger, 'Spalling formation mechanism for gears', *Wear*, vol. 254, no. 12, pp. 1307–1317, Nov. 2003.

[35] W. Wang, H. Liu, C. Zhu, and Z. Sun, 'Evaluation of contact fatigue life of a wind turbine carburized gear considering gradients of mechanical properties', *Int. J. Damage Mech.*, vol. 28, no. 8, pp. 1170–1190, Aug. 2019.

[36] '(2) Very high cycle fatigue of surface carburized CrNi steel at variable stress ratio: Failure analysis and life prediction | Request PDF'.

[37] V. Rajinikanth, M. K. Soni, B. Mahato, and M. Ananda Rao, 'Study of microstructural degradation of a failed pinion gear at a cement plant', *Eng. Fail. Anal.*, vol. 95, pp. 117–126, Jan. 2019.

[38] C. O. F. T. Ruchert, C. I. S. Maciel, and A. E. A. Chemin, 'Sub case origin fatigue in teeth of helical gear of a TA 67n turbo reducer', *Eng. Fail. Anal.*, vol. 108, p. 104286, Jan. 2020.

[39] N. Merah and A. Al-Qutub, 'Premature Failure of an Industrial Mixer Timing Gears', *J. Fail. Anal. Prev.*, vol. 17, Jul. 2017.

[41] G. Henriot, *Engrenages - 8e éd. Conception - Fabrication - Mise en œuvre: Conception - Fabrication - Mise en œuvre*. Paris: Dunod, 2013.

Webography

[1] CITAL website: https://www.cital-dz.com/ . April 2022.

[4] The Urban Transport Magazine website: https://www.urban-transport-magazine.com/en/ . April 2022.

[3] The railway technical website : http://www.railway-technical.com/ . April 2022.

[7] Alstom website : http://www.alstom.com/ . May 2022.

[9] IQS Articles website : https://www.iqsdirectory.com/articles/ . May 2022

[13] 'Reliability Analysis | SpringerLink'. https://link.springer.com/chapter accessed Jul. 07, 2022).

[14] 'Reliability: Engineering & Equipment | Inspectioneering'. https://inspectioneering.com/tag/reliability (accessed Ma. 27, 2022).

[15] 'Jan Claude Ligeron « cours de Fiabilité en Mécanique » (accessed June. 07, 2022).

[16] 'Reliability Study of Parameter Uncertainty Based on Time-Varying Failure Rates with an Application to Subsea Oil and Gas Production Emergency Shutdown Systems 'https://www.mdpi.com (accessed June. 07, 2022).

[18] ‘Distinguez les différents types de systèmes’, *OpenClassrooms*. https://openclassrooms.com/ (accessed Jul. 07, 2022).

[20] ‘Discrete Probability Distribution - Examples, Definition, Types’. https://www.cuemath.com/ (accessed June. 07, 2022).

[21] ‘Continuous Probability Distributions Statistics Review Website’. https://sites.nicholas.duke.edu/statsreview/continuous-probability-distributions/ (accessed June. 07, 2022).

[22] ‘Understanding a Poisson Distribution’, *Investopedia*. https://www.investopedia.com/terms/p/poisson-distribution.asp (accessed June. 07, 2022).

[23] ‘Beta distribution | Properties, proofs, exercises. https://www.statlect.com/probability-distributions/ (accessed June. 08, 2022).

[24] ‘Normal Distribution’, *Investopedia*. https://www.investopedia.com/terms/n/normaldistribution.asp (accessed May 29, 2022).

[25] ‘Exponential Distribution | Definition | Memoryless Random Variable’. https://www.probabilitycourse.com/chapter4/4_2_2_exponential.php (accessed June. 07, 2022).

[27] ‘Reliability: Engineering & Equipment | Inspectioneering | Inspectioneering’. https://inspectioneering.com/tag/reliability (accessed June. 07, 2022).

[30] ‘PREMΛP: Exploring the Design and Materials Space for Gears | Farrokh Mistree - Academia.edu’. https://www.academia.edu (accessed June. 11, 2022).

[31] ‘Machines | Free Full-Text | Dynamic Analysis of a High-Contact-Ratio Spur Gear System with Localized Spalling and Experimental Validation
https://www.mdpi.com/2075-1702/10/2/154 (accessed June. 11, 2022).

[32] ‘(1) Shigley’s Mechanical Engineering Design 8th Edition | CARLOS MIGUEL - Academia.edu’. https://www.academia.edu/ (accessed June. 18, 2022).

[40] ‘DIN 1652-3 Grade 17CrNiMo6 cold-drawn or peeled and treated to ferrite-pearlite structure - Nickel Chromium Molybdenum Steel - Matmatch’. https://matmatch.com/materials (accessed Jul. 10, 2022).

[42] *ENGRENAGES.. Conception, fabrication, mise en oeuvre, 7ème édition - Georges Henriot.* Accessed: June. 11, 2022 https://www.decitre.fr/livres/engrenages

[43] ‘Calcul de la capacité de charge des engrenages cylindriques de transmission de puissance - Présentation et analyse des méthodes I.S.O. 6336’. https://www.editions-ellipses.fr (accessed June. 11,2022).

Appendix

Appendix A

The data of the intervention follow-up provided by CITAL Company

T_i (Hr)	T_e (Hr)	T_{in} (Hr)	T_r (Hr)	TBF (Hr)	TBF_O (Hr)	TBF_{Omin} (min)	Ti_{in} (Hr)	N_i (Hr)
2014-01-28	*2011-04-16*		*2016-01-31*	*1018*	*764*	*870960*	40	2
2014-01-28	*2011-04-16*		*2015-10-19*	*1018*	*764*	*870960*	*20*	*2*
2014-06-15	*2012-03-05*		*2015-10-12*	*832*	*832*	*948480*	*50*	*2*
2014-07-01	*2012-05-28*	*2014-11-06*	*2016-02-10*	*764*	*833*	*949620*	*50*	*2*
2014-07-01	*2012-05-28*		*2015-05-06*	*764*	*1018*	*1160520*	*40*	*2*
2015-03-29	*2012-05-28*		*2016-02-16*	*1035*	*1018*	*1160520*	*80*	*2*
2015-04-20	*2013-01-07*			*833*	*1032*	*1176480*	*50*	*2*
2015-04-26	*2011-04-16*		*2016-03-08*	*1471*	*1035*	*1179900*	*50*	*3*
2015-08-06	*2012-07-05*	*2015-08-06*	*2016-03-16*	*1127*	*1113*	*1268820*	*4*	*3*
2015-08-20	*2012-05-28*		*2016-04-28*	*1179*	*1127*	*1284780*	*2*	*3*
2015-11-05	*2013-01-07*	*2015-12-30*	*2016-04-28*	*1032*	*1179*	*1344060*	*24*	*3*
2016-01-25	*2013-01-07*	*2016-01-25*	*2016-04-28*	*1113*	*1179*	*1344060*	*2*	*3*
2016-03-31	*2013-01-07*	*2016-04-03*	*2016-12-20*	*1179*	*1267*	*1444380*	*20*	*3*
2016-04-27	*2012-05-28*	*2016-05-13*	*2016-07-26*	*1430*	*1386*	*1580040*	*4*	*3*
2016-05-08	*2012-07-05*	*2016-05-12*	*2016-08-03*	*1403*	*1403*	*1599420*	*16*	*3*
2016-05-05	*2012-03-05*	*2016-05-11*	*2016-07-26*	*1522*	*1430*	*1630200*	*7*	*3*
2016-06-19	*2011-04-16*	*2016-07-21*	*2016-08-25*	*1891*	*1471*	*1676940*	*6*	*2*
2016-06-27	*2013-01-07*	*2016-10-31*	*2016-12-15*	*1267*	*1478*	*1684920*	*40*	*2*
2016-07-11	*2011-04-16*	*2016-07-19*	*2016-08-25*	*1913*	*1522*	*1735080*	*8*	*2*
2016-10-24	*2013-01-07*	*2016-11-03*	*2017-03-02*	*1386*	*1605*	*1829700*	*30*	*2*
2016-10-31	*2012-05-28*	*2016-11-20*	*2017-03-02*	*1617*	*1617*	*1843380*	*16*	*2*
2017-01-23	*2011-04-16*	*2017-03-31*	*2017-07-16*	*2109*	*1680*	*1915200*	*150*	*2*
2017-01-24	*2013-01-07*	*2017-02-26*	*2017-06-15*	*1478*	*1706*	*1944840*	*2*	*2*
2017-03-07	*2012-07-05*	*2017-03-12*	*2017-06-15*	*1706*	*1729*	*1971060*	*48*	*2*
2017-04-16	*2011-04-16*	*2017-04-17*	*2017-07-20*	*2192*	*1754*	*1999560*	*16*	*2*
2017-05-21	*2012-07-05*	*2017-07-01*	*2017-08-23*	*1781*	*1765*	*2012100*	*8*	*2*
2017-05-31	*2013-01-07*	*2017-11-20*	*2017-12-24*	*1605*	*1781*	*2030340*	*16*	*2*
2017-06-12	*2011-04-16*	*2017-06-23*	*2017-09-19*	*2249*	*1854*	*2113560*	*20*	*2*
2017-06-21	*2011-04-16*	*2017-07-06*	*2017-08-23*	*2258*	*1891*	*2155740*	*8*	*2*
2017-07-24	*2012-03-05*	*2017-08-03*	*2017-11-07*	*1967*	*1909*	*2176260*	*10*	*2*
2017-08-02	*2012-07-05*	*2017-08-08*	*2017-10-24*	*1854*	*1913*	*2180820*	*8*	*2*
2017-08-05	*2011-04-16*	*2017-08-12*	*2017-10-04*	*2303*	*1924*	*2193360*	*8*	*2*
2017-08-05	*2012-03-05*	*2017-08-15*	*2017-11-09*	*1979*	*1960*	*2234400*	*8*	*2*
2017-08-14	*2013-01-07*	*2017-08-24*	*2017-10-04*	*1680*	*1967*	*2242380*	*8*	*2*
2017-08-26	*2011-04-16*	*2017-09-04*		*2324*	*1979*	*2256060*	*8*	*2*
2017-09-01	*2012-03-05*			*2006*	*1982*	*2259480*	*8*	*2*

2017-10-02	*2013-01-07*	*2017-10-07*	*2017-12-03*	*1729*	*1985*	*2262900*	*8*	*2*
2017-10-26	*2012-03-05*	*2017-11-07*		*2061*	*1990*	*2268600*	*10*	*2*

T_i: *incident date*

T_e: *exploitation date*

T_{in}: *intervention date*

T_r: *return to site date*

TBF: *operating time*

TBF_o: *ordered operating time*

TBF_{omin}: *ordered operating (mi*

T_{in}: *intervention date*

Different Parameter Used in Reliability Analysis

i	*TBF*	TBF_{min}	F_i	$\ln(TBF)$	Y	$R(t)$	$\lambda(t)$
1	*764*	*1100160*	*0,00862069*	*6,63856779*	*-4,7492643*	*0,997*	*0*
2	*764*	*1100160*	*0,01724138*	*6,63856779*	*-4,0517597*	*0,9942*	*0*
3	*832*	*1198080*	*0,02586207*	*6,72383244*	*-3,6419053*	*0,9897*	*0,0001*
4	*833*	*1199520*	*0,03448276*	*6,72503364*	*-3,3498015*	*0,9832*	*0,0001*
5	*1018*	*1465920*	*0,04310345*	*6,9255952*	*-3,1222032*	*0,9741*	*0,0001*
6	*1018*	*1465920*	*0,05172414*	*6,9255952*	*-2,9353933*	*0,9621*	*0,0001*
7	*1032*	*1486080*	*0,06034483*	*6,93925395*	*-2,7767203*	*0,9465*	*0,0002*
8	*1035*	*1490400*	*0,06896552*	*6,94215671*	*-2,6386319*	*0,9269*	*0,0002*
9	*1113*	*1602720*	*0,07758621*	*7,01481435*	*-2,5162567*	*0,903*	*0,0003*
10	*1127*	*1622880*	*0,0862069*	*7,02731451*	*-2,4062682*	*0,8744*	*0,0004*
11	*1179*	*1697760*	*0,09482759*	*7,0724219*	*-2,3062936*	*0,8409*	*0,0004*
12	*1179*	*1697760*	*0,10344828*	*7,0724219*	*-2,2145807*	*0,8026*	*0,0005*
13	*1267*	*1824480*	*0,11206897*	*7,14440718*	*-2,1297988*	*0,7594*	*0,0006*
14	*1386*	*1995840*	*0,12068966*	*7,23417718*	*-2,0509133*	*0,7118*	*0,0007*
15	*1403*	*2020320*	*0,12931034*	*7,24636808*	*-1,9771039*	*0,6601*	*0,0008*
16	*1430*	*2059200*	*0,13793103*	*7,26542972*	*-1,9077092*	*0,6053*	*0,0009*
17	*1471*	*2118240*	*0,14655172*	*7,29369772*	*-1,8421878*	*0,5481*	*0,0011*
18	*1478*	*2128320*	*0,15517241*	*7,2984451*	*-1,7800915*	*0,4896*	*0,0012*
19	*1522*	*2191680*	*0,1637931*	*7,32778054*	*-1,7210445*	*0,4309*	*0,0014*
20	*1605*	*2311200*	*0,17241379*	*7,38087904*	*-1,6647287*	*0,3733*	*0,0015*

21	*1617*	*2328480*	*0,18103448*	*7,38832786*	*-1,6108724*	*0,3179*	*0,0017*
22	*1680*	*2419200*	*0,18965517*	*7,42654907*	*-1,559242*	*0,2658*	*0,0019*
23	*1706*	*2456640*	*0,19827586*	*7,44190673*	*-1,5096347*	*0,218*	*0,0021*
24	*1729*	*2489760*	*0,20689655*	*7,45529849*	*-1,4618734*	*0,1751*	*0,0023*
25	*1754*	*2525760*	*0,21551724*	*7,46965417*	*-1,4158027*	*0,1375*	*0,0025*
26	*1765*	*2541600*	*0,22413793*	*7,47590597*	*-1,3712855*	*0,1055*	*0,0028*
27	*1781*	*2564640*	*0,23275862*	*7,48493028*	*-1,3281997*	*0,0789*	*0,003*
28	*1854*	*2669760*	*0,24137931*	*7,52510075*	*-1,2864368*	*0,0575*	*0,0033*
29	*1891*	*2723040*	*0,25*	*7,54486107*	*-1,2458993*	*0,0408*	*0,0036*
30	*1909*	*2748960*	*0,25862069*	*7,55433482*	*-1,2064997*	*0,0281*	*0,0039*
31	*1913*	*2754720*	*0,26724138*	*7,55642797*	*-1,1681587*	*0,0187*	*0,0042*
32	*1924*	*2770560*	*0,27586207*	*7,56216163*	*-1,1308048*	*0,0121*	*0,0045*
33	*1960*	*2822400*	*0,28448276*	*7,58069975*	*-1,0943725*	*0,0076*	*0,0049*
34	*1967*	*2832480*	*0,29310345*	*7,58426482*	*-1,0588025*	*0,0046*	*0,0052*
35	*1979*	*2849760*	*0,30172414*	*7,59034695*	*-1,0240401*	*0,0026*	*0,0056*
36	*1982*	*2854080*	*0,31034483*	*7,59186171*	*-0,9900353*	*0,0015*	*0,006*
37	*1985*	*2858400*	*0,31896552*	*7,59337419*	*-0,9567421*	*0,0008*	*0,0064*
38	*1990*	*2865600*	*0,32758621*	*7,59588992*	*-0,9241179*	*0,0004*	*0,0069*
39	*2000*	*2880000*	*0,3362069*	*7,60090246*	*-0,8921232*		
40	*2006*	*2888640*	*0,34482759*	*7,60389797*	*-0,8607216*		
41	*2020*	*2908800*	*0,35344828*	*7,61085279*	*-0,8298789*		
42	*2061*	*2967840*	*0,36206897*	*7,63094658*	*-0,7995636*		

$F_i: distribution\ function$

$Y = \ln(\ln(\frac{1}{1-F_i}))$

$R(t): Reliability$

$\lambda(t): failure\ rate$

Appendix B

The charts and tables used in Chapter 4

Tableau 7.2 – $K_{A\text{-}C}$

Machines menantes	Machines menées			
	U Uniforme	L Chocs légers	M Chocs modérés	H Chocs importants
Uniforme	1	1,25	1,50	1,75
Chocs légers	1,10	1,35	1,60	1,85
Chocs modérés	1,25	1,50	1,75	2,00
Chocs importants	1,50	1,75	2	≥ 2,25

Tableau 7.3 – Exemples de machines menantes

Caractéristiques de la transmission	Exemples de machines menantes
Uniforme	– Turbines à vapeur et à turbines à gaz – Moteurs électriques Faible couple de démarrage
Chocs légers	– Turbines – Moteurs électriques Fort couple de démarrage
Chocs modérés	– Moteur à combustion interne à grand nombre de cylindres
Chocs importants	– Moteur à combustion interne Très petit nombre de cylindres

Tableau 7.4 – Exemples de machines menées

Caractéristiques de la transmission	Exemples de machines menées
Uniforme U	Génératrices, convoyeurs à courroies uniformément chargés, élévateurs légers, entraînement d'avance de machines-outils, pompes centrifuges légères, mélangeurs à liquides ou matières homogènes, ventilateurs, etc.
Chocs légers L	Convoyeurs à courroies non uniformément chargés, commande prilateurs de mines et industriels lourds, pompes centrifuges lourdes, mélangeurs pour liquides ou matières non homogènes, pompes de circulation, pompes à pistons multiples, calandres, laminoirs continus, etc.
Chocs modérés M	Extrudeuses pour caoutchouc, mélangeurs avec interruption du travail pour caoutchouc et plastique, broyeurs à boulets, machines à bois, engrenage d'élévateurs, pompe à piston simple, etc.
Chocs importants H	Engrenages d'excavateurs, laminoirs à barres lourds, laminoirs à caoutchouc, broyeurs de minerais, machines de sidérurgie lourdes, pompes d'alimentation lourdes, machines à briques, laminoirs à froid, etc.

A table to determine the value of the Application factor K_A

Tableau 7.6 – Valeur de f_F

Qualité ISO	$K_A \cdot \frac{F_t}{b}$ (N/mm) ≤ 100	200	350	500	800	1 200	1 500	2 000
3	1,96 (1,61)	1,29 (1,18)	1,0	0,88 (0,93)	0,78 (0,86)	0,73 (0,83)	0,70 (0,81)	068 (0,80)
4	2,21 (1,81)	1,36 (1,24)	1,0	0,85 (0,90)	0,73 (0,82)	0,66 (0,77)	0,62 (0,75)	0,60 (0,73)
5	2,56 (2,15)	1,47 (1,34)	1,0	0,81 (0,86)	0,65 (0,74)	0,56 (0,67)	0,52 (0,65)	0,48 (0,62)
6	2,82 (2,45)	1,55 (1,43)	1,0	0,78 (0,83)	0,59 (0,67)	0,48 (0,59)	0,44 (0,55)	0,39 (0,51)
7	3,03 (2,73)	1,61 (1,52)	1,0	0,76 (0,79)	0,54 (0,61)	0,42 (0,51)	0,37 (0,47)	0,33 (0,43)
8	3,19 (2,95)	1,66 (1,59)	1,0	0,74 (0,77)	0,51 (0,56)	0,38 (0,45)	0,33 (0,40)	0,28 (0,35)
9	3,27 (3,09)	1,68 (1,63)	1,0	0,73 (0,75)	0,49 (0,53)	0,36 (0,41)	0,30 (0,36)	0,25 (0,31)
10	3,35 (3,22)	1,70 (1,67)	1,0	0,72 (0,73)	0,47 (0,50)	0,33 (0,37)	0,28 (0,32)	0,22 (0,27)
11	3,39 (3,30)	1,72 (1,69)	1,0	0,71 (0,72)	0,46 (0,48)	0,32 (0,35)	0,27 (0,30)	0,21 (0,24)
12	3,43 (3,37)	1,73 (1,71)	1,0	0,71 (0,72)	0,45 (0,47)	0,31 (0,33)	0,25 (0,27)	0,20 (0,22)

Valeurs pour denture hélicoïdale avec $\varepsilon_\beta \geq 1$.
( ) Valeurs pour denture droite.

A chart to determine the value of f_F

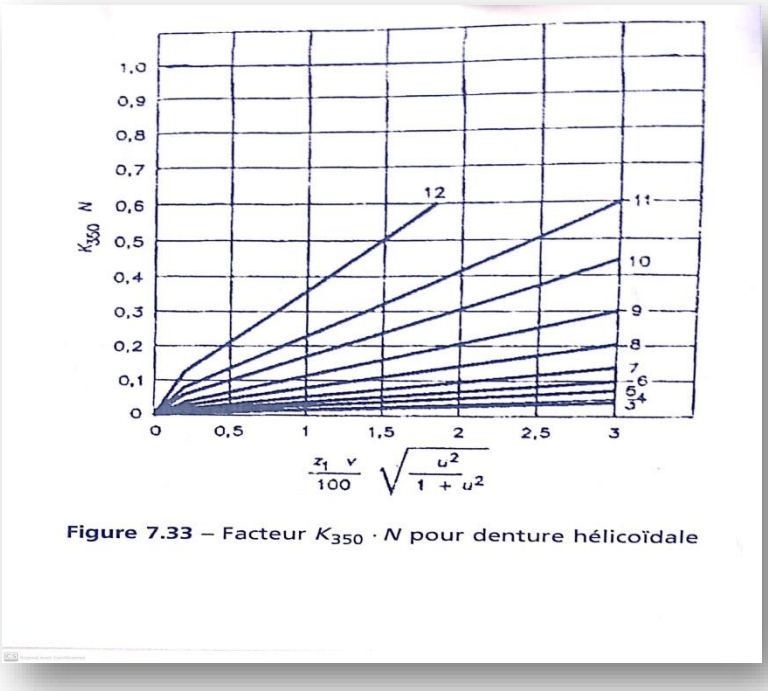

Figure 7.33 – Facteur $K_{350} \cdot N$ pour denture hélicoïdale

A chart to determine the value of the factor $K_{350}.N$ for helical gears

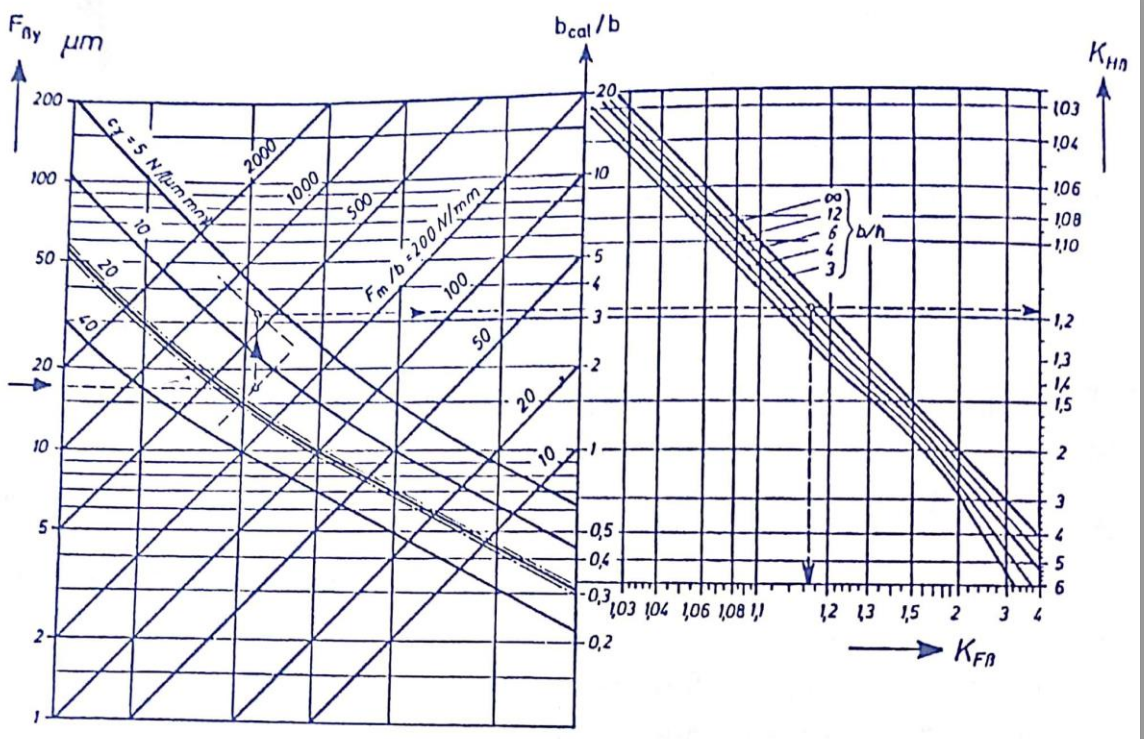

Figure 7.37 – Diagramme par détermination de $K_{H\beta}$ et $K_{F\beta}$ suivant les formules 7.83 et 7.84

A chart to determine the value of gear misalignment after running in $F_{\beta Y}$